The Endoplasmic Spreading Mechanism of Fibroblasts: Showcasing the Integrated Cytoskeleton

Christopher D. Lynch

Submitted in partial fulfillment of the
requirements for the Degree of Doctor of
Philosophy in the Graduate School of Arts
and Sciences

Columbia University

2012

ABSTRACT

The Endoplasmic Spreading Mechanism of Fibroblasts: Showcasing the Integrated Cytoskeleton

Christopher D. Lynch

Cell motility is an essential process that depends on a coherent, cross-linked cytoskeleton that physically coordinates the actions of numerous structural and signaling molecules. In culture, a common feature of cells is the coherent movement of the endoplasm reticulum and membranous organelles toward the periphery during substrate adhesion and spreading. The actin cross-linking protein, filamin (Fln), has been implicated in the support of three-dimensional cortical actin networks capable of both maintaining cellular integrity and withstanding large forces. Although numerous studies have examined cells lacking one of the multiple Fln isoforms, compensatory mechanisms can mask novel phenotypes only observable by further Fln depletion. Indeed, shRNA-mediated knockdown of FlnA in FlnB–/– mouse embryonic fibroblasts (MEFs) causes a novel endoplasmic spreading deficiency as detected by endoplasmic reticulum markers. Microtubule (MT) extension rates are also decreased but not by peripheral actin flow, because this is also decreased in the Fln-depleted system. Additionally, Fln-depleted MEFs exhibit decreased adhesion stability that leads to increased ruffling of the cell edge, reduced adhesion size, transient traction forces, and decreased stress fibers. FlnA–/– MEFs, but not FlnB–/– MEFs, also show a moderate defect in endoplasm spreading, characterized by initial extension followed by abrupt retractions and stress fiber fracture. FlnA localizes to actin linkages surrounding the endoplasm, adhesions, and stress fibers. Thus I suggest that Flns have a major role in the maintenance of actin-based mechanical linkages that enable endoplasmic spreading and MT extension as well as sustained traction forces and mature focal adhesions. I also report that treatment with the calpain

inhibitor N-[N-(N-Acetyl-L-leucyl)-L-leucyl]- L-norleucine (ALLN) restores endoplasmic spreading and focal adhesion (FA) maturation in the absence of Fln. Further, expression of calpain-uncleavable talin, but not full-length talin, also rescues endoplasmic spreading in Fln-depleted cells and indicates a crucial role for stable, mature FAs in endoplasmic spreading. Because FA maturation involves the vimentin intermediate filament (vIF) network, I also examined the role of vIFs in endoplasmic spreading. Wild-type cells expressing a dominant-negative vimentin variant incapable of vIF polymerization exhibit deficient endoplasmic spreading as well as defects in FA maturation. ALLN treatment restores FA maturation despite the lack of vIFs, but does not restore endoplasmic spreading. Consistent with a role for vIFs in endoplasmic spreading, adhesive structures do not contain vIFs when the endoplasm does not spread. Fln-depleted cells also exhibit a microtubule-dependent mistargeting of vIFs. Thus, I propose a model in which cellular force generation and interaction of vIFs with mature FAs are required for endoplasmic spreading. Additionally, I discuss future lines of investigation concerning the role of FlnA in the endoplasmic spreading mechanism as well as mechanosensitive functions of FlnA. Finally, I speculate on a potential application of endoplasmic spreading deficiencies as hallmarks of metastatic breast cancer.

TABLE OF CONTENTS

LIST OF FIGURES

Acknowledgments

First and foremost, I would like to thank my thesis advisor, Mike Sheetz, for graciously allowing me to complete my dissertation work in his lab(s!). Mike provided me excellent advice throughout my years at Columbia, particularly with regards to experimental approach, figure construction, and writing style. Always a source of inspiration, Mike's mantras, including "Grab the bull by the horns!" and "Great papers aren't written. They're rewritten," will echo throughout my future endeavors.

Next, I would like to thank all past and present members of the Sheetz lab for their support and guidance. In particular, Ana Kostic, for being my first mentor and urging me to dive headfirst into filamin research, Nils Gauthier, for transforming me into a cell biologist, Nicolas Biais, for being the most consistent, energetic, passionate, and knowledgeable mentor a student could ask for, Justin Abramson and Matteo Palma for being outstanding office mates and friends, Andre Lazar for making me a better teacher and mentor, as well as carrying the torch, Pere Roca-Cusachs for encouraging me not to write like a scientist and providing helpful translations of Spanish language music videos, Simon Moore for helpful manuscript suggestions and sharing the pain of the dreaded "program," and Xian Zhang and Yunfei Cai for insightful discussions and allowing me to practice my Chinese with them. More recent thanks to Haguy Wolfenson and Thomas Iskratch for helpful suggestions on this thesis.

I would also like to thank all the students and faculty of the Mechanobiology Institute at the National University of Singapore for getting me through "boot camp." In particular, Cheng-han Yu, Feroz Musthafa, Aneesh Sathe, Thomas Masters, Weiwei Luo, Edna Hu, and Felix Margadant made the trip fun, educational, and worthwhile.

Finally, my most sincere thanks to my parents, David and Pauline Lynch, and my fiancée, Annie Cheng, for supporting me through the most difficult, and significant, experience of my life. I truly would not have made it without you.

This work is dedicated to Mom, Dad, and

Annie

Chapter 1 - Introduction

1.1 – Cell motility

Cell motility is a critical aspect of life, and potentially death, for higher organisms. Cells must be motile during development to ensure proper orientation and function of the embryo (Locascio & Nieto, 2001) (Yang & Weinberg, 2008). Cells must also be motile for wounds to heal (Abercrombie & Heaysman, 1954). Unregulated motility, however, has the potential to develop into metastatic cancer (Friedl & Gilmour, 2009). Consequences of motility aside, the mechanisms involved in cell motility are complex, involving hundreds of molecules and coordinated signaling events (Zaidel-Bar, Itzkovitz, Ma'ayan, Iyengar, & Geiger, 2007). Additionally, not all cell types move in similar ways (Hatten, 1999), thereby complicating efforts to simplify cell motility into a series of universal steps. Model cell systems and predictable assays are useful in this respect. In this thesis, I utilize mouse embryonic fibroblasts (MEFs) and cell spreading assays in an effort to mechanistically understand the movement of the endoplasm (defined later in section 1.13). The remainder of this chapter introduces necessary background information. Chapters 2 and 3 each cover experimental results at the start, and end with discussion of the meaning of these results in a broader context. Chapter 4 looks ahead to future work concerning the endoplasm and related molecular players. I conclude by suggesting a possible role for my studies in diagnosing cancer.

1.2 – Fibroblasts as a model system

Cell motility is a vast and fascinating subject. Different cell types move in different ways to different cues, complicating efforts to define motile components universal to all cells. One system in which motility is frequently studied is the fibroblast (Dokukina & Gracheva, 2010) (Giannone & Sheetz, 2006) (Figure 1).

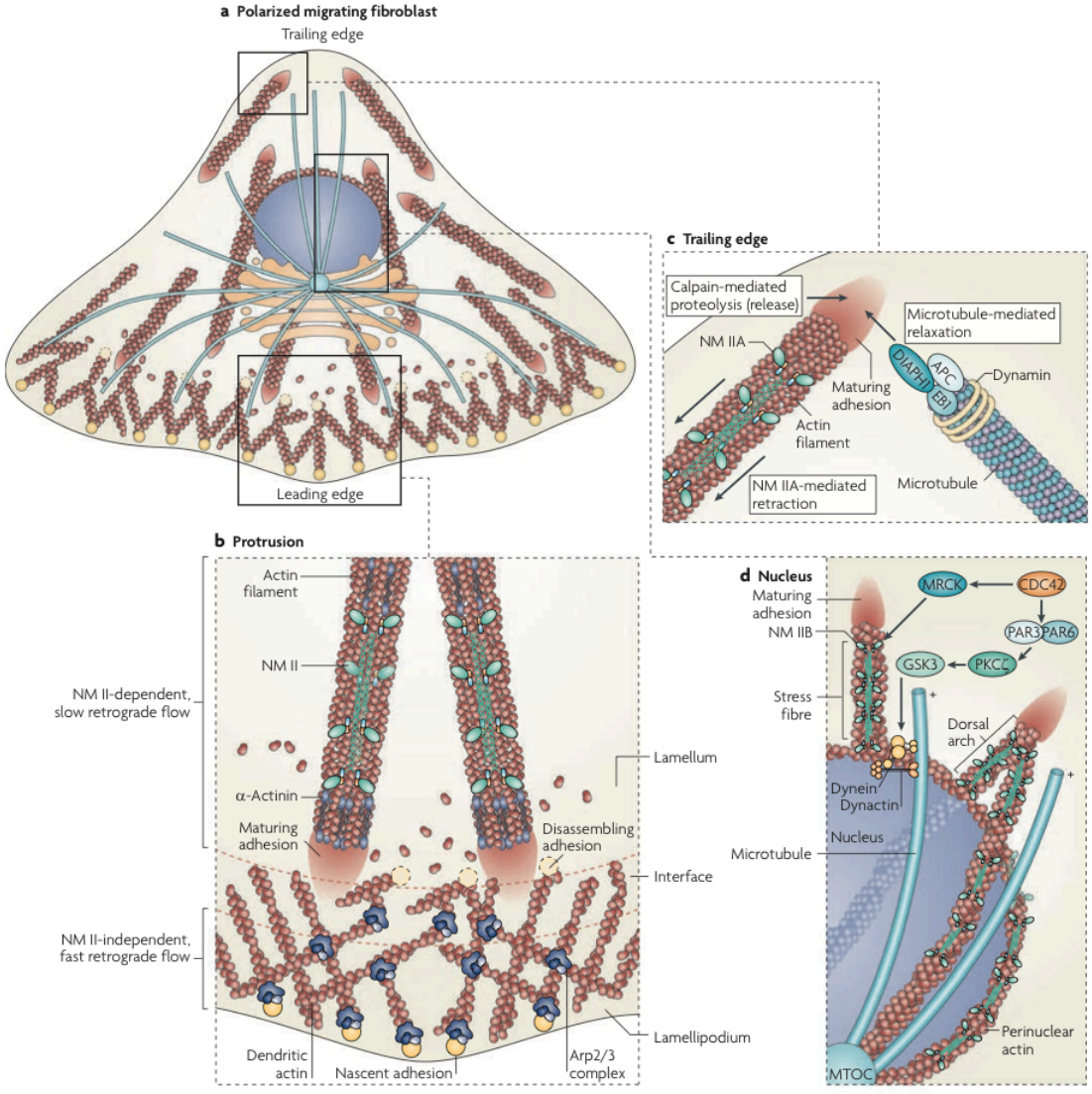

Figure 1 – Schematic of a migrating fibroblast and cytoskeletal structures related to motility (Vicente-Manzanares, Ma, Adelstein, & Horwitz, 2009)

Fibroblasts are derived from the mesoderm and make up the connective tissue that provides support in our bodies (Tarin & Croft, 1969). One of the main functions of fibroblasts is to secrete the extracellular matrix (ECM) (Leiss, Beckmann, Giros, Costell, & Fassler, 2008). The ECM is a complex, three-dimensional web of secreted proteins and glycosaminoglycans that gives structural support to the cells embedded within it. Furthermore, ECM proteins elicit outside-in signaling events in cells, thereby modulating cellular behavior (Leiss, Beckmann, Giros, Costell, & Fassler, 2008). Different ECM proteins, such as fibronectin and collagen, trigger distinct events in cells, particularly related to their motility (Kostic, Lynch, & Sheetz, 2009).

Fibroblast motility is a well-studied phenomenon, with certain aspects seen in other cell types (Kostic & Sheetz, 2006) (Kostic, Sap, & Sheetz, 2007). That said, studying the motile processes of this cell type is an enormous and somewhat daunting task since cells do not exhibit all of their motile processes in any convenient time period for *in vivo* observation. Indeed, cell motility is often thought of as a modular process (Dobereiner, 2005), with certain modules used only in response to very specific, and sometimes rare, stimuli. Modules used only in healing a wound, for example, would never be seen while observing an unwounded organism. Likewise, modules used only in the early stages of development or activated during neoplastic growth would also be difficult to observe. Before discussing these modules further, an overview of the relevant cellular structures is required.

1.3 – Fibroblast architecture

In the same way that the skeletal system provides structure and support for our bodies, the cytoskeleton provides structure and support for cells. However, unlike our skeletal system, the cytoskeleton is a highly dynamic structure that responds to intracellular and extracellular cues. Three of the main functions of the cytoskeleton are intracellular trafficking, cellular stability, and cell motility. As such, the fibroblast cytoskeleton has three subsystems that roughly correlate with these functions: microtubules, intermediate filaments, and microfilaments (though, to be clear, due to the high level of interdependence between these systems, discussed in section 1.12, it is difficult to assign a unique function to any one cytoskeletal element).

Microtubules (MTs) are highly dynamic, hollow, tube-like polymers of α- and β-tubulin heterodimers that serve a number of important roles in the cell, including acting as a platform for intracellular transport, forming the mitotic spindle, providing structural support, and functioning in motility (Nogales, 2000). MTs are seeded by α-β tubulin heterodimers (Weisenberg, Borisy, & Taylor, 1968) that arrange end-to-end to form linear protofilaments. 13 protofilaments arrange around a central axis, resulting in a tubular structure (Desai & Mitchison, 1997). The MT (+) end refers to the β-tubulin-capped end while the (-) end refers to the α-tubulin-capped end. Both α- and β-tubulin bind GTP, but only the GTP on β-tubulin is hydrolysable (Weisenberg, Deery, & Dickinson, 1976). The term "dynamic instability" describes the assembly and disassembly mechanisms of MTs (Mitchison & Kirschner, 1984). GTP-loaded tubulin adds to the growing (+) end, but shortly after incorporation into the MT, GTP is hydrolyzed to GDP. The kinetics of GDP-tubulin favor depolymerization, but GDP-tubulin cannot be removed from a MT unless it is at the (+) end. Therefore, unless GTP-

tubulin has subsequently added onto the (+) end, a cycle of depolymerization will be initiated, usually referred to as a catastrophe (Figure 2).

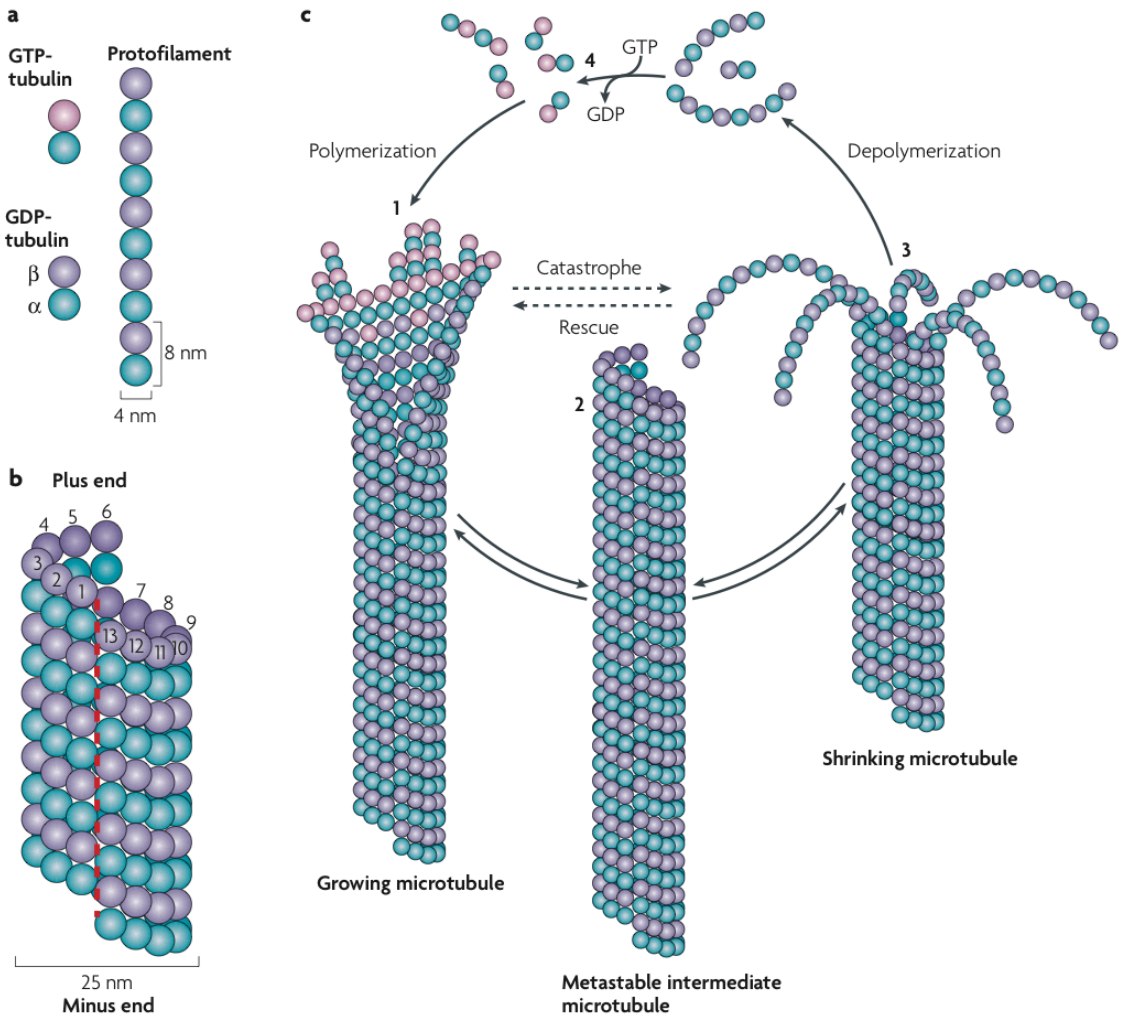

Figure 2 – Schematic of microtubule dynamics (Akhmanova & Steinmetz, 2008).

Intermediate filaments (IFs) are less dynamic structures than MTs, that are classically thought to provide the cell with structural support and resilience against outside forces (Helfand, Chang, & Goldman, 2003). There are two distinct IF networks in cells, one nuclear, and one cytoplasmic (Herrmann & Aebi, 2004). The nuclear IF network makes up the nuclear lamina that supports the inner nuclear membrane (Gruenbaum, Margalit, Goldman, Shumaker, & Wilson, 2005). The cytoplasmic IF

network connects the nuclear membrane with peripheral adhesive structures that function to create a stable link between cells and their surroundings. Similar to MTs, cytoplasmic IFs play a role in motility as well. In humans, IF proteins are encoded by over 65 genes and grouped into five types based on sequence homology (types 1-5) (Fuchs & Weber, 1994) (Herrmann, Bar, Kreplak, Strelkov, & Aebi, 2007). They are also diverse between cell types, including keratins and desmins in epithelial and muscle cells, respectively (Herrmann, Bar, Kreplak, Strelkov, & Aebi, 2007). However, for the purposes of this thesis and fibroblasts in particular, further discussion of IF proteins will focus on another IF protein, vimentin.

Microfilaments, comprised mainly of actin, are highly dynamic polymers that provide structural support as well as drive cell motility via actin polymerization against the cell membrane (Insall & Machesky, 2009). Actin polymerization is an extremely complicated process involving several actin-binding partners that function in nucleation of filamentous actin (F-actin) from globular actin (G-actin), sequestration of G-actin,

filament elongation, capping, and severing, as well as branching and bundling (Figure 3).

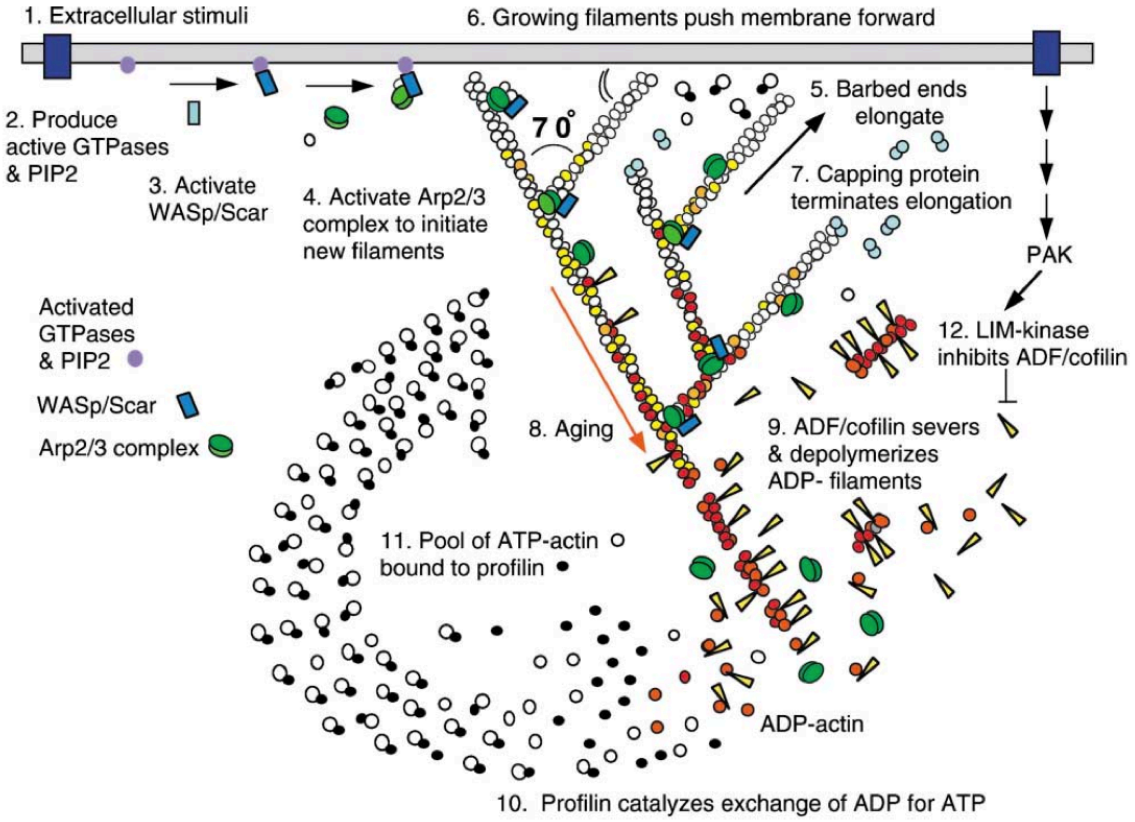

Figure 3 – Mechanisms and proteins involved in actin-driven membrane protrusion (Pollard & Borisy, 2003)

In brief, actin polymerization proceeds through the three phases known as lag, elongation, and steady-state. In the lag phase, G-actin monomers assemble into unstable, short oligomers. After reaching a threshold length, the elongation phase begins at both ends of the filament. Finally, in the steady-state phase, G-actin continues to add onto F-actin, but the total mass of F-actin does not change. G-actin concentration plays a central role in this process. For each end of a filament, a critical concentration exists below which elongation does not take place. The end with the lower critical concentration is referred to as the (+) end while the other is the (-) end. At a certain G-actin concentration intermediate between the critical concentrations of the (+) and (-) ends, G-actin is added onto the (+) end at the same rate as it dissociates from the (-) end. The result is a

"treadmilling" filament that displaces, but never changes in length. This process is the basis of actin polymerization exerting an outward force on the cell membrane (Pollard & Borisy, 2003) (Pollard, 1986). Actin microfilaments can also serve as a platform through which other proteins exert force.

1.4 – Force generation

Another critical aspect of cell motility is force generation on the external environment. The field of cell motility is rife with examples of cells using forces to explore and probe their environment (Ananthakrishnan & Ehrlicher, 2007). For example, as alluded to above, actin polymerization exerts an outward force on a cell membrane under tension to drive cell protrusion (Le Clainche & Carlier, 2008), the cell membrane resists actin polymerization forces with tensile forces directed inward (Gauthier, Fardin, Roca-Cusachs, & Sheetz, 2011), traction forces are exerted on the substrate during cell migration (Oliver, Dembo, & Jacobson, 1995) (Harris, Wild, & Stopak, 1980), and forces associated with rigidity sensing allow the cell to respond to the rigidity of its surroundings (Kostic & Sheetz, 2006) (Kostic, Lynch, & Sheetz, 2009) (Kostic, Sap, & Sheetz, 2007). In fibroblasts, the majority of forces are exerted through myosins (Cai, et al., 2010). Myosins comprise a large family of ATP-dependent motor proteins that associate with actin (Sweeney & Houdusse, 2010). In fibroblasts, myosin II is the predominant isoform involved in force generation on the ECM (Vicente-Manzanares, Ma, Adelstein, & Horwitz, 2009). Three pairs of polypeptides make up non-muscle myosin II: two heavy, two regulatory light and two essential light chains. In mammals, three heavy chain genes *myh9*, *myh10* and *myh14* form myosin IIa, IIb and IIc, respectively.

Upon ATP hydrolysis, the head domains of myosin heavy chain produce what is referred to as a power stroke, in which myosin II pulls on its associated actin microfilaments and generates contractile forces. To migrate, a cell must be able to exert contractile forces on a stable substrate, and for this, a cell must form connections with the substrate.

1.5 – Focal adhesions

The fluid lipid bilayer known as the cell membrane determines the cellular volume, defining the cell interior and exterior. The cell membrane also integrates a number of polysaccharides and proteins that allow communication between interior and exterior cellular regions. For the purposes of this thesis, cells connect to a substrate through focal adhesions (other connections exist, such as tight junctions and hemidesmosomes in epithelial layers, but they will not be a focus of this work). Focal adhesions are large, dynamic multimolecular plaques that mature from smaller, punctate, focal contacts (Geiger & Bershadsky, 2001). In the context of fibroblast cell motility, focal adhesions connect to the aforementioned ECM proteins coating the substrate, sometimes eliciting different cellular responses depending on the type of ECM protein (Kostic, Lynch, & Sheetz, 2009). Within focal adhesions, integrins are the primary molecular connections between the cell and ECM proteins (Miranti & Brugge, 2002). Integrins are heterodimeric transmembrane proteins that interact with ECM proteins at the cell exterior and cytoskeletal mediator proteins, like talin and filamin (Fln), inside the cell (Kiema, et al., 2006). These mediator proteins connect focal adhesions to the actin cytoskeleton, allowing forces generated within the cytoskeleton to be transmitted through focal adhesions, to the substrate (Fournier, Sauser, Ambrosi, Meister, & Verkhovsky,

2010). Overall, more than a hundred proteins are associated with focal adhesions at some point in the lifetime of an adhesion (Figure 4) (Zaidel-Bar, Itzkovitz, Ma'ayan, Iyengar, & Geiger, 2007).

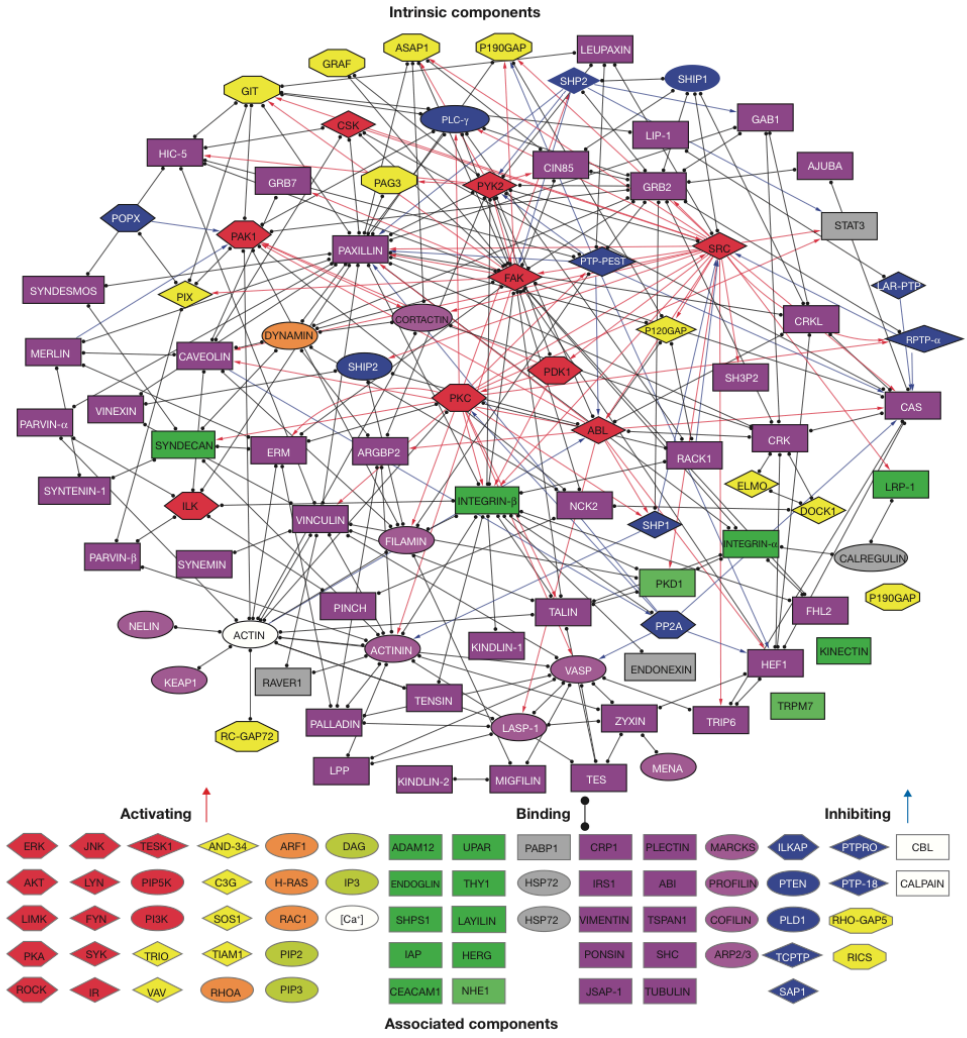

Figure 4 – Focal adhesion proteins are numerous and promiscuous in their binding (Zaidel-Bar, Itzkovitz, Ma'ayan, Iyengar, & Geiger, 2007)

Having covered the general terminology and basic components behind cell motility and fibroblast behavior, the remainder of this section delves deeper into the focal points of this thesis.

1.6 - Fibroblast Spreading

As discussed previously, cell motility is a modular process (Dubin-Thaler, et al., 2008). Certain modules are common between cell types, making information gathered from model systems relevant to other, more specialized systems (rigidity sensing mechanisms discovered in fibroblasts were also found to be relevant in neurons) (Kostic & Sheetz, 2006) (Kostic, Sap, & Sheetz, 2007). On the other hand, some modules can only be observed at specific time points in an organism's life cycle, making a comprehensive study of cell motility onerous. To address this difficulty, our lab and others developed fibroblast spreading assays with high spatial and temporal resolution in two dimensions (Dubin-Thaler, Giannone, Dobereiner, & Sheetz, 2004). Fibroblast spreading assays involve dropping a suspension of fibroblasts onto cover slips coated with ECM proteins and allowing them to spread (see Figure 17A). ECM proteins help replicate an *in vivo*-like environment, since fibroblasts naturally secrete these proteins. *In vivo,* fibroblasts experience integrin-ECM interactions involving a number of ECM proteins, complicating efforts to isolate that aspect of the system. Furthermore, *in vivo* motility assays suffer from low resolution that is not appropriate for answering certain questions, for example, how proteins stretch in the cell (discussed later in section 4.2). Three-dimensional (3-D) motility assays suffer from similar issues (Harunaga & Yamada, 2011). Two-dimensional (2-D) spreading assays, on the other hand, offer high spatial and temporal resolution and greater control over experimental conditions (Dobereiner, 2005). In addition, spreading assays give researchers greater control over the outside-in signaling experienced by the cell. Of course, any 2-D assay designed to replicate an *in vivo* environment will fall short in some aspects, as cells are known to behave in

completely different ways in response to 2-D and 3-D environments (Cukierman, 2001). That said, cells only have a set number of motility modules, and while the manner in which the modules are utilized may differ from 2-D to 3-D, the 2-D system still showcases the modules in a cell's motility arsenal.

Early studies of fibroblast spreading assays led to yet another reason to use these assays to study motility. Dobereiner and colleagues, among others, observed that fibroblast spreading is a predictable process that allows the observation of most motility modules in under an hour (Dobereiner, 2005). Any differences that arise as a result of genetic manipulations or chemical treatments can therefore by readily assessed, no matter which motility module they relate to (Zhang, Jiang, Cai, Monkley, Critchley, & Sheetz, 2008).

1.7 – Phases of fibroblast spreading

A wild-type fibroblast undergoes cell spreading in a predictable, highly reproducible manner. When a fibroblast in suspension contacts an ECM-coated surface, the cell starts by "tiptoeing" on the surface, essentially touching down in some regions and lifting up in others (Ryzhkov, Prass, Gummich, Kuhn, Oettmeier, & Dobereiner, 2010). This is generally regarded as an exploratory phase preceding the basal phase, or phase 0 (P0), of spreading (Dobereiner, Dubin-Thaler, Giannone, Xenias, & Sheetz, 2004). During P0, the cell determines the chemical suitability of the substrate and shows little to no signs of an increase in spread area. If appropriate molecules (such as ECM proteins) are present at the correct concentrations, the cell begins the P1 stage of spreading. P1 is characterized by the cell achieving the majority of its fully spread area.

As this phase usually lasts between 5-10 minutes, it is sometimes referred to as the fast spreading phase. Expansion of the spread area during P1 primarily involves actin polymerization at the leading edge of the cell exerting force on the cell membrane, causing the cell to expand outward (Dobereiner, Dubin-Thaler, Giannone, Xenias, & Sheetz, 2004). Observing this process is similar to watching pancake batter spreading in a fry pan. Punctate focal contacts begin to form during this stage as well. Because the cell membrane is, at least initially, of a constant area, expansion necessarily leads to the cell eventually reaching the maximum of its supply of membrane area. This causes an increase in membrane tension (forces directed inward by the membrane) (Gauthier, Fardin, Roca-Cusachs, & Sheetz, 2011). Put simply, as the cell spreads to a greater area, its membrane begins to become taut.

The next phase of fibroblast spreading is P2, often referred to as the contractile phase. During P2, the cell continues spreading, but intermittently, between cycles of myosin contraction (Giannone, et al., 2007). These contractions serve a number of purposes. For one, they allow cell membrane area to increase via exocytosis (membrane-bound intracellular vesicles add to membrane area by fusing with the cell membrane and releasing their contents) (Gauthier, Rossier, Mathur, Hone, & Sheetz, 2009). They also allow the cell to sense the physical properties of the surface. Surface conformation (Mathur, Moore, & Sheetz, 2012) and rigidity have the capacity to affect cell motility (Kostic & Sheetz, 2006) (Kostic, Lynch, & Sheetz, 2009) (Kostic, Sap, & Sheetz, 2007), just as chemical composition of the surface does (Weiss, 1958) (Curtis & Wilkinson, 1997). Since the cell is no longer continuously spreading, this phase is sometimes referred to as slow spreading.

Importantly, significant traction forces are generated in P2 (Cai, et al., 2010), which of course require a physical link between the cell and the substrate. To accomplish this, the aforementioned punctate focal contacts enlarge and mature into focal adhesions, yielding strong, stable connections to the surface that can withstand high levels of force generated intracellularly by myosin II.

1.8 – Adhesion maturation and disassembly

Mature focal adhesions can experience binding of more than 100 different proteins during their lifetime (Zaidel-Bar, Itzkovitz, Ma'ayan, Iyengar, & Geiger, 2007). The evolution of a focal contact to a focal adhesion is a complex process involving a number of these proteins, but its essence can be broken down into a series of steps (Figure 5).

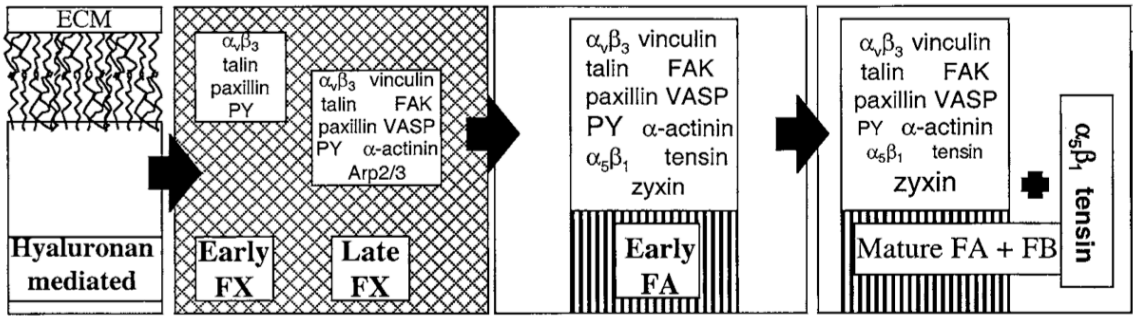

Figure 5 – Schematic showing the stages of focal adhesion maturation and proteins associated with each stage (FX = focal contact, FA = focal adhesion, FB = fibrillar adhesion (Zaidel-Bar, Cohen, Addadi, & Geiger, 2004)

First, during P1, hyaluronan-mediated contacts form between the cell and the ECM-coated surface. Hyaluronan is a glycosaminoglycan found in the plasma membrane of

cells. Hyaluronan-mediated contacts are transient and last on the order of tens of seconds (Zaidel-Bar, Cohen, Addadi, & Geiger, 2004).

Following establishment of a hyaluronan-mediated contact, additional proteins are recruited to the contact region, qualifying it a focal contact, by definition. Focal contact-associated proteins include integrin heterodimers αV-β3, integrin-cytoskeleton mediator proteins talin, vinculin, and α-actinin, the scaffolding protein paxillin, and the signaling protein focal adhesion kinase (FAK) (Zaidel-Bar, Cohen, Addadi, & Geiger, 2004). In fact, both focal contacts and focal adhesions contain integrin-binding proteins, actin-binding proteins, and scaffolding proteins that are arranged in a hierarchical manner. (Figure 6) (Kanchanawong, et al., 2010).

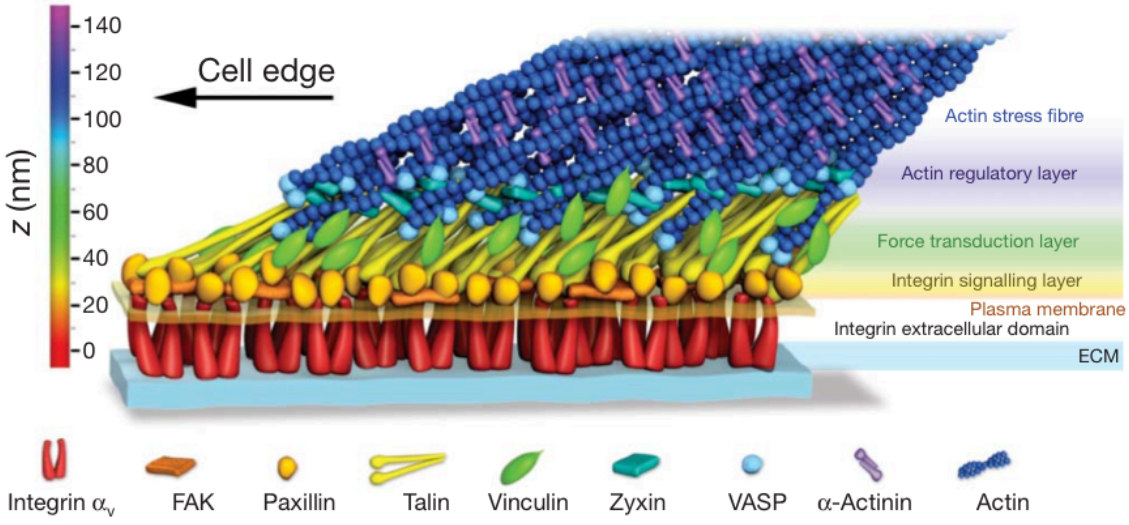

Figure 6 – Hierarchical assembly of focal adhesions away from the ventral surface of the cell. (Kanchanawong, et al., 2010)

During P2, focal contacts become focal adhesions and disassemble. Again, this transformation reflects recruitment of various proteins. In this case, proteins such as the adaptor protein zyxin define the structure.

Another aspect of focal adhesions is their disassembly. Focal adhesion disassembly is accomplished through proteolysis of adhesion proteins. Specifically, the calcium-dependent protease calpain cleaves talin and filamin, as well as other adhesion proteins like paxillin, vinculin, and zyxin. Importantly, calpain-mediated talin proteolysis is a rate-limiting step in adhesion disassembly (Franco, et al., 2004). Put simply, if talin is not cleaved by calpain, adhesions will not turnover and will instead grow and mature. In terms of size, focal adhesions are larger in area than focal contacts. In fact, adhesion area tends to increase with applied contractile force (Riveline, et al., 2001). Contractile forces applied to adhesions originate from actomyosin structures.

1.9 – Actomyosin structures

Actin microfilaments come together to form several types of structures. In particular, microfilaments can aggregate to form stress fibers and 3-D networks of actin. Stress fibers are one of the primary means that forces are exerted on the surface through focal adhesions. Actin networks give the cell shape and structure. Both actin-based structures are highly dynamic and can contain contractile elements.

Cells generate three types of stress fiber: ventral stress fibers, dorsal stress fibers, and transverse arcs (Figure 7).

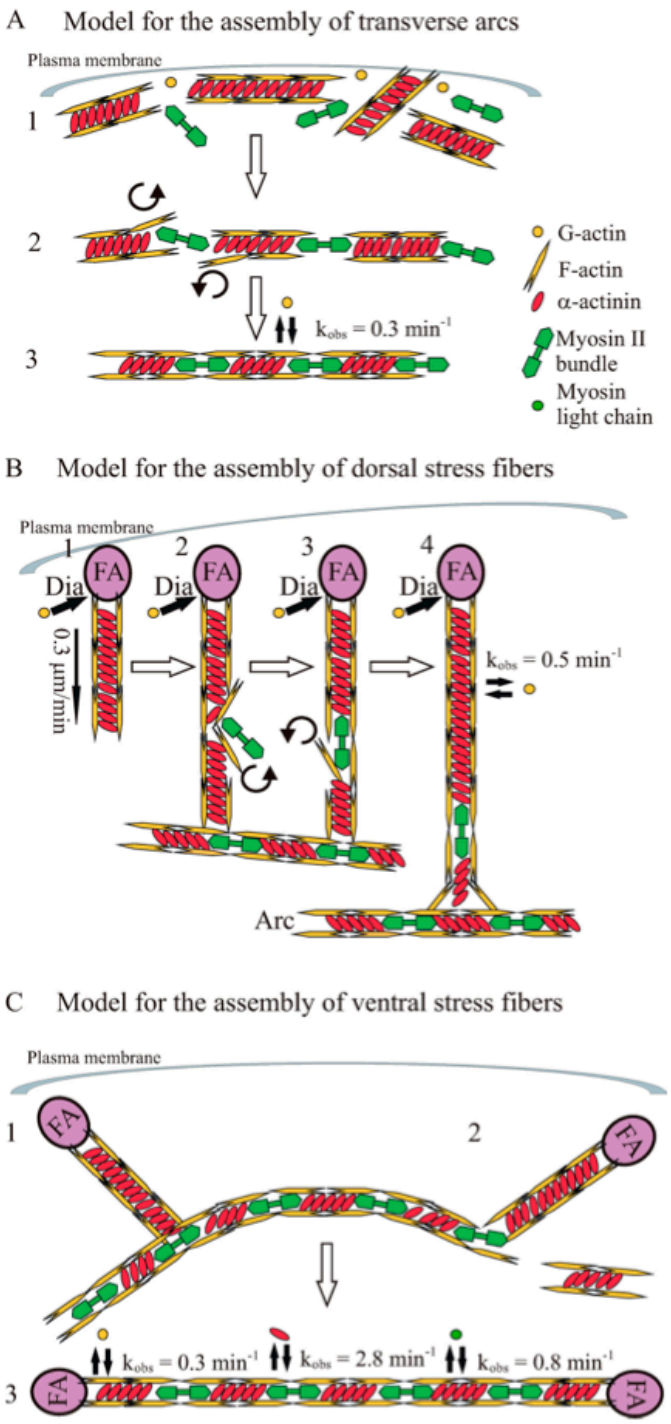

Figure 7 – Stress fiber varieties and assembly mechanisms (Hotulainen & Lappalainen, 2006)

Ventral stress fibers join distant focal adhesions on the ventral surface. Through a combination of cell membrane tensile forces pushing inward on the polymerizing actin network at the cell edge and contractile forces within the network itself, a meshwork of

microfilaments becomes a thick stress fiber known as a transverse arc. Transverse arcs flow rearward, toward the cell center, in a process known as retrograde flow. Once close to the cell center, transverse arcs accumulate and surround the endoplasm, the organelle-rich, central region of the cell (covered in section 1.13).

Dorsal stress fibers initiate at focal adhesions and extend from the ventral surface of the cell toward the dorsal surface. Dorsal stress fibers connect at actin-rich nodes with the transverse arcs accumulated around the endoplasm. In this way, forces generated by myosin anywhere within connected transverse arcs and dorsal stress fibers will be transmitted to the surface (Hotulainen & Lappalainen, 2006).

All of these structures originate from three-dimensional actin networks that require supporting proteins to "prop up" the network. In fibroblasts, this role is filled by Flns.

1.10 – Filamins

Flns have been implicated in numerous aspects of cellular shape and motility. Flns are ~280 kDa, ~80 nm long protein monomers consisting of an N-terminal actin-binding domain followed by 24 IgG-like domains that have the ability to homo- and heterodimerize (Hartwig & Stossel, 1975) and support the formation of three-dimensional actin networks (Hartwig & Shevlin, 1986) (Gorlin, et al., 1990) (Takafuta, Wu, Murphy, & Shapiro, 1998) (Flanagan, 2001) as well as affect membrane-cytoskeleton interactions (Cunningham, Gorlin, & Kwiatkowski, 1992) (Stossel, et al., 2001) (Figure 8) .

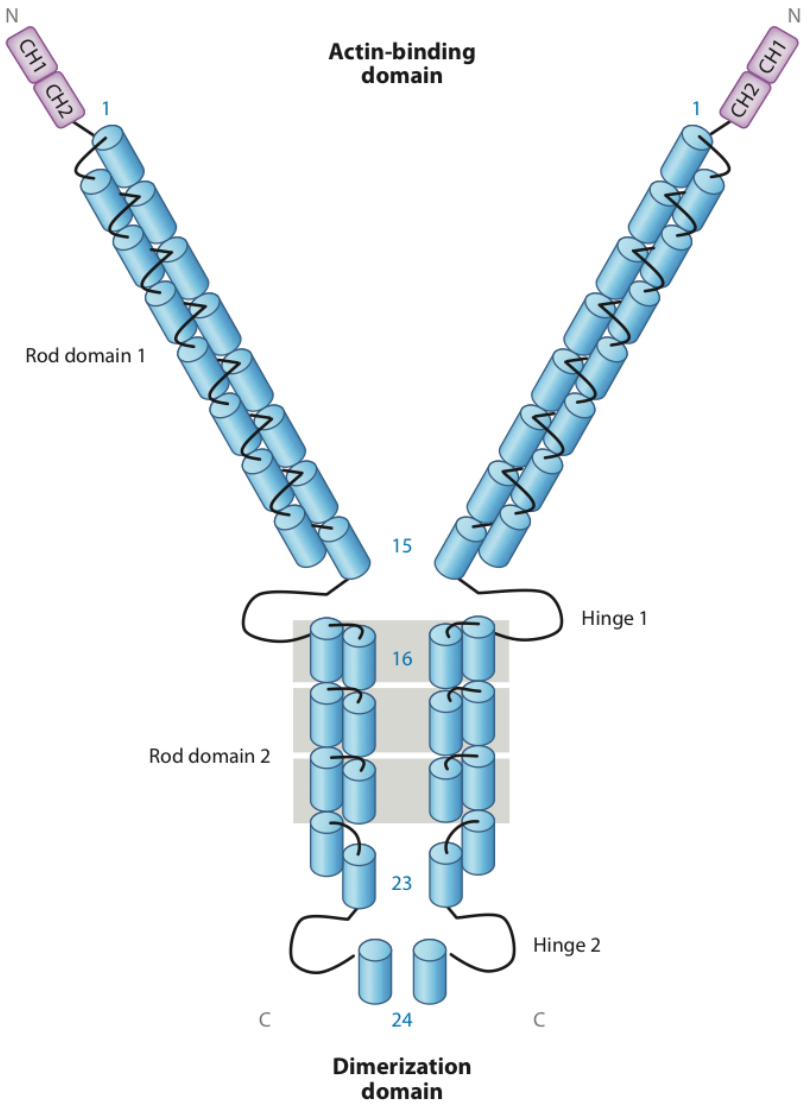

Figure 8 - Schematic showing domain structure of filamin (CH = calponin-homology) (Razinia, Makela, Ylanne, & Calderwood, 2012)

FlnA and FlnB are the two major Fln isoforms expressed in fibroblasts (Stossel, et al., 2001), representing ~90% of total Fln levels (Baldassarre, Razinia, Burande, Lamsoul, Lutz, & Calderwood, 2009). Recent rheological studies on Fln/actin gels have determined that Flns enable a high degree of resilience in actin networks (Kasza, et al., 2009) (Schmoller, Lieleg, & Bausch, 2009), giving the cell the ability to form relatively soft actin networks at low Fln concentrations and bundle stress fibers at high Fln

concentrations (Tseng, An, Esue, & Wirtz, 2004) (Esue, Tseng, & Wirtz, 2009). Flns also bind to integrins (Sharma, Ezzell, & Arnaout, 1995) (Loo, Kanner, & Aruffo, 1998) . In fact, both Fln and the integrin-cytoskeleton mediator protein talin bind to overlapping sites on integrins, and integrin phosphorylation can serve to modulate both talin and Fln binding (Kiema, et al., 2006) (Takala, et al., 2008).

While FlnA knockout mouse embryonic fibroblasts (MEFs) have shown minimal motility defects (Feng, et al., 2006), numerous studies on the FlnA-deficient M2 melanoma cell line have found extensive blebbing and motility-related defects (Cunningham, Gorlin, & Kwiatkowski, 1992) (Flanagan, 2001), malformed actin architecture (Flanagan, 2001), and the inability to sense external rigidity (Byfield, et al., 2009) and control cellular stiffness (Kasza, et al., 2009). Additionally, Fln mutations can cause periventricular nodular heterotopia (PVNH) in humans, reflecting neuronal motility deficiencies (Fox, et al., 1998). On the other hand, FlnB -/- MEFs have been reported to have motility defects and disrupted actin architecture (Zhou, et al., 2007). Importantly, there is high homology between Fln isoforms (Stossel, et al., 2001), and they appear to compensate for each other (Baldassarre, Razinia, Burande, Lamsoul, Lutz, & Calderwood, 2009).

Clearly, Flns have a dramatic impact on the actin cytoskeleton. Importantly, they also link the actin cytoskeleton to the IF cytoskeleton by interaction with the IF protein vimentin.

1.11 – Vimentin

Vimentin is to IFs as actin is to microfilaments. Vimentin is one of many proteins that make up IFs, however in mesenchymal cells, vimentin is the primary IF precursor (Mendez, Kojima, & Goldman, 2010). Structurally, vimentin is a type 3 IF protein composed of globular head and tail domains connected by an α-helical rod domain (Figure 9).

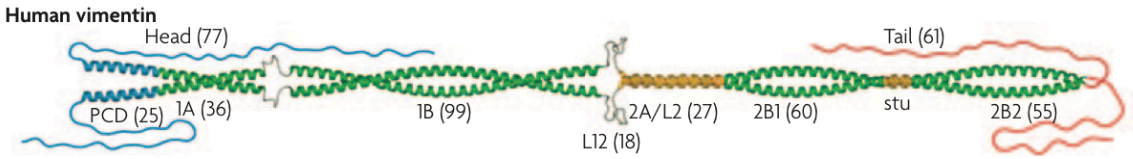

Figure 9 - Ribbon structure of vimentin (Herrmann, Bar, Kreplak, Strelkov, & Aebi, 2007)

Vimentin monomers interact in parallel along their rod domains to form coiled-coil dimers. Dimers associate with one another in a staggered, anti-parallel fashion, giving rise to non-polar tetramers. Vimentin tetramers associate laterally to form unit-length filaments, ~ 60 nm-long IFs. Unit length filaments then anneal laterally, forming longer vimentin intermediate filaments (vIFs) (Figure 10) (Herrmann & Aebi, 2004).

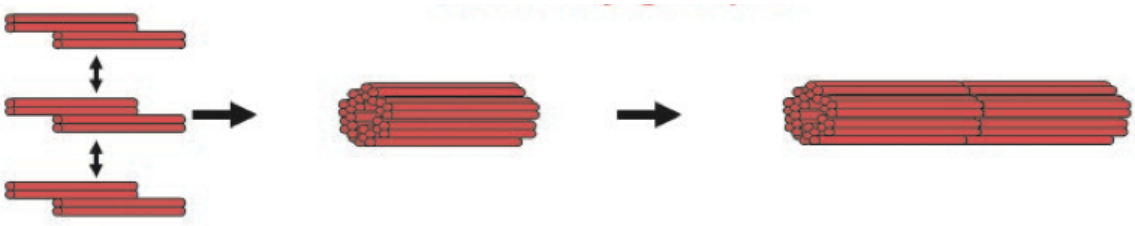

Figure 10 – Intermediate filament formation from tetramers, to unit length filaments, to mature intermediate filaments (Herrmann & Aebi, 2004)

Considering the important role of the IF cytoskeleton, it is surprising that vimentin knockout mice showed no signs of abnormal development (Colucci-Guyon, Portier, Dunia, Paulin, Pournin, & Babinet, 1994). However, upon closer examination,

vimentin knockout mice exhibited numerous defects. For example, vimentin knockouts are prone to renal failure due to a lack of vascular adaptation (Terzi, et al., 1997). In fact, vimentin is crucial in directing the physical responses of the vasculature after changes in blood pressure (Schiffers, et al., 2000) (Davies, Spaan, & Krams, 2005). Loss of vimentin also causes impaired motor coordination and delay of the regeneration of injured dorsal root ganglion neurons (Colucci-Guyon, Gimenez Y Ribotta, Maurice, Babinet, & Privat, 1999). Additionally, expression and distribution of adhesion molecules in lymphocytes is altered upon vimentin loss (Nieminen, Henttinen, Merinen, Marttila-Ichihara, Eriksson, & Jalkanen, 2006). Overall, though its absence is not lethal to an organism, vimentin is critical in diverse cellular processes.

Vimentin's interaction with FlnA is a recent development. Though the specific binding site of vimentin on FlnA has not yet been discovered, co-immunoprecipitation and dot-blot studies have shown that vimentin interacts with FlnA along FlnA domains 1-8 (Kim & McCulloch, 2011) (Kim, Nakamura, Lee, Hong, Perez-Sala, & McCulloch, 2010) (Kim, Nakamura, Lee, Shifrin, Arora, & McCulloch, 2010). Thus, the FlnA-vimentin interaction provides a direct link between the microfilament and IF cytoskeletal systems, though other proteins are known to mediate this type of linkage as well (Fuchs & Karakesisoglou, 2001).

1.12 – Interplay of cytoskeletal systems

Each cytoskeletal system interacts with the others through various mediator proteins. Therefore, perturbations of one cytoskeletal system will likely have consequences for the others (Eckert, 1986). Importantly, interaction of cytoskeletal

systems mediates the positioning of the nucleus and other organelles (Jefferson, Leung, & Liem, 2004) and provides the cell with higher stiffness than any cytoskeletal system alone (Esue, Carson, Tseng, & Wirtz, 2006). Additionally, all three cytoskeletal systems interact with focal adhesions. The actin cytoskeleton affects focal adhesions primarily through the application of force (Ananthakrishnan & Ehrlicher, 2007) (Fournier, Sauser, Ambrosi, Meister, & Verkhovsky, 2010). As discussed previously, forces applied via actomyosin structures stimulate adhesion growth. Notably, IFs and MTs can influence focal adhesions as well. Specifically, IFs have been shown to induce focal adhesion maturation and growth (Tsuruta, 2003) while MTs stimulate degradation of adhesions (Krylyshkina, et al., 2002) (Krylyshkina, et al., 2003).

1.13 – Thesis rationale

In order to better understand the functions of Fln in cell motility, I initially focused on the well-characterized process of cell spreading and polarization (Giannone, et al., 2007) where a standard behavior can be reproducibly observed (Dubin-Thaler, et al., 2008). In that context, I found that a major defect emerged in the spreading of the endoplasm in Fln-depleted MEFs. As mentioned previously, the endoplasm is the central, membranous organelle-rich region of the cell. A second region, the ectoplasm, surrounds the endoplasm and is depleted of organelles due to the presence of a dense actin network (Figure 11) (Nishizaka, Shi, & Sheetz, 2000).

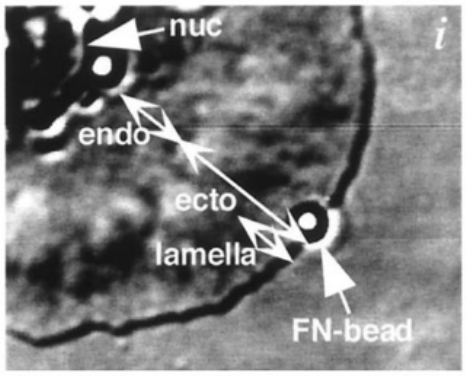

Figure 11 – Differential interference contrast micrograph highlighting the endoplasm and ectoplasm (Nishizaka, Shi, & Sheetz, 2000)

Endoplasmic spreading refers to the flattening and subsequent increase in area of the endoplasm during cell spreading.

Despite hundreds of articles describing the spreading of the cell edge, relatively few have approached the subject of endoplasmic spreading, potentially due to a lack of systems in which endoplasmic spreading is perturbed. With this in mind, I focused on Fln-depleted MEFs in an effort to elucidate other phenotypes associated with defective endoplasmic spreading. Adhesion maturation/growth emerged as a key process in the endoplasmic spreading mechanism, leading us to investigate the role of vimentin intermediate filaments in endoplasmic spreading. Our results implicate all three cytoskeletal systems, as well as focal adhesions, in the spreading of the endoplasm.

Chapter 2 – Filamin Depletion Blocks Endoplasmic Spreading and Destabilizes Force-Bearing Adhesions (Lynch, et al., 2011)

2.1 - Depletion of FlnA in FlnB-/- MEFs Causes a Spreading Defect

FlnA levels were knocked down by transfecting FlnB -/- MEFs with an expression vector for FlnA-targeting shRNA, GFP, and a puromycin resistance sequence. A non-targeting shRNA was similarly expressed as a negative control. GFP-expressing cells transfected with either vector were sorted from untransfected cells by fluorescence activated cell sorting (FACS) and subsequently lysed for Western blot analysis. Cells expressing the FlnA-targeting sequence showed an average of ~75% knockdown when compared to controls (Figure 12A). Additionally, representative immunofluorescence of the GFP-expressing cells with an antibody to FlnA showed an ~ 80-85% depletion of FlnA levels compared to controls in the same field (Figure 12D).

These Fln-depleted MEFs exhibited a spreading defect in that the central organelle-rich region was confined to a smaller area than controls (Figure 12B). Further, the level of knockdown correlated with the level of condensation of the organelle rich region (Figure 12D). The phenotype was rescued by expression of human FlnA-GFP in Fln-depleted MEFs (Figure 12C). Also, Fln-depleted MEFs exhibited a thicker central

region than controls (Figure 12E) by approximately a factor of 2 (Figure 12F).

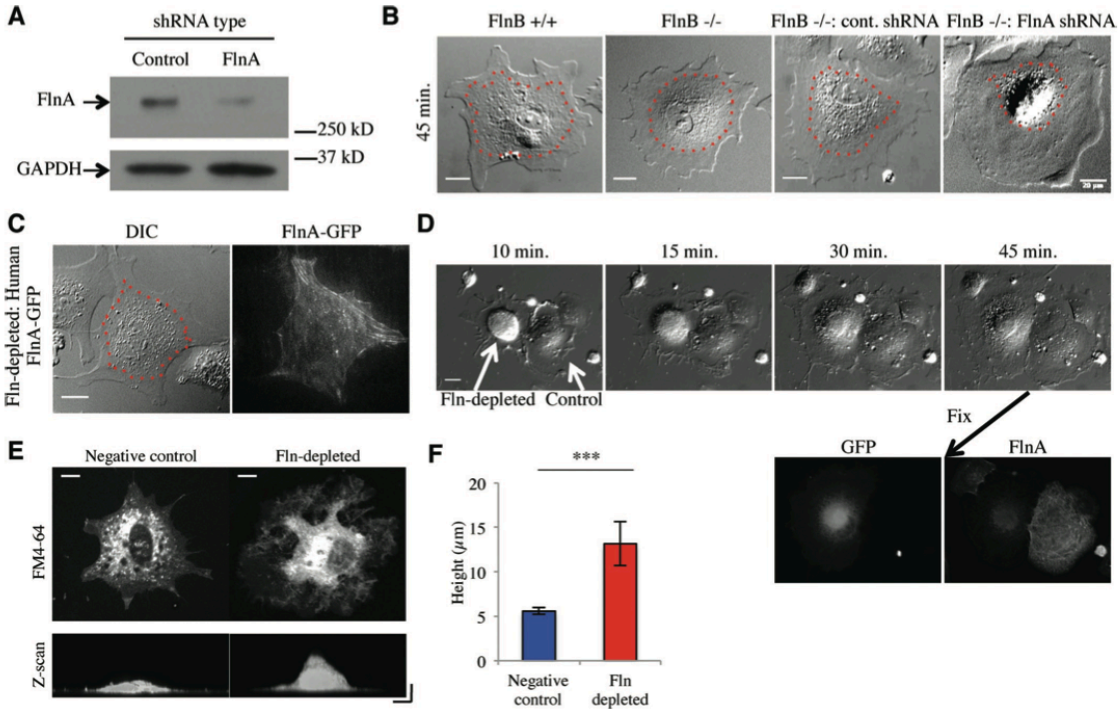

Figure 12 – Fln depletion causes an early endoplasmic spreading defect (Lynch, et al., 2011)

(A) Western blot of FlnB–/– MEFs transfected with nontargeting or FlnA-targeting shRNA vectors expressing GFP sorted from untransfected cells by FACS. FlnA levels were reduced 73% ± 5% (SEM) compared with the control (n = 3). (B) Cell lines were spread on FN-coated glass for 45 min and imaged. Endoplasmic regions are smaller in Fln-depleted MEFs compared with controls. Dotted red lines indicate endoplasmic regions. Scale = 20 μm. (C) Human FL FlnA-GFP rescued the endoplasmic spreading defect when transfected into Fln-depleted MEFs. Scale = 20 μm. (D) Fln-depleted MEFs (cell on left) exhibited an early spreading defect of the endoplasm when spread on 10 μg/ml FN-coated glass. Scale = 20 μm. The cells were fixed and immunostained for FlnA, resulting in correlation of GFP expression with FlnA knockdown and the endoplasmic spreading defect. (E) Fln-depleted and negative control MEFs were plated on 10 μg/ml FN-coated glass for 40 min and fixed. Cells were verified for GFP expression, treated with FM4-64 at 5 μg/ml in PBS for at least 5 min and imaged. Scale = 10 μm. Confocal z-scan along the x-axis of cells shown exhibits disparate thickness of endoplasmic region between Fln-depleted and control MEFs. Scale = 10 μm on both axes. (F) Quantification of cell heights over three separate experiments, at least 15 cells counted for cell type, ***$p < 0.001$, error bars = standard error (SE).

2.2 - Fln Depletion Blocks Spreading of the Endoplasm from the Initiation of Spreading

The spreading defect associated with Fln depletion appeared to be affecting the spreading of the endoplasm, a region previously described as the slightly raised region near the cell center containing the majority of membrane-bound organelles and

surrounded by the ectoplasm, the peripheral region of dense actin arrays that exclude organelles (Nishizaka, Shi, & Sheetz, 2000). However, to confirm the molecular nature of this region I transfected Fln-depleted MEFs and controls with a construct expressing an RFP-tagged endoplasmic reticulum (ER) marker, namely the calreticulin ER targeting sequence and the KDEL retention sequence. Fixation of transfected cells showed a smaller ER area in Fln-depleted MEFs (Figure 13B) compared to controls (Figure 13A).

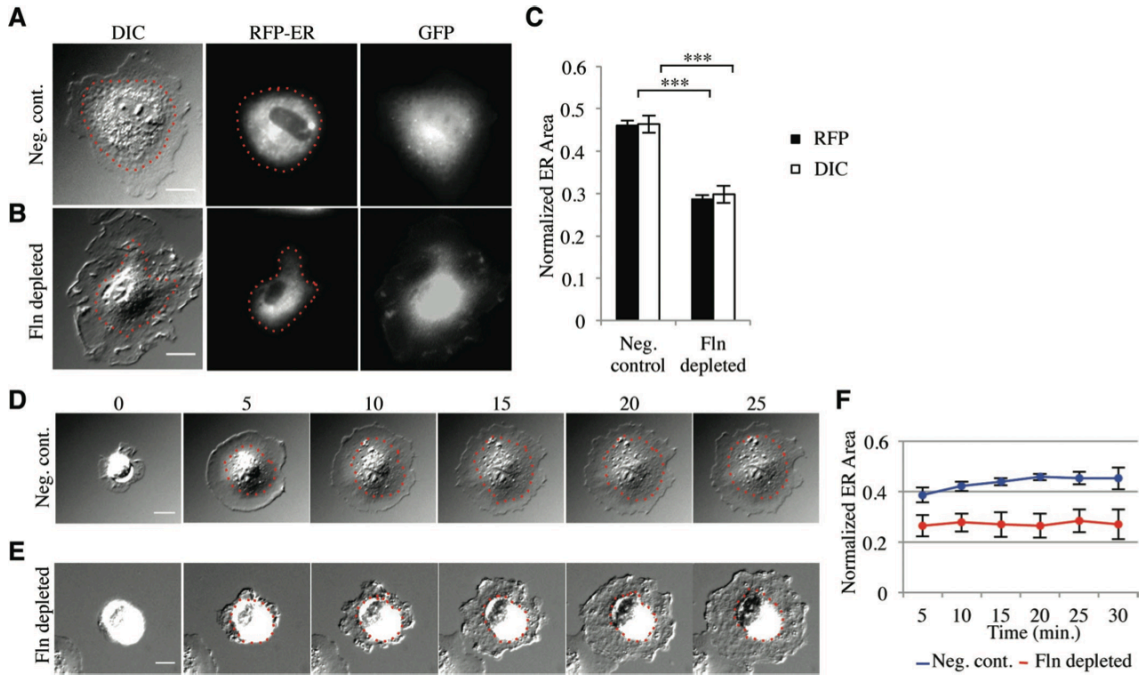

Figure 13 - Fln depletion results in a reduction of ER spread area (Lynch, et al., 2011)

(A) FlnB–/– MEFs transfected with negative control shRNA vector and RFP-ER were plated on FN-coated glass for 30 min and fixed. GFP signal served as a marker for shRNA transfection. Scale = 20 μm. (B) Same as in A, but transfected with FlnA-targeting shRNA. (C) ER area was measured by either RFP signal or DIC and normalized to the whole cell area as measured by DIC (***$p < 0.001$, $n = 44$). (D and E) Time-lapse images of negative control and Fln-depleted MEFs on FN. Scale = 20 μm. (F) Normalized endoplasm area over time ($n = 8$, $p < 0.001$), all error bars = SE.

Because ER area is highly dependent on overall cell area, I measured the ratio of fluorescent ER area to DIC whole cell area to determine the percentage of total area occupied by the ER. Fln-depleted MEFs exhibited an approximately 40% decrease in

normalized ER area compared to controls (Figure 13C), confirming that Fln depletion causes a spreading defect of the ER. Importantly, I observed no significant difference between the area of Fln-depleted MEFs and controls while the difference in ER areas was significant, even before normalization. Additionally, the vesicle-rich endoplasm was measured using video-enhanced DIC and the area of the endoplasm was equal to the area of the ER (Figure 13C), showing that using DIC micrographs alone was suitable for analyzing ER area.

When viewed from early times in spreading, Fln-depleted MEFs often had a particularly granular appearance in the periphery and showed increased ruffling (Figure 13E) when compared to controls (Figure 13D). The endoplasm also failed to spread. Normalized endoplasm areas for Fln-depleted cells were significantly decreased compared to controls independent of the time of spreading (Figure 13F).

2.3 - Microtubules are confined in Fln-depleted MEFs

Because restriction of the ER to the cell center may result from the restriction of microtubules (MTs) (Waterman-Storer & Salmon, 1998), I stained Fln-depleted MEFs with anti-tubulin antibodies after one hour on FN-coated glass (Figure 14A).

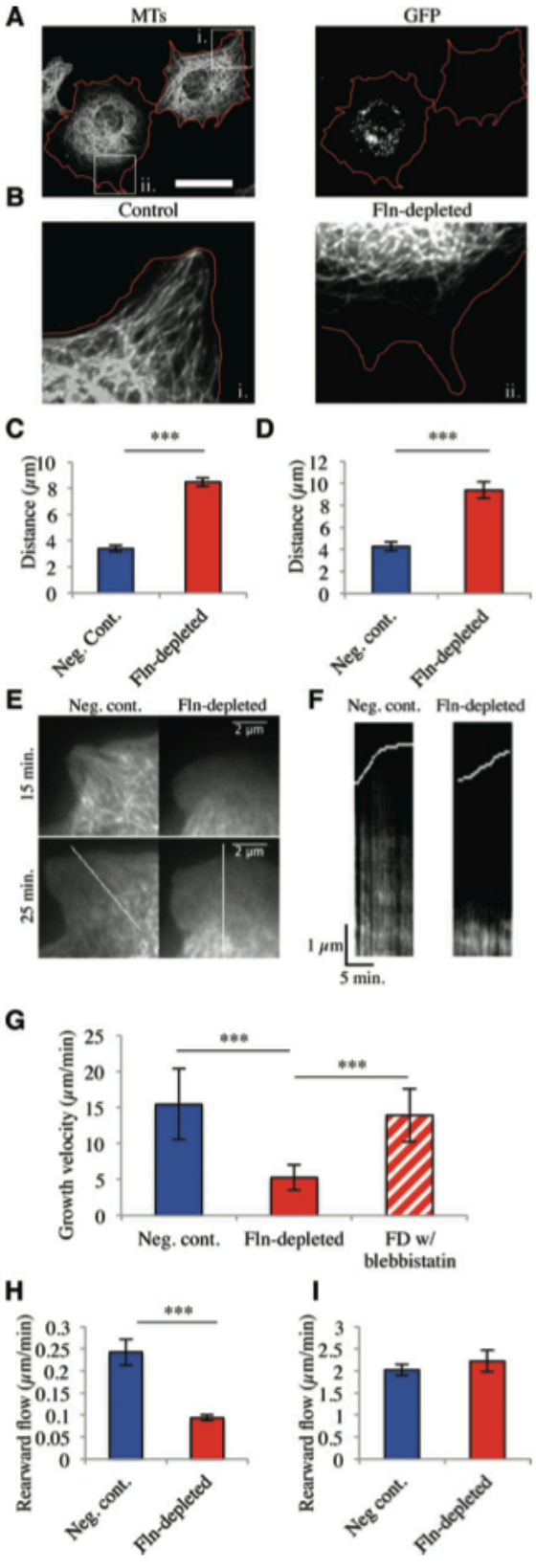

Figure 14 - Fln depletion causes diminished MT extension in spreading MEFs (Lynch, et al., 2011)

(A) FlnB–/– MEFs treated with FlnA shRNA were spread for 1 h on FN-coated glass, fixed, and stained for MTs. GFP-expressing cells were considered transfected and therefore Fln-depleted. Red lines demarcate cell edges. Scale = 50 μm.(B) Enlarged regions from A showing that Fln-depleted MEFs exhibit a larger distance between the MT boundary and the cell edge than do controls. (C) Quantification of distance from MT boundary to cell edge in Fln-depleted MEFs and controls after 15 min of spreading on FN-coated glass measured in TIRF (at least 10 measurements per cell, n = 3) (***p < 0.001). (D) Quantification of distance from MT boundary to cell edge in Fln-depleted and controls after 30 min of spreading on FN-coated glass measured with epifluorescence (at least 10 measurements per cell, n = 33) (***p < 0.001). (E) Fln-depleted MEFs and controls were transfected with 3x-ensconsin-GFP, allowed to spread, and imaged in TIRF. (F) Kymographs taken along white lines from E show a persistently larger distance between the MT boundary and the cell edge in Fln-depleted MEFs compared with controls.(G) Quantification of MT dynamics during the first 30 min of spreading by assessing EB3-RFP growth velocity. Fln-depleted MEFs exhibited slower MT extension than controls (multiple measurements per cell,n = 10 cells) (***p < 0.001), whereas 50 μM blebbistatin treatment rescued this phenotype (multiple measurements per cell, n = 7 cells) (***p < 0.001). (H) Quantification of actin rearward flow velocities by assessing LifeAct-Ruby dynamics from the initiation of spreading. Kymographs of Fln-depleted MEFs showed slower rearward flow than controls (multiple kymographs per cell, n = 6 cells/line) (***p < 0.001). (I) Rearward flow velocities gathered from cells spread for at least 30 min. Fln-depleted MEFs show no significant difference from controls (n = 11 cells/line), all error bars = SE.

MTs in Fln-depleted MEFs were confined to the cell center compared to untransfected cells in the same field (Figure 14B). When the distance between the MT boundary and the cell edge was quantified, the MT boundary was twice as far from the edge in Fln-depleted MEFs as in controls in both TIRF and epifluorescence (Figure 14C, D). To determine if MTs were only partially extending or if they were extending then retracting, I tracked MTs using fluorescent ensconsin (3xEMTB-GFP). MTs were constrained and did not extend to the cell edge from early times (Figure 14E, F).

MT restriction can occur due to either MT stabilization or abnormally rapid actin rearward flow. To determine if MTs had become stabilized, time-lapse observations of EB3-RFP were performed. MTs in the Fln-depleted system exhibited lower growth rates than controls during the first 30 minutes of spreading (Figure 14G). Also, 50 μM blebbistatin treatment rescued Fln-depleted MT growth rates (Figure 14G). Additionally, actin rearward flow rates were measured from spreading initiation and during late spreading (> 30 minutes) using LifeAct-Ruby. Rearward flow rates were significantly

slower in Fln-depleted MEFs at early time points (Figure 14H), while at later times there was no difference between Fln-depleted and controls (Figure 14I).

2.4 - Focal adhesions are small, transient, and unable to support edge extension in Fln-depleted MEFs

MT targeting is believed to be involved in focal adhesion dynamics (Krylyshkina, et al., 2003) (Krylyshkina, et al., 2002) (Kaverina, Krylyshkina, & Small, 1999). Since MTs do not extend to the periphery in Fln-depleted cells, peripheral focal adhesions may also be altered. To test this possibility, Fln-depleted MEFs and untransfected controls were spread for one hour and stained with anti-paxillin antibodies and phalloidin (Figure 15B). Fln-depleted cells exhibited small foci of paxillin accumulation and a disorganized actin cytoskeleton that was deficient in stress fibers compared to untransfected controls in the same field (Figure 15C).

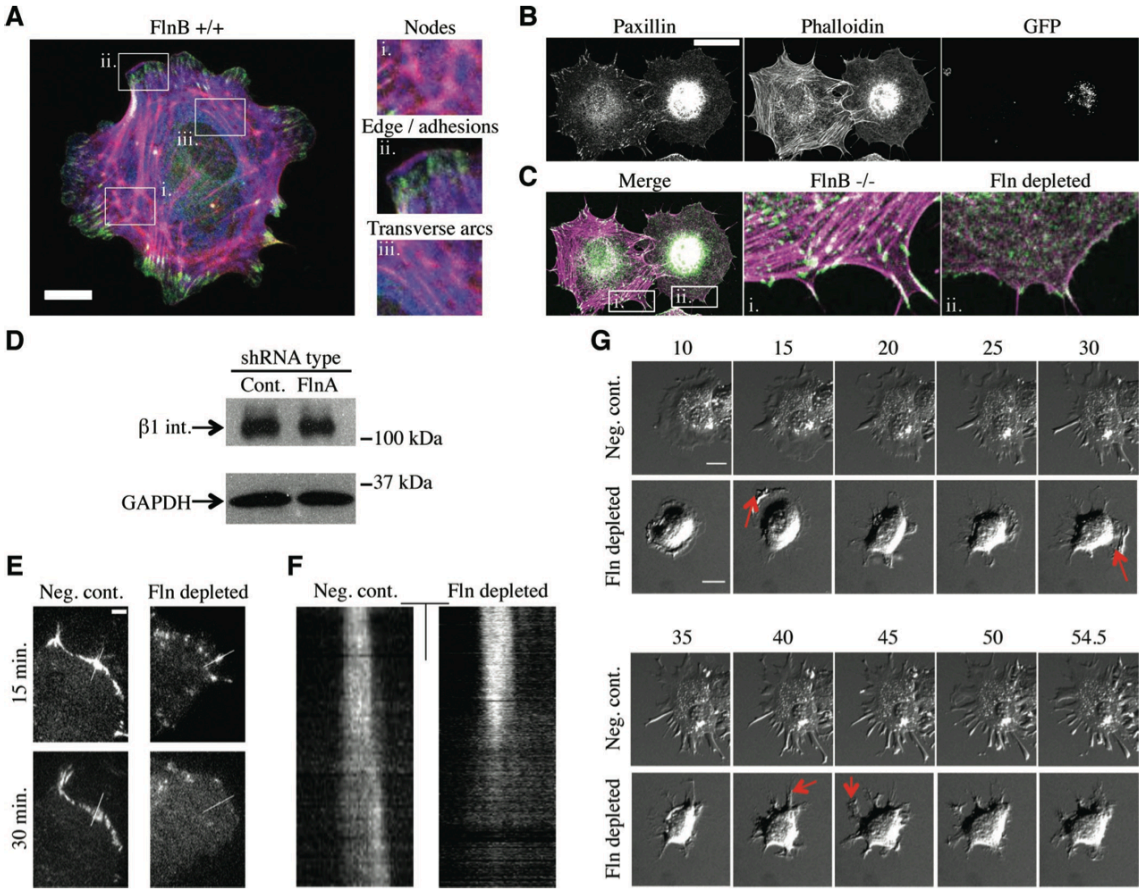

Figure 15 - Fln depletion causes adhesion defects (Lynch, et al., 2011)

(A) Merged confocal sections of FlnB+/+ MEF 30 min after plating on FN-coated glass. Scale = 20 μm; green = paxillin, red = phalloidin, blue = FlnA). Enlarged regions highlight areas of FlnA enrichment, including large nodes at stress fiber junctions, the cell edge, adhesions, and transverse arcs surrounding the endoplasm. (B) FlnB–/– MEFs treated with FlnA shRNA were spread for 1 h on FN-coated glass, fixed, and stained for paxillin and phalloidin. GFP-expressing cells were considered transfected and therefore Fln-depleted. Scale = 50 μm. (C) Merged images of paxillin and F-actin panels show that Fln-depleted MEFs exhibited a highly disorganized, stress fiber-free, actin meshwork surrounding the endoplasm as well as a lack of focal adhesions compared with nontransfected cells. Scale = 50 μm; green pseudocoloring = paxillin, magenta = phalloidin). (D) FlnB–/– MEFs were transfected with nontargeting or FlnA-targeting shRNA expression vectors, sorted by FACS, and lysed. GFP-expressing cells from these populations exhibit no difference in β1 integrin expression. (E) Fln-depleted MEFs and controls expressing paxillin-RFP were spread on FN-coated glass and imaged with TIRF microscopy. Scale = 5 μm.

Since these controls were in fact FlnB -/- MEFs, it was important to examine FlnA localization in wild-type cells. I observed FlnA enrichment in several cytoskeletal structures, including transverse arcs surrounding the endoplasm, nodes of crosslinking connecting mature stress fibers extending above the endoplasm to the transverse arc ring below, as well as at the leading edge and the trailing ends of mature focal adhesions (Figure 15A). The smaller adhesions in Fln-depleted MEFs could be a result of less β1 integrin expression, however this was found not to be the case (Figure 15D).

Because smaller adhesions could be explained by a deficiency in focal adhesion formation or unstable focal adhesions, I transfected Fln-depleted MEFs with paxillin-RFP and found that these cells formed focal contacts, but over time, these contacts were unstable and were disassembled (Figure 15E, F). When the lifetime of the contacts was measured for the Fln-depleted cells after onset of contraction, paxillin-RFP contacts had a much shorter lifetime (~8.5 minutes s.e.m. = 0.05 minutes, n = 45) compared to control adhesions that outlasted the time course of the experiment (> 15 minutes). These results indicated that adhesions in Fln-depleted MEFs are more dynamic than controls. Because this suggests that these adhesions would not be able to support high levels of force, I induced contraction with the MT polymerization inhibitor nocodazole (Kolodney &

Elson, 1995). Fln-depleted MEFs showed more rapid retraction of edge contacts and lamellipodial extensions whereas controls maintained even narrow extensions (Figure 15G).

2.5 - High Forces Are Generated in Fln-depleted MEFs but Rapidly Release

Because unstable focal adhesions could result in defects of force generation, I measured the traction forces of Fln-depleted MEFs using an array of polydimethylsiloxane (PDMS) pillars (Tan, Tien, Pirone, Gray, Bhadriraju, & Chen, 2003) (du Roure, et al., 2005). When Fln-depleted MEFs were spread and imaged on PDMS pillars for ~ 30 minutes, they exhibited more narrow extensions than controls (Figures 16A, B).

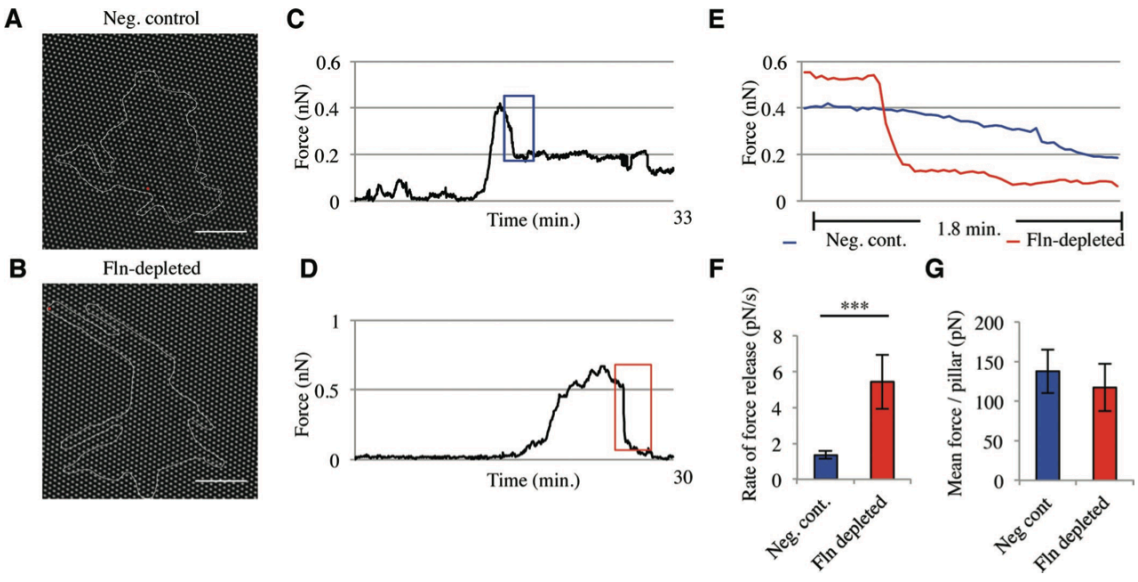

Figure 16 - Fln-depleted MEFs exhibit an inability to sustain large, controlled forces on FN-coated pillars (Lynch, et al., 2011)

(A and B) Fln-depleted MEFs and controls were spread on FN-coated PDMS pillars for ~30 min. Scale = 20 μm.(C and D) Representative traces of single pillar movements tracked over ~30 min of spreading in control (C) and Fln-depleted (D) MEFs (traces taken from pillars marked by a red dot in A and B). (E) Colored regions from C andD reveal rapid force release in Fln-depleted MEFs compared with controls. (F) Average rate of force-release events on pillars. Fln-depleted MEFs exhibited a significantly higher rate of force release compared with controls (5.42 pN/s ± 1.50 pN/s compared with 1.36 pN/s ± 0.21 pN/s, n = 29, ***p < 0.001). (G) Mean force/pillar of Fln-depleted MEFs and controls shows no significant difference in force generation capability (n = 12; >3 experiments), all error bars = SE.

Representative force vs. time traces from single pillar measurements exhibited similar or higher levels of peak force generation (Figures 16C, D), however the release of force occurred at a higher rate in Fln-depleted cells when compared to controls (Figure 16E). In Fln-depleted cells, the average rate of force release was nearly four times that of the control (Figure 16F). Because this behavior could result from impaired traction force generation, I measured whole-cell force generation and found a slightly lower traction force per pillar in Fln-depleted MEFs, but the average value was not significantly different from controls (Figure 16G).

2.6 - FlnA-/- Cells Have Many Characteristics of Fln-depleted Cells

Given the dramatic motility defects in Fln-depleted MEFs, I asked whether these phenotypes could be attributed to either FlnA or FlnB. FlnA -/- MEFs exhibited a weaker ER spreading deficiency than Fln-depleted MEFs (Figure 17A) while FlnB -/- MEFs appeared very similar to controls (Figure 12B). Averaged normalized ER areas of FlnA -/- (Figure 17B) but not FlnB -/- MEFs, were significantly decreased when compared to

controls.

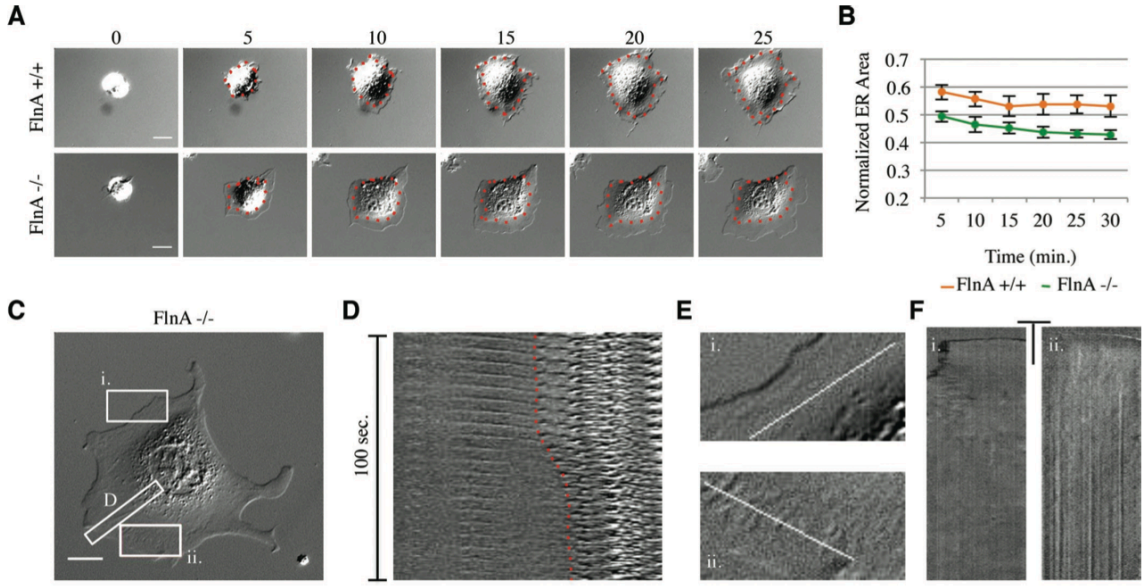

Figure 17 - FlnA is the major Fln isoform involved in endoplasmic spreading defects (Lynch, et al., 2011)

(A) Representative montages of single FlnA+/+ and FlnA–/– MEFs spread for 25 min on FN (red dotted lines demarcate endoplasm regions). (B) Averaged normalized endoplasm areas for each cell line represented in A. Data shown are mean ± SEM (n = 17). Differences were significant throughout the time course ($p < 0.001$, two-way repeated measures ANOVA). (C) FlnA–/– MEF spread on FN-coated glass for 50 min. Scale = 20 μm. (D) Montage of stress fiber demarcated in C. After stress fiber breakage, the endoplasm is contracted rearward as indicated by red dotted line. (E) Enlarged images demarcated in A. Gaps are seen in ii., with a normal, coherent ectoplasm shown in i. for comparison. (F) Kymographs from lines seen in E. Gaps begin to appear 15 min after the initiation of spreading and persist throughout. Scale: 10 μm and 10 min, all error bars = SE.

Also, while FlnA -/- MEFs form stress fibers late in spreading, it was common for them to experience a contraction of the endoplasm that was not seen in controls or Fln-depleted MEFs. This contraction was often associated with stress fiber breakage and the appearance of gaps at the endoplasm boundary of FlnA -/- MEFs (Figure 17C), suggesting that the cytoskeleton network was formed but was not able to sustain force at the endoplasm boundary. Stress fiber breakage was correlated with endoplasm retraction (Figure 17D) and gaps in the cytoplasm were observed at the endoplasm boundary of FlnA -/- MEFs (Figure 17E) during the contractile phase of spreading (Figure 17F).

2.7 - Endoplasmic spreading requires the calpain-cleavability and integrin-binding functions of FlnA

To further understand Fln's role in the Fln-depleted endoplasmic spreading phenotype, Fln-depleted MEFs were transfected with RFP-ER and human full-length (FL) FlnA, calpain-uncleavable FlnA, or FlnA Δ19-21, the latter missing the primary integrin-binding site of FlnA.

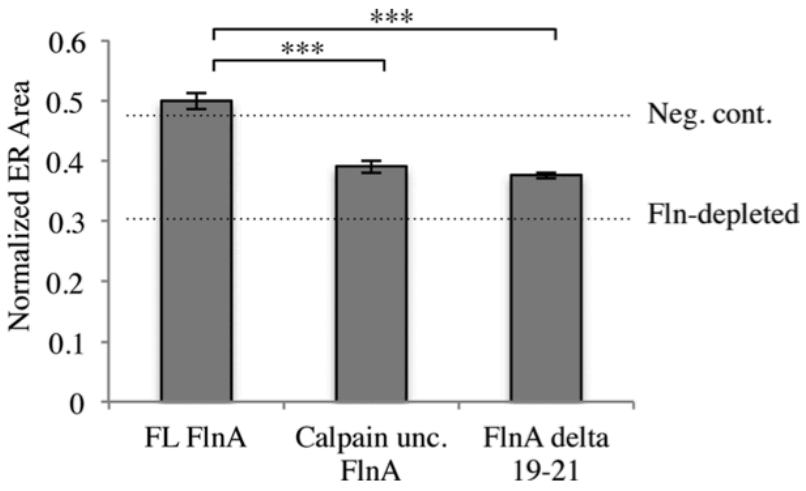

Figure 18 - Calpain cleavability and integrin-binding are FlnA functions critical in the ER spreading phenotype (Lynch, et al., 2011)

Fln-depleted MEFs were transfected with RFP-ER and FL FlnA, calpain-uncleavable FlnA, or FlnA lacking domains 19–21. FL FlnA recovers the ER spreading phenotype to above control levels, whereas calpain-uncleavable FlnA and FlnA lacking domains 19–21 exhibit only partial recovery (n = 36) (***p < 0.001), all error bars = SE.

Normalized ER areas showed complete rescue of endoplasmic spreading upon FL FlnA addition, while calpain-uncleavable FlnA and FlnA Δ19-21 showed only partial rescue (Figure 18), indicating that both integrin binding and calpain cleavage play significant roles in Fln organization and function.

2.8 - Summary and Discussion

Although previous studies of Fln isoform knockouts or mutants show interesting phenotypes (Cunningham, Gorlin, & Kwiatkowski, 1992) (Feng, et al., 2006) (Zhou, et al., 2007), the depletion of multiple Flns shows a novel phenotype that has, as yet, not been ascribed to the loss of Flns: namely a deficiency in endoplasmic spreading. When the spreading of the endoplasm and ectoplasm is coupled, endoplasm area stabilizes at 50-60% of total cell area in controls (Figure 17B). The Fln-depleted deficiency in endoplasmic spreading results in a reduction of endoplasmic area to ~30% of total cell area (as assessed by a fluorescent ER marker) (Figure 13F) and is associated with a significant decrease in MT extension rate (Figure 14G). In addition, Fln-depleted cells lack stress fibers and have very dynamic adhesions (Figure 15B, C, E, F). Although the traction forces generated by Fln-depleted cells are only slightly lower than control cells (Figure 16G), the rate of loss of tension is dramatically higher indicating that Fln is important for maintaining mechanical forces on adhesions (Figure 16F). These changes are consistent with a role for Fln in stabilizing the actin cytoskeleton under force.

Since the ER typically spreads along MTs, it is expected that the MT arrays are condensed in Fln-depleted cells (Figure 14). This condensation was found to be partially due to the fact that MTs have lower extension rates in Fln-depleted MEFs than in controls (Figure 14G). Another possibility that has been shown previously (Terasaki & Reese, 1994) is that MT condensation could be a result of high rates of actin rearward flow preventing extension to the periphery. However, rearward cortical actin flow rates were actually lower in Fln-depleted MEFs than in controls during the period when MT extension rates were measured (Figure 14H) and not significantly higher than controls later in spreading (Figure 14I). We also accounted for the directionality of MT extension

in our analysis. MTs in control cells moved in a vector direction toward the periphery whereas MTs in Fln-depleted MEFs were more randomized (data not shown). However, this did not affect our assessment of MT growth rates as we measured the velocity over the EB3 distance traveled, not simply the displacement. The further observation that blebbistatin treatment rescues MT condensation in Fln-depleted MEFs (Figure 14G) indicates that MT extension is hindered by a contractile actin network surrounding the endoplasm that, without Fln crosslinking, is presumably too dense to permit typical MT extension. As a result, MTs in Fln-depleted cells could potentially experience higher rates of catastrophe and pauses in growth.

This raises the question of whether the absence of MTs in the periphery would alter adhesion dynamics, membrane traffic or other parameters. MTs are implicated in the process of adhesion turnover but adhesions must form initially for this to occur. In the Fln-depleted cells, there is extensive ruffling of the edge that is indicative of a lack of stable adhesions in the periphery as is observed (Figure 15B, C, E, F) and perhaps an alteration in the process leading to mature stress fibers (Figure 15B, C) (Hotulainen & Lappalainen, 2006). Further, the inability of the endoplasm to spread appears to precede the loss of early adhesions, which indicates that the primary defect is in adhesion maturation or in coupling of the microtubule ends to the peripheral adhesions to enable it to extend.

In considering adhesion maturation, it is useful to compare the adhesions that form after Fln depletion with the lack of even early adhesions after talin depletion. Fln-depleted cells formed early adhesions that quickly disassembled as indicated by RFP-paxillin dynamics (Figure 15E, F). In contrast, talin-depleted MEFs did not exhibit

extensive spreading or adhesion formation (Zhang, Jiang, Cai, Monkley, Critchley, & Sheetz, 2008). I speculate that since Fln depletion appears to reduce the lifetime of adhesions, Fln may contribute to stabilization of adhesions and/or maintenance of the force-generating actomyosin network. Indeed, a recent study of Fln ligand-binding sites has shown Flns to have the capacity to bind multiple integrin β tails at once, potentially allowing Fln to cluster integrins, and thereby replace talin in the formation of mature adhesions (Ithychanda, et al., 2009).

I found additional evidence that Fln is involved in stabilizing adhesions from the dynamics of force generation of Fln-depleted MEFs on PDMS pillars. Because many *in vivo* environments are discontinuous (there are micron-sized gaps in the cornea (Nishida, Yasumoto, Otori, & Desaki, 1988) and the intestinal mucosa (Toyoda, Ina, Kitamura, Tsuda, & Shimada, 1997)), PDMS pillar arrays provide a relevant measure of cellular forces while still allowing for the accurate quantification of forces exerted by specific cellular regions (Tan, Tien, Pirone, Gray, Bhadriraju, & Chen, 2003) (du Roure, et al., 2005). The rate of force release on single pillars is ~four-fold higher after Fln depletion compared to controls (Figure 16F). Whole-cell force measurements indicated a trend toward lower force exerted / pillar in the Fln-depleted system, though these findings were not significant (Figure 16G). Similar, but stronger results were found using M2 cells (Kasza, et al., 2009).

In the case of Fln-depleted fibroblasts, the presence of early adhesions, high traction forces, and rapid force release all indicate that the matrix-integrin linkage to the cytoskeleton forms but is not sustained. As further support of this hypothesis, nocodazole treatment causes dramatic collapse of lamellipodial extensions in Fln-

depleted MEFs (Figure 15G). Whether the collapse occurs at the level of the adhesion or the actin cytoskeleton is a subject for future studies, since Fln has both roles in stabilizing the actin cytoskeleton and linking integrins to actin filaments.

In addition to a role in traction force generation, Fln appears to play a structural role in stabilizing force-bearing structures within the cytoskeleton, since it is concentrated in interior regions of cytoplasm. The primary localization of FlnA is in structures surrounding the endoplasm both near the ventral surface and in nodes of cross-linked actin as well as in dorsal stress fibers (Figure 15A). Additionally, Fln appears to be found in the proximal regions of focal adhesions (or in stress fibers emerging from focal adhesions, though super resolution studies may be necessary to confirm this) (Figure 15A), suggesting an important role in linking adhesions to the cytoskeleton proper. Accordingly, in time-lapse DIC movies of spreading FlnA -/- MEFs, I find stress fiber breakage that results in endoplasm retraction (Figure 17D). I observe breakage events near adhesive contacts as well as in the middle of stress fibers, suggesting that the inability to sustain high levels of local force generation in Fln-depleted MEFs could be a result of weakness in both the dynamic actin cytoskeleton and the connections to adhesions.

It is logical that Flns may stabilize the structural linkages by spreading force among multiple actin filaments in dynamic cytoskeletal links within the actin network surrounding the endoplasm, in stress fibers, and in force-generating contacts on pillars. The observation that calpain-uncleavable FlnA and FlnA Δ19-21 do not completely rescue the endoplasmic spreading deficiency (Figure 18) supports this notion. In addition, Fln has an affinity for the membrane, as shown through the well-characterized blebbing

of M2 melanoma cells (Cunningham, Gorlin, & Kwiatkowski, 1992). Gaps in the membranes of FlnA-/- cells are indicative of that role as well (Figure 17C, E, F).

2.9- Potential Model of Endoplasmic Spreading

There appears to be two different roles for Fln in endoplasmic spreading (Figure 19).

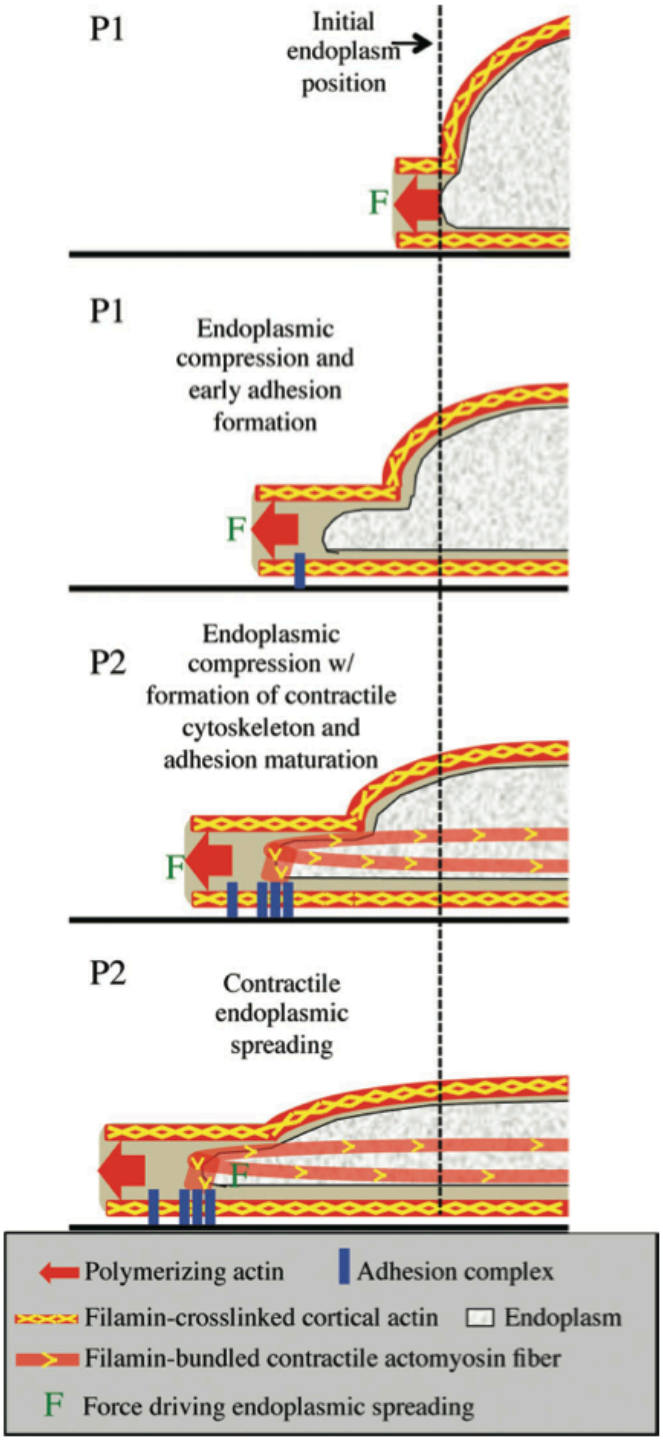

Figure 19 – Schematic model of endoplasmic spreading (Lynch, et al., 2011).

Initially the cell begins to spread via actin polymerization against the cell membrane. Cortical actin is cross-linked by Fln along the membrane. As the cell continues to spread, actin polymerization forces at the edge are transmitted back through the Fln-cross-linked cortex to the cell center, causing flattening of the endoplasm. At the same time, early adhesions begin to form. At the onset of contraction, cells exert contractile forces through mature focal adhesions, Fln-bundled actin stress fibers, and Fln-cross-linked actin meshworks (not shown for simplicity), allowing the endoplasm to spread in the direction of the edge despite being already flattened. Fln-depleted MEFs do not exhibit endoplasmic compression because they lack cortical cross-linking while they also do not experience contractile endoplasmic spreading due to unstable focal adhesions and a lack of strong actin stress fibers and cross-linked actin capable of stably supporting large forces exerted on the substrate.

During the initial phases of spreading (P0 and P1), the cortical cytoskeleton is flattened, which will cause the endoplasm to flatten as well. Upon the activation of contraction (P2), the endoplasm will spread because of forces developed on the peripheral adhesions. In the absence of Fln, both mechanisms of spreading are weakened because of the loss of crosslinks in the actin network. Connections between the endoplasm and surrounding cortical actin are particularly sensitive, explaining why gaps in the membrane form in this region in the FlnA-/- cells and why there are abrupt retractions of the endoplasmic boundary (Figure 17D). High forces generated within the contractile actin network surrounding the endoplasm that are normally transmitted through these connections would resist extension of MTs and the endoplasm boundary with the cell edge. This is still the case when calpain uncleavable FlnA and FlnA Δ19-21 are added to the Fln-depleted system, underlining the importance of the Fln-adhesion linkage as well as the dynamic nature of actin crosslinks (Figure 18).

Additionally, it should be noted that while our study concentrates on Fln-depleted and FlnA -/- MEFs, FlnB -/- MEFs did exhibit similar but less severe phenotypes. I suggest that the endoplasmic spreading deficiency that I report may be caused by a general Fln deficiency, rather than a deficiency of FlnA or FlnB specifically. Indeed,

FlnA and FlnB show high homology (van der Flier & Sonnenberg, 2001) while FlnA typically comprises ~60% of expressed Flns in fibrosarcoma cells (Baldassarre, Razinia, Burande, Lamsoul, Lutz, & Calderwood, 2009), indicating that loss of FlnA has a greater impact on cellular Fln levels than FlnB loss. FlnC undoubtedly plays a role as well, since FlnC's expression is increased upon depletion of FlnA and FlnB in fibrosarcoma cells (Baldassarre, Razinia, Burande, Lamsoul, Lutz, & Calderwood, 2009). Nonetheless, total Fln levels are lower in doubly depleted cells than in single knockdowns and controls, indicating that the endoplasmic spreading deficiency truly is linked to low levels of Fln expression.

In summary, I suggest that the primary role of Flns during cell spreading is to stabilize the transmission of forces through adhesions to cross-linked and bundled actin structures to enable formation of a cohesive cytoskeleton that supports endoplasmic spreading and organelle dispersal. Although Fln itself may have no direct role in bearing tensile forces, its depletion results in major cytoskeletal disruptions as cells generate force. Further, Flns stabilize stress fibers and the actin cytoskeleton linkages to focal adhesions and membranes. Thus, I suggest that the endoplasmic reticulum- and microtubule-rich cytoplasm behaves as a separate mechanical unit that is contractile and must be spread by pulling forces exerted on peripheral adhesions.

Chapter 3 – Endoplasmic spreading requires interaction between vimentin intermediate filaments and force-bearing focal adhesions (Lynch, et al., in preparation)

3.1 - ALLN restores focal adhesion maturation and endoplasmic spreading in Fln-depleted MEFs

Recent studies indicated a role for FlnA in stabilizing focal adhesions, since FlnA depletion leads to increased rates of disassembly (Xu, et al., 2010) (Lynch, et al., 2011). The turnover appeared to be protease dependent, since the calpain inhibitor N-[N-(N-Acetyl-L-leucyl)-L-leucyl]- L-norleucine (ALLN) reversed the increased rates of adhesion turnover in Fln-depleted cells and subsequently restored adhesion maturation (Xu, et al., 2010). Therefore, we tested if ALLN would restore adhesions in Fln-depleted MEFs. Expression of full-length (FL) FlnA restored normal FAs in Fln-depleted MEFs that had smaller adhesions (Figure 20A). Addition of ALLN similarly restored normal FAs. (Figure 20A). Quantification showed that adhesion area in Fln-depleted MEFs was increased two-fold by expressing FL FlnA, and three-fold by ALLN treatment (Figure 20B). Adhesion maturation occurred primarily during P2 of cell spreading (Dobereiner, Dubin-Thaler, Giannone, Xenias, & Sheetz, 2004) (Figure 20C), similar to untreated wild-type (WT) MEFs. If increased turnover of adhesions was linked to the Fln-depleted endoplasmic spreading defect, then treatment of Fln-depleted MEFs with ALLN should restore endoplasmic spreading.

Although differential interference contrast (DIC) micrographs of Fln-depleted MEFs showed a dense endoplasm clustered near the center of the cell, treatment with ALLN caused the endoplasm to spread normally (Figure 20D). Accordingly, the

endoplasm/whole cell area ratio, measured as described previously (Lynch, et al., 2011),

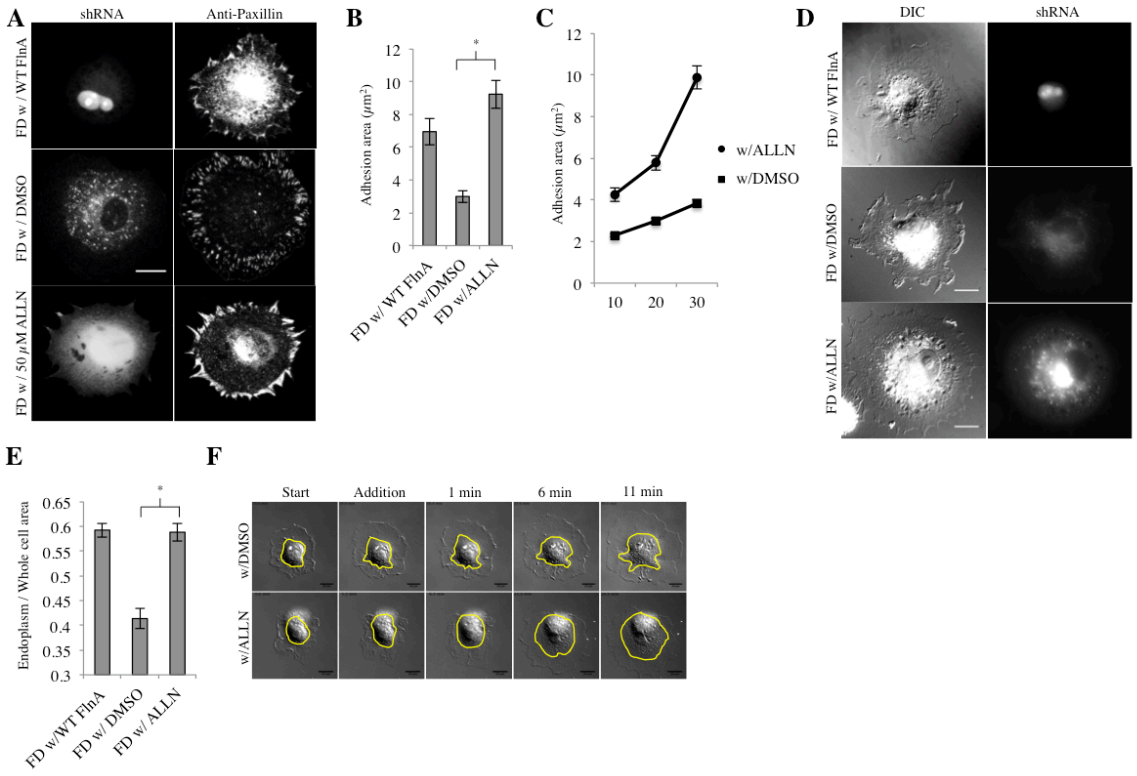

Figure 20 - ALLN rescues endoplasmic spreading in Fln-depleted MEFs (Lynch, et al., in preparation)

A) Fln-depleted MEFs were treated with 50 μM ALLN or an equal volume of DMSO for 22 hours, plated on 10 μg/ml fibronectin (FN)-coated glass for 30 minutes, fixed, stained for paxillin, and imaged with confocal microscopy. GFP signal was associated with successful FlnA shRNA transfection and expression. B) Areas of adhesion plaques were measured manually from a single confocal slice in each condition (Fln-depleted w/FL FlnA: 7 cells, 128 adhesions; Fln-depleted w/DMSO: 10 cells, 305 adhesions; Fln-depleted with ALLN: 12 cells, 323 adhesions; *: $p < 0.001$). C) Adhesion areas were measured at various time points using the same method as in B (w/DMSO, 10 minutes: 6 cells, 39 adhesions; w/DMSO, 20 minutes: 15 cells, 174 adhesions; w/DMSO, 30 minutes: 12 cells, 198 adhesions; w/ALLN, 10 minutes: 16 cells, 295 adhesions; w/ALLN, 20 minutes: 9 cells, 168 adhesions; w/ALLN, 30 minutes: 10 cells, 213 adhesions). D) Fln-depleted MEFs were transfected with RFP-ER, treated with 50 μM ALLN or an equal volume of DMSO for 22 hours, plated on FN-coated glass for 30 minutes, and fixed. E) Endoplasm/whole cell area was determined by measuring RFP-ER area and whole cell area in fluorescent and DIC channels respectively (w/ FL FlnA: 34 cells; w/DMSO: 40 cells; w/ALLN: 41 cells; *: $p < 0.001$). F) Fln-depleted MEFs were plated on FN-coated glass followed by addition of either DMSO or ALLN into the media, all error bars = SE.

of Fln-depleted MEFs was increased to control levels by treatment with ALLN compared to untreated Fln-depleted MEFs (Figure 20E). This effect was observed within 3-5 minutes of ALLN addition (Figure 20F). Taken together, these results indicate that the

defect in focal adhesion maturation was correlated with the endoplasmic spreading deficiency previously reported in Fln depleted MEFs.

3.2 - Expression of a low-turnover talin variant rescues endoplasmic spreading in Fln-depleted MEFs

Because calpain-mediated proteolysis is a rate-limiting step in focal adhesion turnover (see section 1.8), preventing talin cleavage may promote adhesion growth and endoplasmic spreading. To test this possibility, I transfected Fln-depleted MEFs with the GFP-calpain-uncleavable talin (NC Talin) that can stabilize adhesions for further maturation (Franco, et al., 2004).

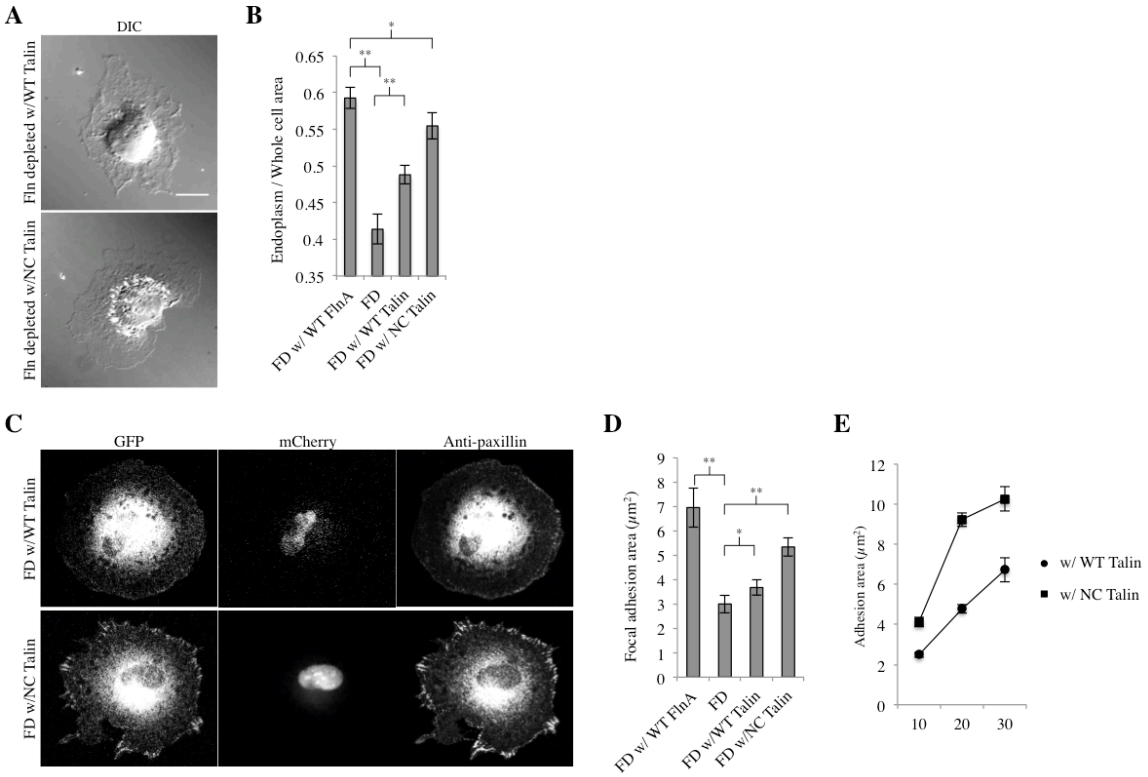

Figure 21 – Expression of a low-turnover talin variant rescues endoplasmic spreading in Fln-depleted MEFs (Lynch, et al., in preparation)

A) Fln-depleted MEFs were co-transfected with GFP-tagged talin, either full-length (FL) or calpain uncleavable (NC), spread for 30 minutes and fixed. B) Endoplasm/whole cell area ratios were measured using differential interference contrast (DIC) images for Fln-depleted MEFs co-transfected with GFP-tagged FL FlnA, FL talin, or NC talin (at least 17 cells analyzed/experimental condition; * : $p > 0.1$, ** : $p < 0.001$). C) Fln-depleted MEFs, expressing mCherry as an shRNA marker, were co-transfected with GFP-tagged FL or NC talin, spread on FN for 30 minutes, fixed, and stained for paxillin. D) Areas of adhesion plaques were measured manually from a single confocal slice in each condition (Fln-depleted w/FL FlnA: 7 cells, 128 adhesions; Fln-depleted: 10 cells, 305 adhesions; Fln-depleted w/ FL Talin: 11 cells, 166 adhesions; Fln-depleted w/ NC Talin: 5 cells, 82 adhesions; *: $p > 0.1$, **: $p < 0.01$). E) Fln-depleted MEFs transfected with either FL or NC Talin were allowed to spread and fixed at various time points (min.). Cells were stained for paxillin and adhesion area was measured as in D, all error bars = SE.

In Fln-depleted MEFs, expression of NC Talin restored endoplasm spreading whereas expression of FL Talin had no effect (Figure 21A). Endoplasm/whole-cell area ratios measured in Fln-depleted MEFs expressing NC Talin were indistinguishable from the Fln-depleted MEFs expressing FL FlnA (Figure 21B). Like Fln-depleted MEFs treated with ALLN, expression of NC Talin produced more elongated and mature adhesions than did expression of FL Talin (Figure 21C). Likewise, adhesion area was significantly greater in Fln-depleted MEFs transfected with NC Talin compared to Fln depleted MEFs with or without FL Talin (Figure 21D) and adhesion growth showed a similar trend (Figure 21E). Thus, inducing adhesion maturation using two distinct approaches, ALLN treatment and NC Talin expression, rescued Fln-depleted endoplasmic spreading.

3.3 - Endoplasmic spreading requires vimentin intermediate filaments

Because adhesions associated with vimentin intermediate filaments (vIFs) tend to be larger and more stable (Burgstaller, Gregor, Winter, & Wiche, 2010) (Tsuruta, 2003), I investigated the role of vIFs in endoplasmic spreading. I transfected RPTPα +/+ MEFs with either a full-length vimentin-GFP construct (GFP-FL Vim) or a GFP-tagged dominant negative vimentin variant expressing only amino acids 1-138 (GFP-Vim 1-138) (Chang, et al., 2009). These amino acids only code for the vimentin globular head

domain and a small portion of the α-helical rod domain, so their incorporation into growing vIFs halts elongation. Spread cells expressing GFP-Vim 1-138 lacked polymerized vIFs compared to controls expressing GFP-FL Vim (Figure 22A). Similar to the Fln-depleted system, cells expressing GFP-Vim-1-138 were unable to spread the endoplasm (Figure 22A) and had endoplasm/whole cell area ratios that were significantly lower than controls (Figure 22C). FAs were also smaller, more punctate, and failed to mature as in Fln-depleted MEFs (Figure 22B, E), resulting in adhesion areas that were significantly less than controls (Figure 22D). Together, these results demonstrated marked phenotypic similarities between the Fln-depleted system and cells expressing GFP-Vim 1-138 and indicated that vIFs were required for endoplasmic spreading.

3.4 – Both vimentin intermediate filaments and mature focal adhesions are required for endoplasmic spreading

Since expression of GFP-Vim 1-138 inhibited FA maturation as well as vIF assembly, there was a question of whether both or only one of these factors was sufficient for endoplasmic spreading. However, Fln-depleted MEFs have vIFs with a contracted

endoplasm, indicating that vIFs are not sufficient for endoplasmic spreading.

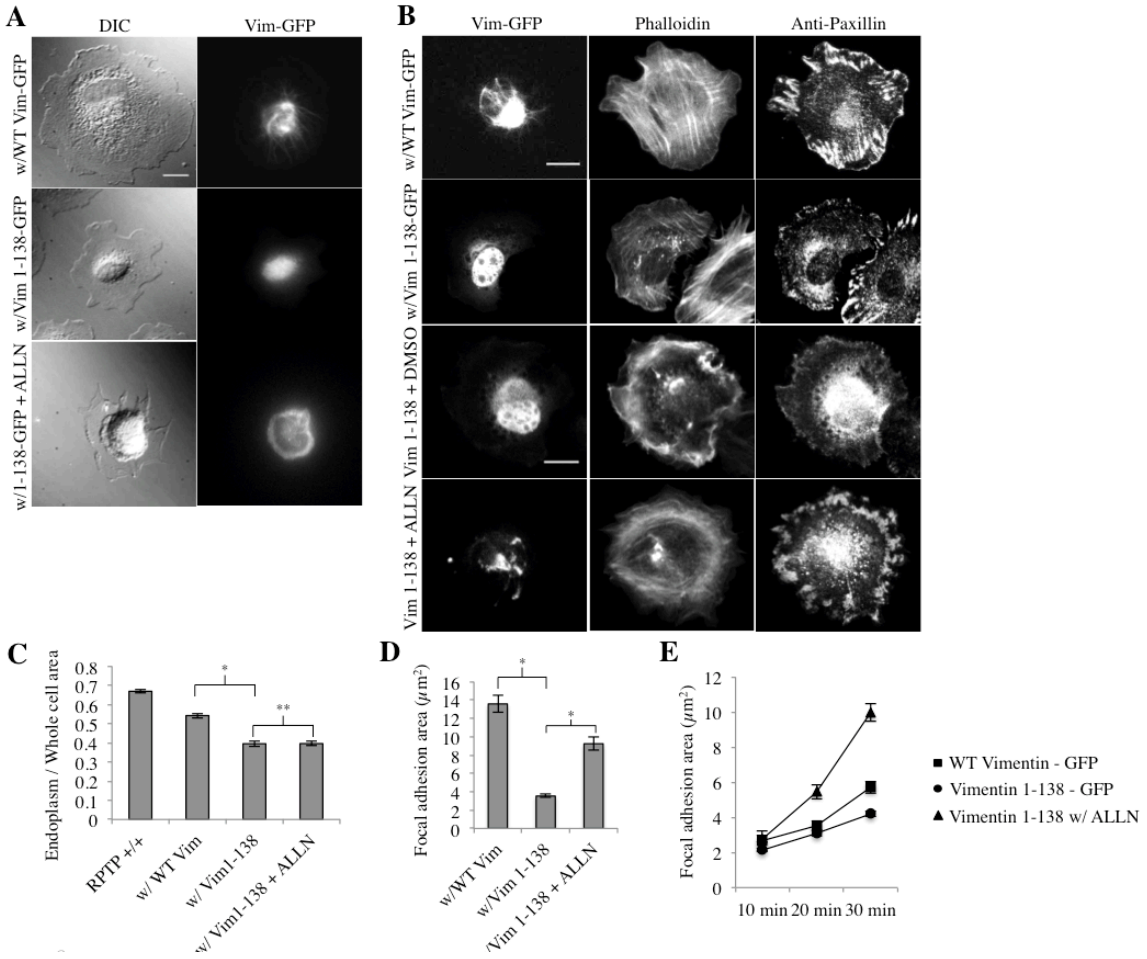

Figure 22 – Vimentin intermediate filaments and mature focal adhesions are required together for endoplasmic spreading (Lynch, et al., in preparation)

A) RPTPα +/+ MEFs were transfected with full-length vimentin-GFP or vimentin 1-138-GFP, spread for 30 minutes on FN-coated glass, and fixed. vIFs are do not polymerize in the latter condition. B) RPTPα +/+ MEFs were transfected and spread as in A, with subsequent immunostaining for paxillin. C) Endoplasm/whole cell ratios were measured as in Figure 2B (RPTPα +/+: 30 cells, w/FL Vim: 39 cells, w/Vim1-138: 30 cells, w/Vim1-138 + ALLN: 45 cells; *: $p < 0.001$, **: $p > 0.1$). D) Adhesions areas were measured manually from a single confocal slice in each condition (w/FL Vim: 6 cells, 120 adhesions; w/ Vim1-138: 6 cells, 120 adhesions; w/ Vim1-138 + ALLN: 9 cells, 222 adhesions; *: $p < 0.001$). E) Adhesion plaque areas were measured at various time points using the same method as in D (w/FL Vim: 10 min: 4 cells, 42 adhesions; 20 min: 6 cells, 114 adhesions; 30 min: 170 adhesions; w/Vim1-138: 10, 20, 30 min: 5 cells each, 100 adhesions each), all error bars = SE.

To determine if mature FAs are sufficient for endoplasmic spreading in the absence of vIFs, I transfected wild-type MEFs with GFP-Vim 1-138 and treated them with ALLN overnight. After spreading on FN-coated glass, vIFs did not form (Figure 22A), but

adhesions matured (Figure 22B, D, E). Interestingly, the endoplasm did not spread (Figure 22A) and endoplasm/whole cell area ratios were unchanged from the GFP-Vim 1-138-expressing cells without ALLN (Figure 22C). Thus, mature FAs were not sufficient for endoplasmic spreading. Both vIFs and mature FAs were needed for endoplasmic spreading to occur.

3.5 - Vimentin intermediate filaments and mature focal adhesions must co-localize for efficient endoplasmic spreading

If endoplasmic spreading required both vIFs and mature FAs, then it followed that the two might be physically linked during the endoplasmic spreading process. In control cells transfected with paxillin-GFP and stained for vimentin, vIFs coalesced at FA sites in a directed fashion (Figure 23E) and vIFs contacted a high percentage of total FAs (Figure 23D). In Fln-depleted cells, vIFs extended into the periphery, without linking to FAs (Figure 23E) and only ~35% of FAs in Fln-depleted MEFs were in contact with vIFs (Figure 23D). To further test the role of vIFs, I treated RPTPα +/+ MEFs with Withaferin A (WFA), an inhibitor of vimentin cytoskeleton spreading that allowed vIFs to form while blocking their extension to the periphery (Thaiparambil, et al., 2011). In WFA-treated cells, vIFs formed but were restricted to the perinuclear region (Figure 23A, E) with no discernible changes in the actin cytoskeleton (Figure 23A). As in Fln-depleted MEFs, vIFs in WFA-treated cells contacted only about 30% of total FAs (Figure

23D).

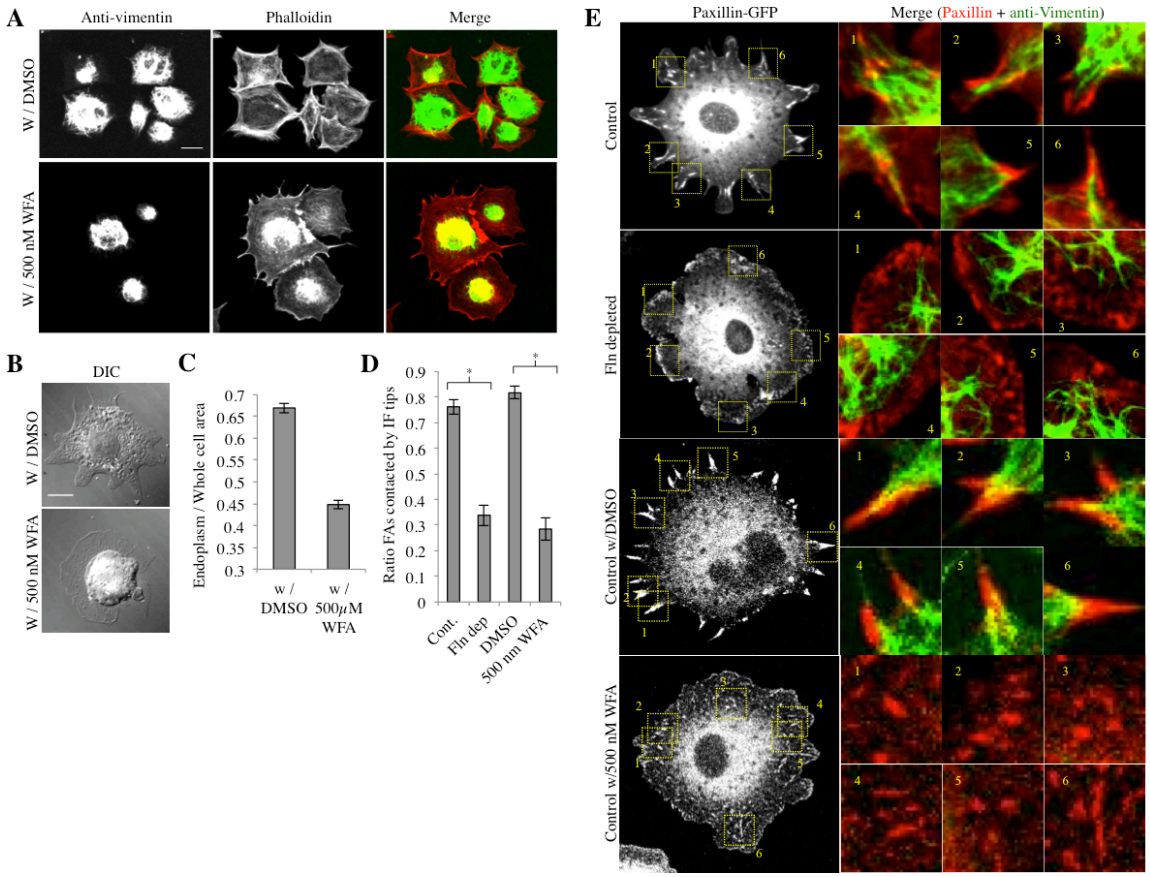

Figure 23 – Endoplasmic spreading requires co-localization of vimentin intermediate filaments and mature focal adhesions (Lynch, et al., in preparation)

A) RPTPα +/+ MEFs were treated with 500 nM withaferin A (WFA) overnight, spread on FN-coated glass for 30 minutes, fixed, and stained for vimentin, and subsequently subjected to fluorescent confocal imaging (green: anti-vimentin, red: phalloidin). B) Cells were treated with WFA as in A, fixed, and imaged with DIC. C) Endoplasm / whole cell area ratios were significantly lower for cells treated with WFA than controls (30 cells measured for each condition, $p < 0.001$). D) Each cell type was plated on FN-coated glass for 30 minutes, fixed, and stained for vimentin and paxillin. FA plaques co-localizing with vIF tips were quantified as a percentage of total FA plaques (Cont.: 8 cells, Fln-depleted: 4 cells, Cont. w/ DMSO: 6 cells, Cont. w/ WFA: 7 cells; *: $p < 0.001$). E) Sample images used to generate D. Cells were prepared as described in D and subjected to confocal imaging, all error bars = SE.

Intriguingly, WFA-treated cells also showed a defect in adhesion maturation (Figure 23E) and an unspread endoplasm (Figure 23B) with endoplasm/whole cell area ratios that were approximately 30% lower than controls (Figure 23C). Thus, under several different conditions, endoplasmic spreading was correlated with a high level of co-localization

between vIFs and mature FAs. Cells deficient in either component or missing an interaction between them were unable to spread the endoplasm.

3.6 – In Fln-depleted MEFs, vIFs extend past FAs in a microtubule-dependent manner

Because there appeared to be a need for a linkage between vIFs and FAs, we carefully examined vIF distribution in Fln-depleted MEFs and their controls. Fln-depleted MEFs had a more extensive vIF network covering a larger fraction of the cell area compared to controls (Figure 24A). The average distance between the cell edge and areas containing vIFs was nearly half that of controls in Fln-depleted MEFs (Figure 24B). Much of the vIF network extended to regions without FAs in the absence of Fln. Nocodazole, the MT polymerization inhibitor, reversed this phenotype (Figure 24A), causing confinement of vIFs to the cell center and increasing the distance between vIFs and the cell edge (Figure 24B). Thus, miss targeting and over-extension of vIFs in Fln-depleted MEFs is a microtubule-dependent process.

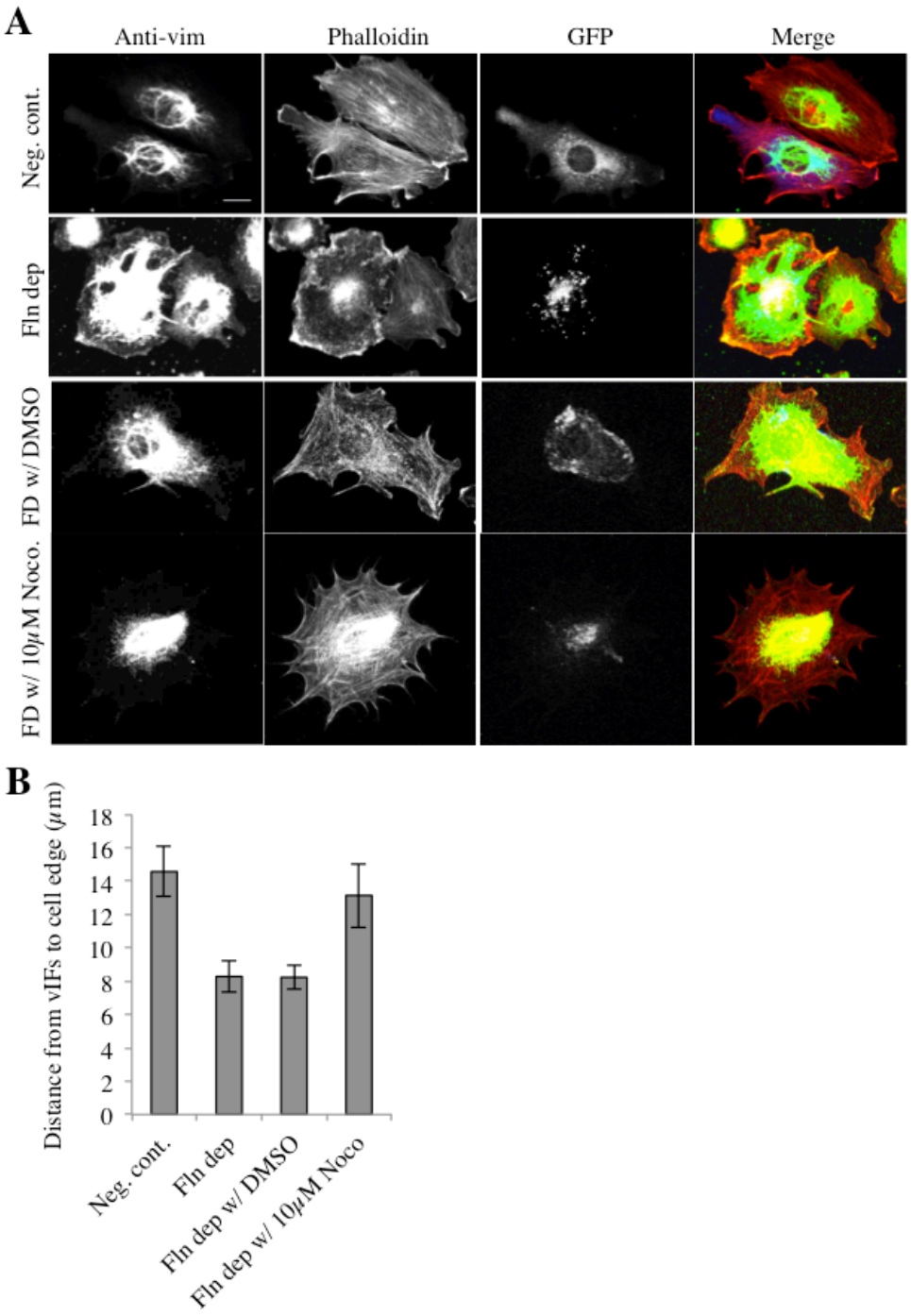

Figure 24 - VIFs extend closer to the cell edge in Fln-depleted MEFs in a microtubule-dependent manner (Lynch, et al., in preparation)

A) In each condition, MEFs were plated on FN-coated glass for 30 minutes, fixed, and stained for vimentin and phalloidin, with GFP signal corresponding with shRNA expression. Cells treated with nocodazole were exposed 30 minutes prior to spreading. Vimentin signal was overexposed in all images to highlight vIFs in the periphery. B) Distances of vIFs to the cell edge was determined by averaging the distance from the vIF boundary to the cell edge at ten points in the cell, using at least six cells per cell type (*: $p < 0.001$, **: $p < 0.05$), all error bars = SE.

3.7 - Endoplasmic spreading requires myosin II contractile activity

Lastly, I sought to determine if contraction plays a role in endoplasmic spreading. I allowed RPTPα +/+ MEFs to spread in the presence of blebbistatin, a myosin II inhibitor (Straight, et al., 2003), and found that the endoplasm was not spread after 30 minutes (Figure 25A).

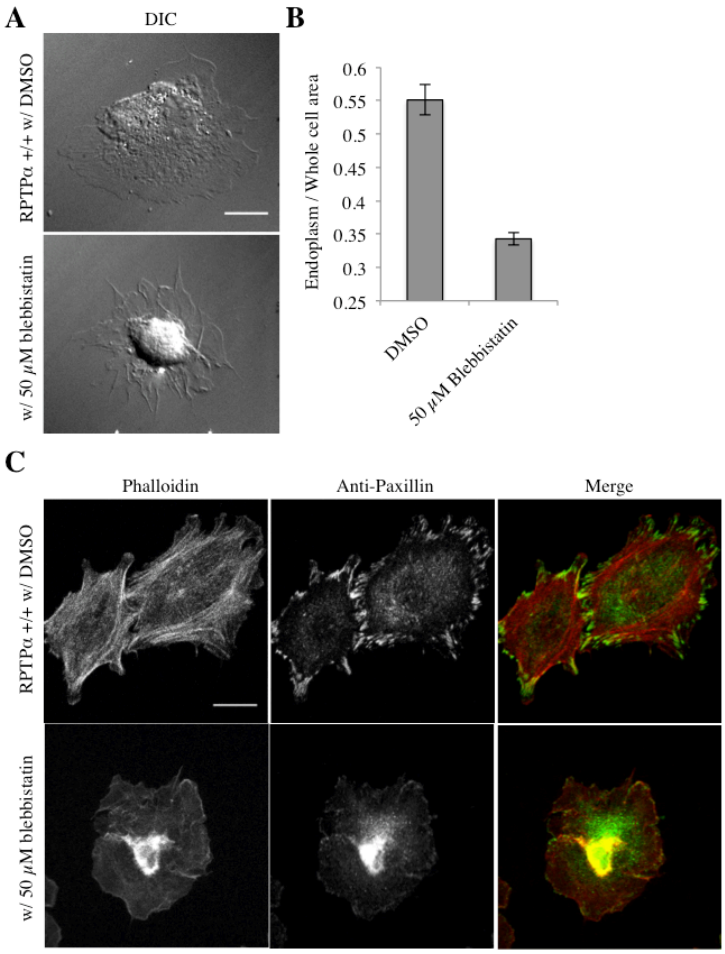

Figure 25 – Endoplasmic spreading requires myosin II-mediated contraction (Lynch, et al., in preparation)

A) RPTPα +/+ MEFs were treated with 50 μM blebbistatin or an equal volume of DMSO and plated on 10 μg/μl FN for 30 minutes. B) Endoplasm / whole cell ratios show a reduction in endoplasmic spreading upon blebbistatin treatment. C) As in A, cell were then fixed and stained for phalloidin and paxillin, all error bars = SE.

Endoplasm/whole-cell area ratios in blebbistatin-treated cells were lower than controls (Figure 25B). In accordance with the endoplasmic spreading deficiency observed in Fln-depleted MEFs, cells expressing GFP Vim 1-138, and WFA-treated cells, this deficiency was coupled with a defect in adhesion maturation (Figure 25C). Thus, inhibiting myosin II blocked endoplasmic spreading, indicating that force generation, in addition to interaction of vIFs with FAs, was necessary for endoplasmic spreading.

3.8 – Summary and discussion

My earlier studies focused on the role of Flns in cell spreading and indicated that depletion of Fln levels caused an endoplasmic spreading defect (Lynch, et al., 2011). However, the spreading could depend upon the linkage between vIFs and mature adhesions and may have an indirect dependence upon Fln depletion. Indeed, either ALLN or NC-talin rescues endoplasmic spreading in a Fln depleted background (Figure 20E, Figure 21B). Thus, Fln levels do not seem to be the only determinative factor in endoplasmic spreading, but large, mature adhesions are critical. Further, we show that vIFs are linked to FAs in endoplasmic spreading and disruption of vIFs or the linkage leaves the endoplasm unspread. Thus, we suggest that both mature adhesions and vIF connections are needed for endoplasmic spreading.

In a model suggested recently (Xu, et al., 2010), mature adhesions can only form when there is competition between talin and Fln for calpain-mediated proteolysis. When Fln levels are depleted, calpain-mediated proteolysis quickly turns over talin at the adhesion, precluding further maturation. Adding FL FlnA back to the Fln depleted system restores talin-Fln competition for calpain proteolysis, thereby spreading calpain

cleavage between both talin and Fln and allowing adhesion maturation to occur. Inhibiting calpain cleavage in Fln-depleted cells allows further maturation to occur since talin now has a longer half-life at the adhesion. Overexpressing NC talin achieves the same result, but bypasses the calpain cleavage step.

Interestingly, FL talin expression does not rescue the Fln-depleted endoplasmic spreading defect (Figure 21B). Under the model from Xu et al., adding to the pool of calpain cleavable molecules should decrease adhesion turnover and, according to our results, rescue endoplasmic spreading. This is not the case however, potentially reflecting a cellular preference for Fln to be at the adhesion to allow further maturation. In this scenario, ALLN treatment of Fln-depleted cells or overexpression of NC talin would make the ~15% remaining cellular FlnA (Figure 12A) sufficient to allow adequate adhesion maturation to occur. This is a subject for further inquiry. Overall, our results indicate that mature adhesions are required for endoplasmic spreading.

VIFs promote adhesion maturation and stabilization (Tsuruta, 2003), but the role of this phenomenon in the context of endoplasmic spreading has not been explored. The effects of vIF disruption have been reported in a number of systems, with a lack of polarization and raised central cellular regions being typical results (Ivanova, Margolis, Vasiliev, & Gelfand, 1976) (Goldman, Khuon, Chou, Opal, & Steinert, 1996) (Eckert, 1986). Our results with GFP-Vim 1-138 quantify the latter effect (Figure 22C), since reduced endoplasmic spreading necessarily results in a thicker central cellular region. I also show GFP-Vim 1-138-transfected cells to be similar to Fln-depleted cells and Fln-depleted cells transfected with FL Talin in that adhesion maturation correlates with an endoplasmic spreading defect (Figure 22D). Similar to the Fln depleted system, a lack of

vIFs, immature adhesions, or both could cause the GFP-Vim 1-138-associated endoplasmic spreading defect. ALLN treatment once again shed light on this issue: adhesions matured without vIF formation (Figure 22B) and, contrary to the Fln depleted case, endoplasmic spreading was not rescued (Figure 22C). Therefore, neither vIFs nor mature adhesions are sufficient for endoplasmic spreading on their own. This result is in agreement with that observed in the Fln depleted system: vIFs are present but proper adhesion maturation does not occur, perhaps because of the loss of the vIF-FA linkage. Hence, endoplasmic spreading does not occur.

The necessity for both vIFs and mature FAs in the endoplasmic spreading mechanism leads to the logical conclusion that they most likely interact in some way during the process. This interaction has been shown in other systems (Bershadsky & Tint, 1987), but has never been approached in the context of endoplasmic spreading. The GFP-Vim 1-138 system was unsuitable to probe this issue, as vIFs do not polymerize in the presence of this variant. WFA treatment provided an alternative since WFA inhibited endoplasmic spreading (Figure 23C) and adhesion maturation (Figure 23E), yet still allowed vIF formation (Figure 23A). In this system, as in Fln depleted cells, vIFs were not co-localized with or directed toward adhesive structures (Figure 23E), indicating that the vIF-FA interaction is required for endoplasmic spreading. One caveat to using WFA, as with other chemical treatments, is that though it's primary mechanism of action is known (covalent modification of vimentin monomers), it is unclear if it has any off-target effects, particularly on focal adhesion maturation. We postulate that adhesions do not mature in WFA-treated cells because of a lack of interaction with vIFs, however WFA may affect this process as well. An important control to be explored in the future would

be to determine if WFA-treated cells have the ability to mature adhesions. This could be accomplished through dual treatment of wild-type cells with WFA and ALLN. If ALLN rescued adhesion maturation, then the effects of WFA would be limited in our system to inhibiting vIF extension to the periphery.

Recent work (Burgstaller, Gregor, Winter, & Wiche, 2010) suggests that vimentin filament fragments must be transported along MTs and aggregate at adhesions before they form vIFs. This aggregation is due to the presence of the plectin isoform P1f. Plectins are members of the plakin family of proteins that bind to each cytoskeletal system (MTs, IFs, and MFs) as well as to integrins (Jefferson, Leung, & Liem, 2004). VIFs overextend past peripheral adhesions in Fln depleted cells, suggesting that Fln depletion disrupts vIF fragment aggregation at adhesive sites. Interestingly, I did not observe P1f in any of our wild type or experimental systems (data not shown). This may be a result of disparities in the timing of experiments as I performed mine at 30 minutes after the initiation of spreading while Burgstaller et al. completed theirs at much later time points (~16 hours after spreading). Early time points may require a different protein that, like P1f, associates with mature adhesions and vimentin, thereby promoting vIF co-localization at adhesions. Zyxin is one such candidate (Lee, Mruk, Conway, & Cheng, 2004), however I detected no differences in zyxin localization between Fln-depleted cells and their controls (data not shown). Another protein that associates with both adhesions and vimentin is Fln (Kim, Nakamura, Lee, Shifrin, Arora, & McCulloch, 2010). ALLN- and NC talin-mediated rescue of endoplasmic spreading in Fln depleted cells seemingly show that Fln is dispensable for endoplasmic spreading and adhesion maturation. However, Fln depleted cells still express ~15% of cellular FlnA levels (not to mention

relatively small quantities of FlnC). Either ALLN treatment or NC Talin expression in Fln depleted cells could promote adhesion maturation adequately enough so that vIFs could aggregate at mature adhesions with low levels of Fln mediating the interaction. Future studies will focus on this intriguing possibility.

Because vIFs must interact with mature adhesions to allow endoplasmic spreading, we postulated that contraction was necessary to perform the actual spreading of the endoplasm. Indeed, I found this to be the case as blebbistatin treatment blocked endoplasmic spreading and adhesion maturation (Figure 25). Collectively, my results suggest a robust mechanism for endoplasmic spreading (Figure 26). The essential interaction of vIFs with mature adhesions connects contractile elements surrounding the endoplasm to the substrate, thus allowing force generation and subsequent spreading of the endoplasm. As presented previously (Burgstaller, Gregor, Winter, & Wiche, 2010) (Lynch, et al., 2011), a cage-like structure of actin interspersed with IFs surrounds the endoplasm. MTs typically extend toward the periphery as MT motors transport vimentin fragments outward. As adhesions begin to mature, a vimentin-binding protein associated with mature adhesions causes the aggregation of vIFs at adhesions and subsequent elongation toward the central cage.

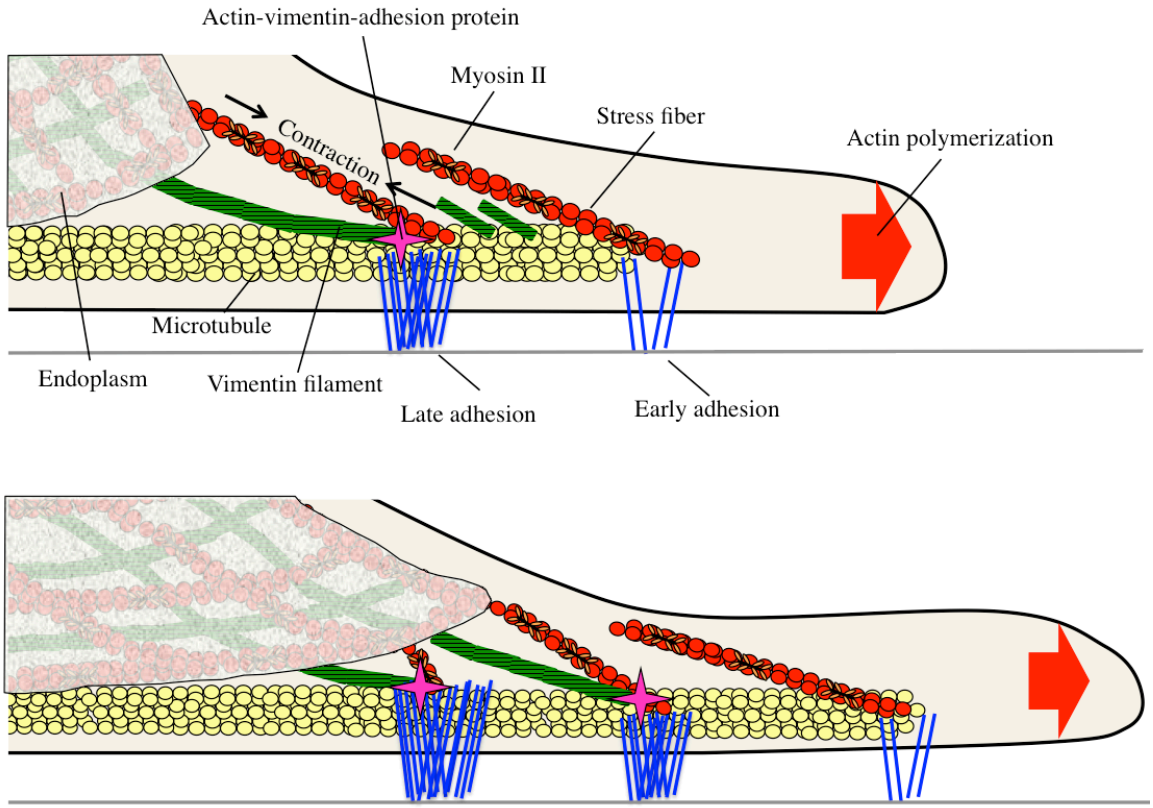

Figure 26 - Endoplasmic spreading is a continuous process dependent on interaction between vimentin intermediate filaments and force-bearing adhesions (Lynch, et al., in preparation)

A cage-like structure surrounds the endoplasm from the beginning of spreading. As microtubules migrate outward, vimentin fragments are transported out to maturing adhesions. Vimentin fragments collect at maturing adhesions, subsequently forming vimentin filaments that can interact with the central endoplasmic cage. Myosin II contraction in stress fibers and the endoplasmic cage causes the endoplasm to pull forward on the connection to the maturing adhesion, resulting in further maturation. Vimentin filaments collect at the next round of adhesions, connecting with the spreading endoplasmic cage and allowing endoplasmic spreading to continue, regardless of the height of the cell.

Once vIFs interact with the central cage, any contraction of elements comprising the cage or in connected stress fibers should result in endoplasmic spreading as long as a strong, stable connection exists between the cage and the substrate.

Our previous work suggested two different phases of endoplasmic spreading, an initial flattening phase followed by a later contractile phase (Lynch, et al., 2011). I proposed that once the cell was flat, forces exerted by polymerizing actin on the cell

membrane of the leading edge would no longer be able to flatten the endoplasm further, necessitating a different mechanism. Our current results lead to a contractile endoplasmic spreading model that plays a role throughout cell spreading, even allowing the coherent spreading of the endoplasm once the cell flattens. After the steps outlined above, the continuous extension of MTs into the periphery promotes a new round of vimentin aggregation at more peripheral, "younger" adhesions. These adhesions would then connect with the now more expansive central cage. Contractile forces would pull on the substrate and spread the endoplasm further. Interestingly, this model may also provide an explanation for the plateauing of endoplasm spreading at ~60-70% of cell area because the endoplasm would only spread into regions exhibiting mature adhesions and vIFs.

In summary, our work provides a deeper understanding of the players involved in endoplasmic spreading that has, thus far, been elusive. Numerous studies documented various aspects of the process but until now, their relation to endoplasmic spreading has not been fully realized. Important questions linger however, including how vIFs interact with mature adhesions at early stages of spreading as well as temporal aspects of the process. These will be assessed in future studies, potentially providing a more global understanding of coherent cell spreading.

Chapter 4 – Future perspectives

4.1 – Further investigations of FlnA function in endoplasmic spreading

This thesis provides a framework for further studies into Fln's role in cell motility as well as potential applications of the endoplasmic spreading mechanism. Indeed, a number of important questions arise from the results of my research. For instance, it is critical to continue characterizing the endoplasmic spreading mechanism and endoplasmic spreading defects. An important point is that for all the mechanistic details I elucidated in this work, it remains unclear what is at the heart of an endoplasmic spreading defect; is it a disconnect in coherent force transmission between vIFs, the actin cytoskeleton, and mature focal adhesions? If so, what binding partners mediate the vIF/mature focal adhesion interaction that is required for endoplasmic spreading?

Flns may be these critical mediators. Of course, it is possible that their depletion simply leads to a lack of adhesion maturation and that this is the source of the Fln-depleted endoplasmic spreading defect. As already discussed briefly, FlnA binds vimentin and interacts with mature adhesions. To further understand if FlnA is essential for endoplasmic spreading, I transfected Fln-depleted MEFs with GFP-tagged FlnA fragments comprising either FlnA domains 1-8, 8-15, 16-23, or 16-24. Since vimentin binds FlnA along domains 1-8 and cryptic integrin-binding sites are located along the entire length of the FlnA molecule (Ithychanda, et al., 2009), I hypothesized that FlnA domains 1-8 would rescue the Fln-depleted endoplasmic spreading defect while the other FlnA fragments would not. Unfortunately, I found no variation in the effects of any fragments on endoplasmic spreading, i.e. none of them rescued the endoplasmic spreading deficiency (Figure 27).

There are a number of possible explanations for this result. For one, it is possible that cryptic integrin-binding sites on FlnA domains 1-8 are not uncovered in the absence of the rest of the molecule. Since FlnA is a mechanosensitive protein (see section 4.2), this is a definite possibility.

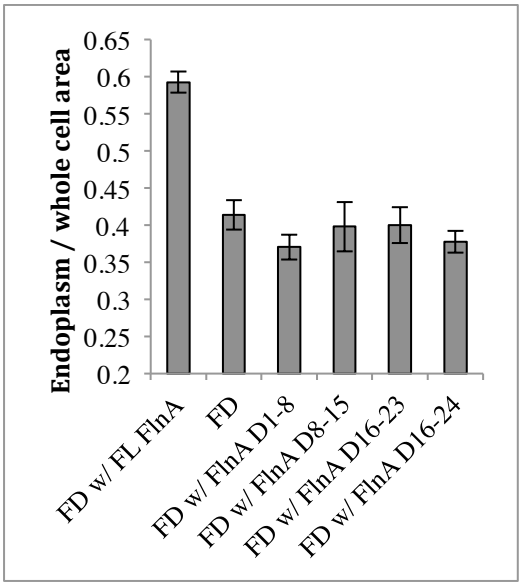

Figure 27 – FlnA fragments do not rescue the Fln-depleted endoplasmic spreading defect.

Fln-depleted MEFs were transfected with the indicated GFP-tagged FlnA fragments. None of the FlnA fragments rescued the Fln-depleted endoplasmic spreading deficiency, all error bars = standard deviation (SD).

The fragment would be able to bind vimentin, but not integrins, so forces generated within the endoplasm would still not be transmitted to the surface and the endoplasm would not spread. Another possibility is that the N-terminal actin-binding domain of FlnA is required for endoplasmic spreading. Of course, FlnA simply may not be the missing link between vIFs and mature adhesions. Yet another possibility is that endoplasmic spreading defects arise not directly from a missing protein or cellular

component, but from another process that takes over in the absence of FlnA or vIFs. In any case, this is an important subject for further inquiry.

4.2 – Mechanosensitive functions of FlnA (Lynch & Sheetz, 2011)

Regardless of its potential role in endoplasmic spreading, FlnA is an incredibly important cellular protein with diverse functions. For example, FlnA is mechanosensitive (Yamazaki, Furuike, & Ito, 2002) (Pentikainen & Ylanne, 2009) (Lad, et al., 2007) (Kolahi & Mofrad, 2008) (Johnson, Tang, Carag, Speicher, & Discher, 2007) (Heikkinen, et al., 2009) (Furuike, Ito, & Yamazaki, 2001) and plays a role in mechanotransduction. Cellular mechanotransduction is the process by which cells detect external and internal mechanical signals and convert them to chemical responses. In the context of cell adhesion to a substrate, externally applied forces produce similar effects as internally generated forces (Riveline, et al., 2001). Focal adhesions grow and mature, while motile velocity decreases (Calderwood, et al., 2001). How does the cell coordinate these responses at the molecular level? Ehrlicher *et al*. suggested that mechanical strain in a FlnA-actin network would alter important interactions between the network and the cell. To test their hypothesis, they used a novel fluorescence microscopy-based method for measuring protein binding kinetics (Ehrlicher, Nakamura, Hartwig, Weitz, & Stossel, 2011). Two critical aspects of cellular mechanics were addressed by their study, cytoskeletal network linkage to the extracellular matrix and the dynamics of actin in the cytoskeleton. Both were found to be responsive to strain on FlnA.

As pointed out earlier, FlnA is a large, rod-like protein comprised of an N-terminal actin-binding domain and 24 IgG-like domains that can bind numerous proteins.

The first 15 IgG-like domains are referred to as rod 1. These domains interact end-to-end to produce an elongated structure that binds actin filaments along its length. Domains 16-23 make up rod 2 (Nakamura, Osborn, Hartemink, Hartwig, & Stossel, 2007), a more compact region where domains interact in complex ways that result in cryptic binding sites only exposed when the molecule is under tension (Pentikainen & Ylanne, 2009). The C-terminal IgG-like domain allows the protein to homodimerize. Each subunit of a FlnA dimer is capable of binding lengthwise along an actin filament via interactions with rod 1, thereby orthogonally crosslinking two actin filaments and creating a network of actin filaments. Although a Fln-crosslinked network is capable of transmitting forces over long distances (Wang, Tytell, & Ingber, 2009); cohesive propagation of forces in cells between adhesions depends upon myosin contractility (Cai, et al., 2010) (Rossier, et al., 2010). In cells, the loss of Flns results in the loss of normal focal adhesions and reduced linkage between cytoskeletal compartments (Baldassarre, Razinia, Burande, Lamsoul, Lutz, & Calderwood, 2009) (Lynch, et al., 2011). However, the Fln network can have other roles than just crosslinking. As a mechanotransducer, strain generated within this network (internally or externally) can strain the FlnA dimer at its crosslinks. One way to explain the effects of FlnA on many cell activities is that strain of FlnA could alter its binding affinity for other components as has been shown for cell cytoskeletons in general (Sawada & Sheetz, 2002).

Ehrlicher *et al*. tested this hypothesis using a novel technique known as fluorescence loss after photoconversion, or FLAC. Conceptually similar to fluorescence recovery after photobleaching (Sprague, Pego, & Stavreva, 2004), a given protein's binding partner is tagged with a photoactivatable fluorophore that does not fluoresce until

excited by a pulse of high energy light. Once fluorescent, unbound proteins rapidly diffuse away from the site of excitation while proteins bound to the actin-FlnA network must first release. The result is typically a two-component exponential decay in fluorescence intensity (a very rapid, unbound and slow, bound component). Although a high density of FlnA can result in rebinding and multiple release steps, small activation volumes and excess binding protein reduce the possibility. Thus, the slow decay component can be a measure of the off-rate constant for the bound complex. Assuming that the on-binding rate is unchanged, changes in off-rate constant would reflect changes in the equilibrium binding constant, i.e. the fraction bound.

Ehrlicher *et al*. then used an *in vitro* FLAC assay to test how strain in a FlnA-actin network would alter binding. The experimental apparatus consisted of a stationary cover glass on the bottom, a reconstituted FlnA-actin network in the middle that also contained a specific FlnA binding partner, and a piezo-driven upper plate capable of applying external, unidirectional strain on the network (Figure 28A).

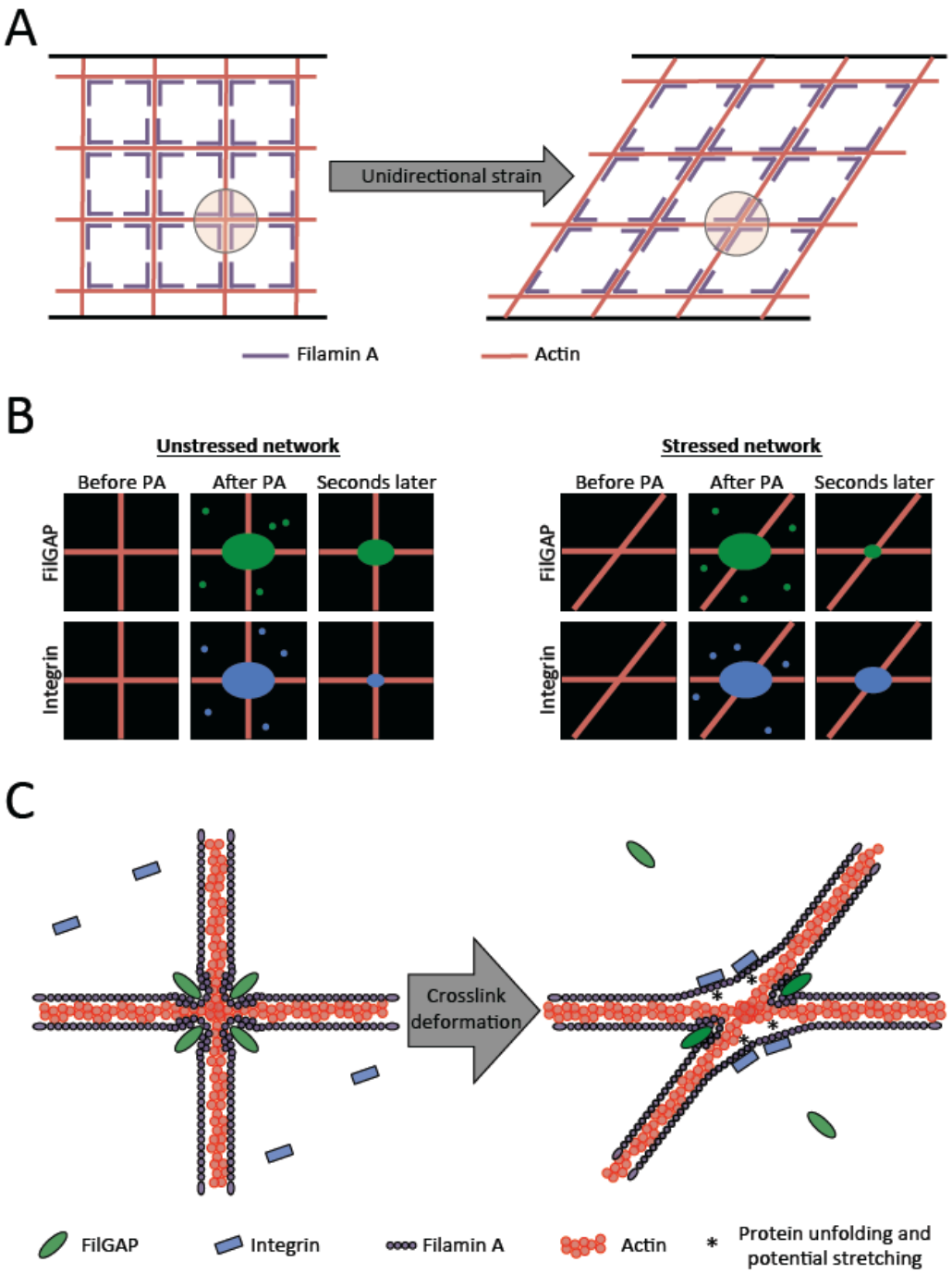

Figure 28 – Strain-induced FlnA stretching causes stronger integrin binding and release of FilGAP (Lynch & Sheetz, 2011)

A) Schematic depicting the effect of unidirectional strain applied to an actin-FlnA network. B) Cartoon of fluorescence loss after photoconversion (FLAC) data for each FlnaA binding partner tested. After photoactivation (PA) on an unstressed network, FilGAP has a longer lifetime than integrin at FlnA crosslinks. After PA in a stressed network, the opposite result is observed. C) Model of FlnA crosslinks before and after deformation. Each panel depicts circled regions from A.

The FlnA binding partners were either a peptide representing the FlnA binding site from integrin β7, which binds at cryptic binding sites on FlnA, or FilGAP, a GTPase that specifically inactivates Rac and binds to domain 23 of FlnA, near its C-terminal dimerization domain. Rac inactivation is typically associated with a shift toward slower actin dynamics and adhesion maturation. Thus, alterations in binding of integrin β7 tail peptide and FilGAP have implications for cytoskeleton-matrix interactions and actin dynamics, respectively. Finally, to determine if cellular motors could produce similar strains, non-muscle myosin II was incubated with the network until all ATP was hydrolyzed. After the network had time to relax, strain was induced by uncaging photolabile ATP, causing further myosin contraction.

The reported results were striking: applying an external strain caused stronger binding of the integrin peptide to FlnA while weakening FilGAP binding. Further, FLAC-based binding kinetics of photoactivatable FlnA showed a turnover time on the order of six minutes. This observation provided an internal control, as any strain exerted on the system would be relaxed over time due to the dynamic nature of FlnA crosslinking. Accordingly, FLAC measurements taken after relaxation of the actin network showed increased FilGAP binding. When the relaxed network contained myosin, contraction induced by ATP uncaging produced internal strain. FLAC measurements of networks undergoing internal strain showed that integrin binding strength increased while FilGAP binding became weaker (Figure 28B). It is interesting to note that the off-rate of FilGAP was decreased in the presence of myosin and contraction did not cause a decrease to the same level as the externally applied strain. However, molecular mechanotransduction

through FlnA generally behaves in a similar manner regardless of whether strain is exerted externally or internally.

How could applied strain elicit stronger binding of one binding partner but weaken the binding of another? There are two major effects of the strain: one would be to alter the angle between the FlnA rods and the other would be to cause domain unfolding as suggested by the fact that the integrin binding site is cryptic. In the first case, the FilGAP binding domain, domain 23, is close enough to the dimerization domain, domain 24, such that lower crosslinking angles could allow FilGAP to simultaneously interact with both subunits of the homodimer. Increasing the crosslinking angle would increase the distance between each subunit's FilGAP-binding domain, potentially weakening the binding strength of FilGAP to FlnA. Alternatively, the applied tension in the network could mechanically stretch FlnA (in vitro measurements of unfolding show that it occurs in a physiological force range (Chen, Zhu, Cong, Sheetz, Nakamura, & Yan, 2011)) exposing its cryptic integrin-binding sites and promoting the integrin-FlnA interaction (Figure 28C).

The findings of Ehrlicher *et al*. provide insights into the complex issues of how matrix-cytoskeleton binding and actin dynamics are regulated by mechanical forces. They also support previous observations related to FlnA. For one, Ithychanda and Qin recently demonstrated that FlnA has the potential to bind integrin at numerous cryptic sites along its length (Ithychanda, et al., 2009). The authors proposed, as have others, that FlnA mediates adhesion maturation by clustering integrins into larger adhesive structures. Recent work from our lab and others shows that cells depleted of Flns cannot generate stable levels of internal force (although peak forces are at control levels) and as

a result, adhesions do not mature (Lynch, et al., 2011), which is in agreement with the finding that internal strain increases integrin binding in FlnA crosslinked actin networks. Furthermore, because local application of forces causes inhibition of cell membrane-proximal Rac in a FilGAP-dependent manner (Shifrin, Arora, Ohta, Calderwood, & McCulloch, 2009), the result that FilGAP binding is weakened by application of stress on the network also fits well with cell-based studies. Ehrlicher *et al*. also suggest that regulation of FilGAP could be purely mechanical in nature, as FilGAP would be tightly bound to FlnA until force generation occurs, at which point the crosslinking angle of FlnA would increase, thereby weakening FilGAP binding and promoting its recruitment to the leading edge of the cell. An alternative explanation is that FlnA stretching results in conformational changes that weaken FilGAP binding without a crosslinking angle change. In any case, these results are important, for many cell activities require that the responses to mechanical strain be robust and include stabilization of matrix-cytoskeleton linkages and alterations of actin dynamics.

FlnA is now added to the list of intracellular proteins that respond to strain by altering either binding (talin), enzymatic (titin), or substrate (p130Cas) functions (Moore, Roca-Cusachs, & Sheetz, 2010). The biochemical complexity of focal adhesions, which can contain over 100 types of molecules (Zaidel-Bar, Itzkovitz, Ma'ayan, Iyengar, & Geiger, 2007) that are potentially mechanosensitive in their binding (Schiller, Friedel, Boulegue, & Fassler, 2011) can be at times discouraging, and mechanotransduction is often thought of as a tangled web of biochemical signaling. Ehrlicher *et al*., however, have shown us that strain in the actin-FlnA network can simultaneously regulate both actin dynamics and adhesion of the actin cytoskeleton to the surrounding matrix. Further

studies, however, are required to elucidate how much stretching of FlnA occurs during cell mechanotransduction and where its activities fit into microenvironmental controls of cell stasis versus growth or differentiation.

4.3 – Stretching of filamin A in live cells

To explore the extent of FlnA stretching in cells, I generated FlnA constructs expressing an N-terminal GFP and a C-terminal mCherry sequence (see Figure 29 for illustration of this concept using talin).

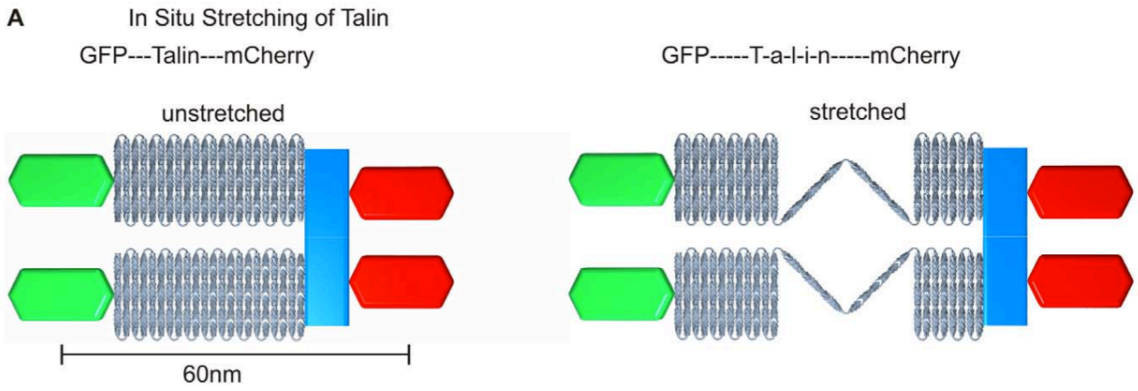

Figure 29 – Schematic of GFP-talin-mCherry fusion protein (Margadant, et al., 2011)

These constructs were expressed in wild-type fibroblasts that were plated on fibronectin-coated glass and visualized in two-color TIRF with high temporal resolution. To prevent photobleaching artifacts, total acquisition time was restricted to two minutes with a time interval of two seconds between frames. An algorithm described previously was used to analyze the resulting image sequences (Margadant, et al., 2011). At a basic level, the algorithm detects signals in one channel that co-exist with signals from the other channel

within a given radius (Figure 30).

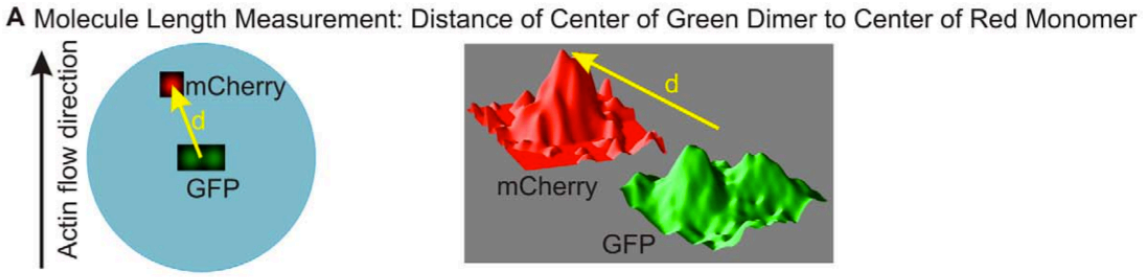

Figure 30 – Schematic showing basic concepts of detecting protein stretching (Margadant, et al., 2011)

Dimers can also be accounted for in various ways (e.g. for FlnA, two N-terminal signals must be associated with a single C-terminal signal to be detected). After filtering signal sets based on signal quality and intensity, the algorithm calculates the displacement between the signal centroids over time, yielding a temporal measure of FlnA stretching length in living cells.

Preliminary results are promising: FlnA appears to be stretched to lengths of about 100-150 nm. FlnA has an unstretched length of approximately 80 nm, so the measured stretched lengths are reasonable. Blebbistatin and Y-27632 (a Rho kinase inhibitor) both appear to decrease FlnA stretching length, suggesting that stretching is subject to mechanical forces. Additionally, comparing results from GFP-talin-mCherry and GFP-FAK-mCherry constructs shows a disparity in stretched length between each of these proteins as well as FlnA. In short, I have begun monitoring FlnA stretching in live cells. Data analysis is ongoing, but should lead to important discoveries for a number of processes related to motility, especially integrin-binding.

4.4 – Endoplasmic spreading as a possible hallmark of metastatic breast cancer

As important and satisfying as basic research can be, a researcher should always consider potential application to real world problems. Biomedical research has revealed a number of organ-specific cancer biomarkers, molecules that, when detected, suggest that a certain tissue may be at risk. Downstream of initial tests, cells and tissues are assayed in a number of ways to determine the likelihood of cancerous transformation. New determinative factors, based on the general properties that all solid cancers must have, would be informative and complementary to any diagnosis. On the most basic level, metastatic solid cancers must have the ability to divide uncontrollably and become motile to other parts of the body.

My thesis work began with a focus on the cell spreading phenotypes associated with various cancer cell types. The experiments were part of a larger study in which we determined that secondary tumor cells had a preference for substrates of certain rigidities that correlated with where the cells metastasized (Kostic, Lynch, & Sheetz, 2009). For our study, we used cancer cells of disparate metastatic potential and tissue tropism. Tissue tropism refers to the preference of a tumor cell to metastasize to a certain tissue over other tissue types.

In brief, human breast cancer cells were inoculated into mouse ventricles, where they eventually metastasized to form bone lesions in the leg. Cells from the lesions were then isolated, expanded, and re-inoculated into mice. Cancer cells were subsequently collected from any resultant lesions. Certain lines formed lesions in bone tissue, while others preferred the lung (Kang, et al., 2003) (Minn, et al., 2005) (Minn, et al., 2005). As such, when we assessed their rigidity sensing capabilities, cells that metastasized to hard regions (bone) preferred spreading on rigid substrates while those that metastasized to

soft regions (lung) preferred spreading on soft substrates. These results indicated that the rigidity sensing response in breast cancer cell lines correlated with the tissue tropism.

I contributed to this work by determining if cells of varying metastatic potential displayed differences in cell spreading. Breast cancer lines (cancerous and non-cancerous) were allowed to spread on fibronectin-coated glass for 30 minutes while being recorded by time-lapse differential interference contrast microscopy. I found no significant correlation between spreading rates and metastatic potential, so I did not pursue the experiments further.

However, after making endoplasmic spreading and its mechanisms the focus of my thesis, revisiting the breast cancer cell motility data revealed a potential defect in endoplasmic spreading amongst cancer cells that was not observed in controls. In particular, scp2, which is metastatic to bone, appeared to have the most severe endoplasmic spreading defect, while scp3, which is metastatic to lung, may carry a lesser defect. Scp21, which is non-metastatic, and MCF10A, the control cells, appeared to spread the endoplasm normally. These preliminary results indicate that an endoplasmic spreading defect may be a hallmark of metastatic breast cancers, particularly those that metastasize to rigid regions of the body (Figure 31). That said, endoplasmic spreading is most likely not directly linked to metastasis. Other phenotypes observed in parallel with defective endoplasmic spreading, such as decreased stress fibers and impaired adhesion maturation, may promote metastasis *in vivo*. Decreased stress fibers could make a cell more motile, since stress fibers are typically associated with strong adhesion to a surface. Impaired adhesion maturation could likewise make cells more motile since mature adhesions tend to be associated with the cell beginning to establish itself in a certain area.

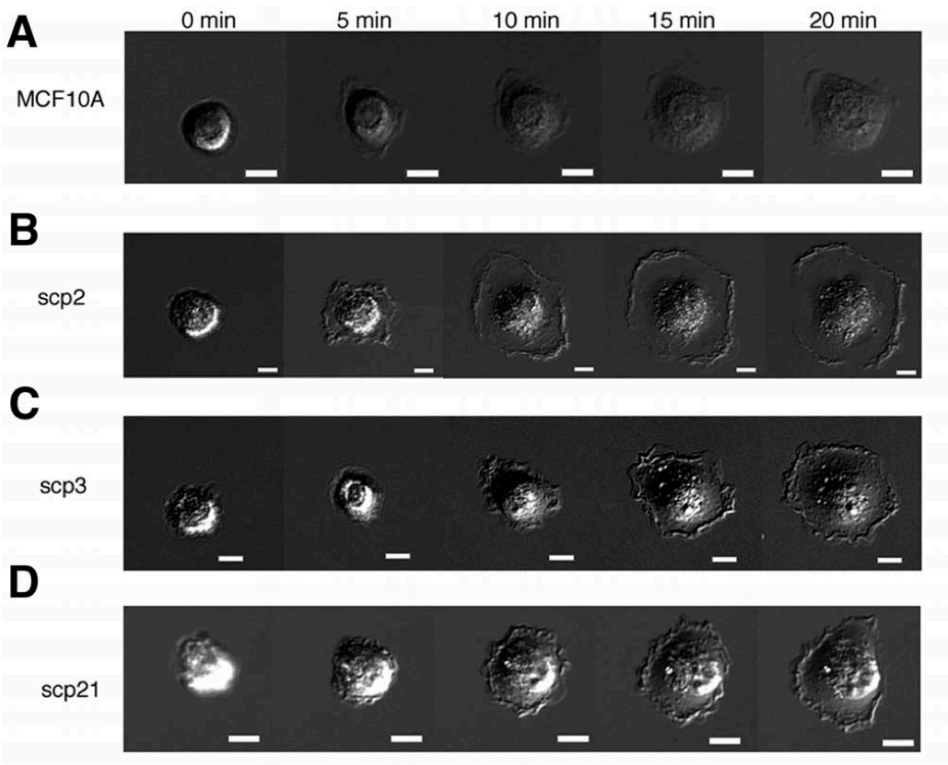

Figure 31 - Potential endoplasmic spreading deficiencies in breast cancer lines (Kostic, Lynch, & Sheetz, 2009)

(A-D) Breast epithelial cell line MCF10A (A), and breast cancer cell lines SCP 2 (B), SCP 3 (C), and SCP 21 (D) were plated on FN-coated glass and their spreading was recorded. SCP 2 was most metastatic to the bone, SCP 3 to the lung, whereas SCP21 was not metastatic. The time course of representative cells is shown. No significant changes in cell area or motility were observed in cells that were observed longer than 20 min (up to 2 h). However, SCP2 appeared to carry an endoplasmic spreading deficiency. SCP 3 and SCP 21 appeared to spread the endoplasm normally.

At this point, though we can speculate, it is unclear why endoplasmic spreading defects might be associated with metastatic breast cancer cells. Also, an endoplasmic spreading defect has not been quantitatively confirmed in metastatic breast cancer cells, only qualitatively observed. Despite this, loss of FlnA causes cells to become metastatic (Xu, et al., 2010), so I suggest that some or all of the phenotypes observed in Fln-depleted MEFs that lead to an endoplasmic spreading deficiency may also be present in metastatic cancer cells in general. This is a topic for future studies.

In summary, this thesis provides a framework for future research on the endoplasm, both basic and applied. Endoplasmic spreading has been largely ignored for many years and it is my hope that this thesis at least underlines the integral role of the endoplasm in cell spreading, and potentially paves the way for further discoveries.

Appendix

First manuscript materials and methods

Antibodies and membrane dyes: Fixable FM1-43x membrane dye and FM4-64 membrane dye were purchased from Molecular Probes. Rabbit polyclonal anti-FlnA, mouse monoclonal anti-paxillin, mouse anti-β-tubulin, mouse anti-GAPDH, and rhodamine-phalloidin were purchased from Novus Biologicals, BD Biosciences, Seven Hills Bioreagents, Santa Cruz Biotechnology, and Molecular Probes, respectively.

Cell culture: FlnA +/+, FlnA -/-, FlnB +/+, FlnB -/-, and Fln-depleted MEFs were maintained in high glucose DMEM (Gibco) + 10% FBS (Gibco) at 37°C.

Constructs and transfection: pSilencer H1-3.1 puro expression vector (Ambion) was used as described previously (Cai et al., 2006) but targeting Mus musculus *flnA* with the sequence: 5'-CCATACTTACTGTATCCGA-3'. Insert design was conducted using the pSilencer insert design tool on the Ambion website. For transfection detection, this vector was engineered to express GFP as well. pSilencer H1-3.1 puro-GFP bearing a non-targeting sequence was used as a control. pLNCX-paxillin-RFP was from Dr. Michael Partridge (Columbia University). pEGFP-3xEMTB was from Dr. Chloe Bulinski (Columbia University). pEGFP-FlnA-full and calpain-uncleavable FlnA-GFP was from Dr. Donald Ingber (Children's Hospital and Harvard Medical School). FlnA Δ19-21-GFP was from Dr. David Calderwood (Yale University). RFP-EB3 was from Dr. Richard Vallee (Columbia University). pRFP-ER was from Clontech. Transfection was accomplished using the Nucleofector system (Amaxa) or FuGENE HD transfection

reagent (Roche). FlnB -/- MEFs were transfected according to manufacturer's protocol, incubated for 1 day, exposed to 1.75 μg/ml puromycin (Sigma) in DMEM for 3 days, and used for experimentation.

FACS and Western blotting: Cells were transfected, allowed to recover for 1 day, exposed to 1.75 μg/ml puromycin in DMEM for 3 days, trypsinized, and resuspended in serum-free DMEM. Samples were sorted by a FACSAria cell sorter (BD Biosciences), centrifuged, and lysed with RIPA buffer. After sonication, samples were stored at -80°C. SDS-PAGE and Western blotting was then performed as described previously (Zhang et al., 2008).

Cover glass treatment and spreading assay preparation: On the day of the experiment, silanized cover glasses were treated with a droplet of 10 μg/ml human plasma fibronectin (FN) (Roche) and incubated at 37°C for 1 hour. Meanwhile, cells were trypsinized and resuspended in serum-free DMEM (w/o phenol red) (Gibco) for 30 minutes (for nocodazole studies, nocodazole was diluted in serum-free DMEM at 10 μM). Cells were then loaded into a sealed live-cell imaging chamber with a FN-coated cover glass on the bottom and an uncoated cover glass on top and spread at 37°C. DIC and epifluorescence microscopy was performed on an Olympus IX70 microscope mounted with a UPlanApo 20x, 0.70 NA objective (Olympus) and a Roper Scientific CoolSnap FX cooled CCD camera (Photometrics) while TIRF microscopy was performed on an Olympus IX81 microscope with a PlanApo 60x, 1.45 NA oil immersion TIRFM objective (Olympus) and a Cascade II camera (Photometrics). Imaging software was SimplePCI (C-Imaging).

Correlative cell spreading assay with immunostaining: Cells were prepared as described above but loaded into a modified imaging chamber consisting of a FN-coated cover glass on the bottom, a circular rubber gasket in the middle, and an uncoated cover glass on top. Cells were then verified for GFP expression by epifluorescence microscopy and imaged with DIC microscopy for 45 minutes. Coated cover glass was then removed from the microscope, fixed and stained as described above, and imaged once again to verify FlnA knockdown.

Immunostaining and FM-143x / FM4-64 staining: Cells were fixed with 3.7% formaldehyde in PBS, quenched with 50 mM ammonium chloride in PBS, and permeabilized with 0.1% Triton X-100 in PBS. Primary and secondary antibody stainings were performed at 37°C for 1.5 hours each. Confocal imaging was completed on an Olympus IX81 microscope with a PlanApo 60X, 1.40 NA oil immersion objective and FluoView imaging software (Olympus). FM1-43x / FM4-64 staining was accomplished by briefly fixing cells with 7.4% (2X) formaldehyde followed by a 5 minute incubation with FM1-43x / FM4-64 in 1X formaldehyde / PBS.

Quantification of distance between MT boundary and cell edge: Fln-depleted cells and their controls were transfected with 3x-ensconsin-GFP and allowed to spread. Distances between the MT boundary and cell edge were determined by drawing lines perpendicular to the cell edge from the edge to the MT boundary. At least ten measurements were made per cell and distances were measured using ImageJ.

Measurement of MT growth rates: EB3 signal was tracked using Nano Tracking plug-in for ImageJ (Nicolas Biais, Columbia University, referenced in (Cai *et al*., 2006; Biais *et al*., 2008)). Displacement plots showed regions of growth, pause, and catastrophe. Regions of highest growth were analyzed for each cell type/condition in Matlab.

Preparation of FN-coated PDMS pillars and force generation assays: PDMS was prepared in a 10:1 ratio of PDMS/curing agent, placed in a vacuum chamber to remove bubbles, and molded over silicon wafers for 14 hours at 65°C. Pillars were peeled in ethanol and quickly transferred to PBS. Pillars were then incubated at 37°C in 10 μg/ml FN for 1.5 hours for coating. After rinsing with PBS, cells were plated with CO_2-independent media and imaged on coated pillars for ~ 30 minutes on an Olympus IX70 microscope mounted with a LUCPlanFl 40x, 0.60 NA objective (Olympus).

Image analysis and statistics: Analysis of Western blots was accomplished using the "Integrated Density" measurement in ImageJ (http://rsb.info.nih.gov/ij/). Endoplasm and whole cell areas of DIC images were measured by hand using the "Area" measurement in ImageJ. While in some cells the endoplasm-ectoplasm boundary is easily identifiable with a still DIC image, all of our measurements were performed on movies at the appropriate time point, making it easier to determine the endoplasm-ectoplasm boundary in DIC by tracking organelle movements. Kymographs were generated in ImageJ with the Multiple Kymograph function (J. Rietdorf and A. Seitz, European Molecular Biology Laboratory, Heidelberg, Germany). Analysis of force generation on PDMS pillars was

completed using Nano Tracking. All other image processing was completed in ImageJ. All graphical data was completed in Excel 2008 (Microsoft) as was the execution of two-tailed t-tests and calculation of standard deviations and standard errors. Statistical analysis was done using SigmaStat (Systat) with two-tailed student's t-test when two cases were compared and with analysis of variance (ANoVA) tests when more comparisons were done. Line art was completed in Powerpoint 2008 (Microsoft).

Second manuscript methods

Antibodies and Reagents: Mouse monoclonal anti-paxillin, mouse monoclonal anti-vimentin, rhodamine-phalloidin and anti-zyxin were purchased from BD Biosciences, Abcam, Molecular Probes, and Abcam respectively. Anti-plectin P1f was obtained from Gerhard Wiche (University of Vienna, Austria) (Baldassarre et al., 2009; Burgstaller et al., 2010). N-[N-(N-Acetyl-L-leucyl)-L-leucyl]- L-norleucine (ALLN), withaferin A (WFA), blebbistatin, and nocodazole were all purchased from Sigma-Aldrich.

Constructs and Transfection: pSilencer H1–3.1 puro expression vector (Ambion, Austin, TX) was used as described previously (Cai et al., 2006) but targeting Mus musculus flnA with the sequence: 5′-CCATACTTACTGTATCCGA-3′. Insert design was conducted using the pSilencer insert design tool on the Ambion Web site. For transfection detection, this vector was engineered to express mCherry in place of GFP. pRFP-ER was obtained from Clontech (Mountain View, CA). Full-length (FL) and Non-Cleavable (NC) Paxillin-GFP, as well as FL/NC Talin-GFP, were obtained from Anna Huttenlocher (University of Wisconsin-Madison) (Cortesio et al., 2011; Franco et al., 2004). FL/NC FlnA-GFP was obtained from Donald Ingber (Children's Hospital and Harvard Medical School, Boston,

MA) (Mammoto et al., 2007). Full-length Vimentin-GFP and Vimentin 1-138 –GFP were obtained from Robert Goldman (Northwestern University) (Chang et al., 2009). Transfections were accomplished using the Nucleofector system (Lonza, Walkersville, MD). FlnB–/– MEFs were transfected according to the manufacturer's protocol, incubated for 1 day, exposed to puromycin at 1.75 μg/ml (Sigma, St. Louis, MO) in DMEM for 3 days, and used for experimentation.

Cell Culture: FlnB-/- and RPTPα+/+ MEFs were maintained in high-glucose DMEM (Life Technologies, Carlsbad, CA) + 10% fetal bovine serum (Life Technologies) at 37°C.

Chemical Treatment: Fln-depleted and negative control MEFs as well as RPTPα+/+ MEFs transfected with Vim-GFP and Vim 1-138 –GFP were incubated in 50μM ALLN in DMSO in serum media (FBS+DMEM) for 22 hours prior to experimentation. Fln-depleted MEFs were incubated with 10μM Nocodazole (an equivalent volume of DMSO for control cells) in serum-free media for 30 minutes. RPTPα+/+ MEFs were incubated with 50μM Blebbistatin (an equivalent volume of DMSO for control cells) in serum-free media for 30 minutes. RPTPα+/+ MEFs were incubated with 500nM WFA (an equivalent volume of DMSO for control cells) in serum media for 22 hours. Cell spreading assays were then conducted, either with live-cell imaging or fixation and immunostaining.

Cover glass treatment and spreading assay preparation: On the day of the experiment, silanized cover glasses were treated with a droplet of FN (Roche) at 10 μg/ml and were incubated at 37°C for 1 hour. Meanwhile, cells were trypsinized and resuspended in

serum-free DMEM (without phenol red) (Life Technologies) for 30 min prior to experimentation. DIC and epifluorescence microscopy were performed on an Olympus IX70 microscope (Center Valley, PA) mounted with a PlanApo 60×, 1.40 NA objective (Olympus) and a Roper Scientific Cool-Snap FX cooled CCD camera (Photometrics, Tucson, AZ). Imaging software used was SimplePCI (Hamamatsu Corporation, Sewickley, PA).

Immunostaining: Cells were fixed with 3.7% formaldehyde in phosphate-buffered saline (PBS), quenched with 50 mM ammonium chloride in PBS, and permeabilized with 0.1% Triton X-100 in PBS. Primary and secondary antibody stainings were performed at 37°C for 1.5 hours each. Confocal imaging was completed on either an Olympus IX81 microscope with a UPlanApo 60×, 1.40 NA oil immersion objective and FluoView imaging software (Olympus), or a Zeiss LSM 700 microscope with a Zeiss Plan-APOCHROMAT 63x 1,4 Oil DIC objective and Zeiss Zen Imaging Suite imaging software. For time-course assays, immunostaining was begun after 10, 20 and 30 minutes.

Image Analysis and Statistics: Endoplasm - whole cell area ratios were measured in the method previously reported (Lynch et al., 2011). Focal adhesion areas were analyzed by hand using the "Area" measurement tool in ImageJ. Paxillin signals smaller than $0.5\mu m^2$ were not considered. Between 10 and 15 representative FA areas per cell were quantified after thresholding. Determination of vIF connection with FAs was quantified by summing the total adhesions per cell and assessing how many were contacted by vIFs. The ratio of those FAs that colocalized with a vimentin IF to the total number of FAs was then calculated. Average distance between vIFs and the cell edge was assessed by measuring 10 regions around each cell for the distance from the tip of a vIF to the cell

edge (orthogonal to the cell edge). All p-values were generated using the Student's t-test and all graphs were generated in Microsoft Excel.

Bibliography

1. Abercrombie, M., & Heaysman, J. E. (1954). Observations on the social behaviour of cells in tissue culture II. *Exp Cell Res. , 6*, 293-306.

2. Akhmanova, A., & Steinmetz, M. O. (2008). Tracking the ends: a dynamic protein network controls the fate of microtubule tips. *Nat Rev Mol Cell Biol , 9* (4), 309-322.

3. Ananthakrishnan, R., & Ehrlicher, A. (2007). The forces behind cell movement. *Int. J. Biol. Sci. , 3*, 303-317.

4. Baldassarre, M., Razinia, Z., Burande, C. F., Lamsoul, I., Lutz, P. G., & Calderwood, D. A. (2009). Filamins regulate cell spreading and initiation of cell migration. *PLoS ONE , 4*, e7830.

5. Bershadsky, A., & Tint, I. (1987). Association of intermediate filaments with vinculin-containing adhesions plaques of fibroblasts. *Cell Motil Cytoskeleton .*

6. Burgstaller, G., Gregor, M., Winter, L., & Wiche, G. (2010). Keeping the vimentin network under control: cell-matrix adhesion-associated plectin 1f affects cell shape and polarity of fibroblasts. *Mol Biol Cell , 21*, 3362-3375.

7. Byfield, F. J., Wen, Q., Levental, I., Nordstrom, K., Arratia, P. E., Miller, R. T., et al. (2009). Absence of filamin A prevents cells from responding to stiffness gradients on gels coated with collagen but not fibronectin. *Biophys J , 96*, 5095-5102.

8. Cai, Y., Rossier, O., Gauthier, N. C., Biais, N., Fardin, M.-A., Zhang, X., et al. (2010). Cytoskeletal coherence requires myosin-IIA contractility. *J Cell Sci , 123*, 413-423.

9. Calderwood, D. A., Huttenlocher, A., Kiosses, W. B., Rose, D. M., Woodside, D. G., Schwartz, M. A., et al. (2001). Increased filamin binding to beta-integrin cytoplasmic domains inhibits cell migration. *Nat Cell Biol , 3*, 1060-1068.

10. Chang, L., Barlan, K., Chou, Y.-H., Grin, B., Lakonishok, M., Serpinskaya, A. S., et al. (2009). The dynamic properties of intermediate filaments during organelle transport. *J Cell Sci. , 122*, 2914-2923.

11. Chen, H., Zhu, X., Cong, P., Sheetz, M. P., Nakamura, F., & Yan, J. (2011). Differential mechanical stability of filamin A rod segments. *Biophys J , 101*, 1231-1237.

12. Colucci-Guyon, E., Gimenez Y Ribotta, M., Maurice, T., Babinet, C., & Privat, A. (1999). Cerebellar defect and impaired motor coordination in mice lacking vimentin. *Glia , 25* (1), 33-43.

13. Colucci-Guyon, E., Portier, M. M., Dunia, I., Paulin, D., Pournin, S., & Babinet, C. (1994). Mice lacking vimentin develop and reproduce without an obvious phenotype. *Cell , 79* (4), 679-694.

14. Cukierman, E. (2001). Taking cell-matrix adhesions to the third dimension. *Science , 294*, 1708-1712.

15. Cunningham, C., Gorlin, J., & Kwiatkowski, D. (n.d.). Actin-binding protein requirement for cortical stability and efficient locomotion. *Science* .

16. Curtis, A., & Wilkinson, C. (1997). Topographical control of cells. *Biomaterials , 18* (24), 1573-1583.

17. Davies, P. F., Spaan, J. A., & Krams, R. (2005). Shear stress biology of the endothelium. *Annals of Biomedical Engineering , 33* (12), 1714-1718.

18. Desai, A., & Mitchison, T. J. (1997). Microtubule polymerization dynamics. *Annu. Rev. Cell Dev. Biol. , 13*, 83-117.

19. Dobereiner, H.-G. (2005). Force sensing and generation in cell phases: analyses of complex functions. *Journal of Applied Physiology , 98*, 1542-1546.

20. Dobereiner, H.-G. (2005). Force sensing and generation in cell phases: analyses of complex functions. *Journal of Applied Physiology , 98*, 2794-2803.

21. Dobereiner, H.-G., Dubin-Thaler, B., Giannone, G., Xenias, H. S., & Sheetz, M. P. (2004). Dynamic phase transitions in cell spreading. *Phys Rev Lett , 93*, 108105.

22. Dokukina, I. V., & Gracheva, M. E. (2010). A model of fibroblast motility on substrates with different rigidities. *Biophys J , 98*, 2794-2803.

23. du Roure, O., Saez, A., Buguin, A., Austin, R. H., Chavrier, P., Silberzan, P., et al. (2005). Force mapping in epithelial cell migration. *PNAS , 102*, 2390-2395.

24. Dubin-Thaler, B. J., Giannone, G., Dobereiner, H.-G., & Sheetz, M. P. (2004). Nanometer analysis of cell spreading on matrix-coated surfaces reveals two distinct cell states and STEPs. *Biophys J , 86*, 1794-1806.

25. Dubin-Thaler, B. J., Hofman, J. M., Cai, Y., Xenias, H., Spielman, I., Shneidman, A. V., et al. (2008). Quantification of cell edge velocities and traction forces reveals distinct motility modules during cell spreading. *PLoS ONE , 3*.

26. Eckert, B. (1986). Alteration of the distribution of intermediate filaments in Ptk1 cells by acrylamide II: Effect on the organization of cytoplasmic organelles. *Cell Motil Cytoskeleton , 6*, 15-24.

27. Ehrlicher, A. J., Nakamura, F., Hartwig, J. H., Weitz, D. A., & Stossel, T. P. (2011). Mechanical strain in actin networks regulates FilGAP and integrin binding to filamin A. *Nature* .

28. Esue, O., Carson, A. A., Tseng, Y., & Wirtz, D. (2006). A direction interaction between actin and vimentin filaments mediated by the tail domain of vimentin. *J Biol Chem , 281* (41), 30393-30399.

29. Esue, O., Tseng, Y., & Wirtz, D. (2009). Alpha-actinin and filamin cooperatively enhance the stiffness of actin filament networks. *PLoS ONE , 4*, e4411.

30. Feng, Y., Chen, M. H., Moskowitz, I. P., Mendonza, A. M., Vidali, L., Nakamura, F., et al. (2006). Filamin A is required for cell-cell contact in vascular development and cardiac morphogenesis. *PNAS , 103*, 19836-19841.

31. Flanagan, L. A. (2001). Filamin A, the Arp 2/3 complex, and the morphology and function of cortical actin filaments in human melanoma cells. *J Cell Biol. , 155*, 511-518.

32. Fournier, M. F., Sauser, R., Ambrosi, D., Meister, J. J., & Verkhovsky, A. B. (2010). Force transmission in migrating cells. *J Cell Biol , 188*, 287-297.

33. Fox, J. W., Lamperti, E. D., Eksjoglu, Y. Z., Hong, S. E., Feng, Y., Graham, D. A., et al. (1998). Mutations in filamin 1 prevent migration of cerebral cortical neurons in human periventricular heterotopia. *Neuron , 21*, 1315-1325.

34. Franco, S. J., Rodgers, M. A., Perrin, B. J., Han, J., Bennin, D. A., Critchley, D. R., et al. (2004). Calpain-mediated proteolysis of talin regulates adhesion dynamics. *Nat Cell Biol , 6*, 977-983.

35. Friedl, S. J., & Gilmour, D. (2009). Collective cell migration in morphogenesis, regeneration and cancer. *Nat Rev Mol Cell Biol. , 10*, 445-457.

36. Fuchs, E., & Karakesisoglou, I. (2001). Bridging cytoskeletal intersections. *Genes Dev , 15*, 1-14.

37. Fuchs, E., & Weber, K. (1994). Intermediate filaments: structure, dynamics, function, and disease. *Annu. Rev. Biochem. , 63*, 345-382.

38. Furuike, S., Ito, T., & Yamazaki, M. (2001). Mechanical unfolding of single filamin A (ABP-280) molecules detected by atomic force microscopy. *FEBS Lett , 498* (1), 72-75.

39. Gauthier, N. C., Fardin, M.-A., Roca-Cusachs, P., & Sheetz, M. P. (2011). Temporary increase in plasma membrane tension coordinates the activation of exocytosis and contraction during cell spreading. *PNAS , 108*, 14467-14472.

40. Gauthier, N. C., Rossier, O. M., Mathur, A., Hone, J. C., & Sheetz, M. P. (2009). Plasma membrane area increases with spread area by exocytosis of a GPI-anchored protein compartment. *Mol Biol Cell , 20*, 3261-3272.

41. Geiger, B., & Bershaksky, A. (2001). Assembly and mechanosensory function of focal contacts. *Curr Opin Cell Biol , 13*, 584-592.

42. Giannone, G., & Sheetz, M. P. (2006). Substrate rigidity and force define form through tyrosine phosphatase and kinase pathways. *Trends Cell Biol. , 16*, 213-223.

43. Giannone, G., Dubin-Thaler, B. J., Rossier, O., Cai, Y., Chaga, O., Jiang, G., et al. (2007). Lamellipodial actin mechanically links myosin activity with adhesion-site formation. *Cell , 128*, 561-575.

44. Goldman, R. D., Khuon, S., Chou, Y. H., Opal, P., & Steinert, P. M. (1996). The function of intermediate filaments in cell shape and cytoskeletal integrity. *J Cell Biol. , 134*, 971-983.

45. Gorlin, J. B., Yamin, R., Egan, S., Stewart, M., Stossel, T. P., Kwiatkowski, D. J., et al. (1990). Human endothelial actin-binding protein (ABP-280, nonmuscle filamin): a molecular leaf spring. *J Cell Biol. , 111*, 1089-1105.

46. Gruenbaum, Y., Margalit, A., Goldman, R. D., Shumaker, D. K., & Wilson, K. L. (2005). The nuclear lamina comes of age. *Nat Cell Biol. , 6* (1), 21-31.

47. Harris, A. K., Wild, P., & Stopak, D. (1980). Silicone rubber substrata: a new wrinkle in the study of cell locomotion. *Science , 208* (4440), 177-179.

48. Hartwig, J. H., & Shevlin, P. (1986). The architecture of actin filaments and the ultrastructural location of actin-binding protein in the periphery of lung macrophages. *J Cell Biol. , 103*, 1007-1020.

49. Hartwig, J. H., & Stossel, T. P. (1975). Isolation and properties of actin, myosin, and a new actin-binding protein in rabbit alveolar macrophages. *J Biol Chem , 250*, 5696-5705.

50. Harunaga, J. S., & Yamada, K. M. (2011). Cell-matrix adhesions in 3D. *Matrix Biol , 30*, 363-368.

51. Hatten, M. (1999). Central nervous system neuronal migration. *Annu. Rev. Neurosci. , 22*, 511-539.

52. Heikkinen, O. K., Ruskamo, S., Konarev, P. V., Svergun, D. I., Iivanainen, T., Heikkinen, S. M., et al. (2009). Atomic structures of two novel immunoglobulin-like domain pairs in the actin cross-linking protein filamin. *Journal of Biological Chemistry , 284* (37), 25450-25458.

53. Helfand, B. T., Chang, L., & Goldman, R. D. (2003). The dynamic and motile properties of intermediate filaments. *Annu. Rev. Cell Dev. Biol. , 19*, 445-467.

54. Herrmann, H., & Aebi, U. (2004). Intermediate filaments: molecular structure, assembly mechanism, and integration into functionally distinct intracellular scaffolds. *Annu. Rev. Biochem. , 73*, 749-789.

55. Herrmann, H., Bar, H., Kreplak, L., Strelkov, S. V., & Aebi, U. (2007). Intermediate filaments: from cell architecture to nanomechanics. *Nature Publishing Group , 8* (7), 562-573.

56. Hotulainen, P., & Lappalainen, P. (2006). Stress fibers are generated by two distinct actin assembly mechanisms in motile cells. *J Cell Biol. , 173*, 383-394.

57. Insall, R. H., & Machesky, L. M. (2009). Actin dynamics at the leading edge: from simple machinery to complex networks. *Developmental Cell , 17*, 310-322.

58. Insall, R. H., & Machesky, L. M. (2009). Actin dynamics at the leading edge: from simple machinery to complex networks. *Developmental Cell , 17*, 310-322.

59. Ithychanda, S. S., Hsu, D., Li, H., Yan, L., Liu, D., Das, M., et al. (2009). Identification and characterization of multiple similar ligand-binding repeats in filamin: implication on filamin-mediated receptor clustering and cross-talk. *Journal of Biological Chemistry , 284*, 35113-35121.

60. Ivanova, O., Margolis, L., Vasiliev, J., & Gelfand, I. (1976). Effect of colcemid on the spreading of fibroblasts in culture. *Exp Cell Res , 101*, 207-219.

61. Jefferson, J. J., Leung, C. L., & Liem, R. K. (2004). Plakins: goliaths that link cell junctions and the cytoskeleton. *Nature Publishing Group , 5* (7), 542-553.

62. Johnson, C. P., Tang, H.-Y., Carag, C., Speicher, D. W., & Discher, D. E. (2007). Forced unfolding of proteins within cells. *Science , 317* (5838), 663-666.

63. Kanchanawong, P., Shtengel, G., Pasapera, A. M., Ramko, E. B., Davidson, M. W., Hess, H. F., et al. (2010). Nanoscale architecture of integrin-based cell adhesions. *Nature , 468* (7323), 580-584.

64. Kang, Y., Siegel, P. M., Shu, W., Drobnjak, M., Kakonen, S. M., Cordon-Cardo, C., et al. (2003). A multigenic program mediating breast cancer metastasis to bone. *Cancer Cell , 3*, 537-549.

65. Kasza, K. E., Koenderink, G. H., Lin, Y. C., Broedersz, C. P., Messner, W., Nakamura, F., et al. (2009). Nonlinear elasticity of stiff biopolymers connected by flexible linkers. *Physical review E, Statistical, nonlinear, and soft matter physics , 79*.

66. Kasza, K. E., Nakamura, F., Hu, S., Kollmannsberger, P., Bonakdar, N., Fabry, B., et al. (2009). Filamin A is essential for active cell stiffening but not passive stiffening under external force. *Biophys J , 96*, 4326-4335.

67. Kaverina, I., Krylyshkina, O., & Small, J. V. (1999). Microtubule targeting of substrate contacts promotes their relaxation and dissociation. *J Cell Biol. , 146*, 1033-1044.

68. Kiema, T., Lad, Y., Jiang, P., Oxley, C. L., Baldassarre, M., Wegener, K. L., et al. (2006). The molecular basis of filamin binding to integrins and competition with talin. *Mol Cell , 21*, 337-347.

69. Kim, H., & McCulloch, C. A. (2011). Filamin A mediates interactions between cytoskeletal proteins that control cell adhesion. *FEBS Lett. , 585*, 18-22.

70. Kim, H., Nakamura, F., Lee, W., Hong, C., Perez-Sala, D., & McCulloch, C. A. (2010). Regulation of cell adhesion to collagen via beta1 integrins is dependent on interactions of filamin A with vimentin and protein kinase C epsilon. *Exp Cell Res* .

71. Kim, H., Nakamura, F., Lee, W., Shifrin, Y., Arora, P., & McCulloch, C. A. (2010). Filamin A is required for vimentin-mediated cell adhesion and spreading. *Am J Physiol, Cell Physiol , 298*, C221-36.

72. Kolahi, K. S., & Mofrad, M. R. (2008). Molecular mechanics of filamin's rod domain. *Biophys J , 94* (3), 1075-1083.

73. Kolodney, M. S., & Elson, E. L. (1995). Contraction due to microtubule disruption is associated with increased phosphorylation of myosin regulatory light chain. *PNAS , 92* (22), 10252-10256.

74. Kostic, A., & Sheetz, M. P. (2006). Fibronectin rigidity response through Fyn and p130Cas recruitment to the leading edge. *Mol Biol Cell. , 17*, 2684-2695.

75. Kostic, A., Lynch, C. D., & Sheetz, M. P. (2009). Differential matrix rigidity response in breast cancer cell lines correlates with the tissue tropism. *PLoS ONE , 4*, e6361.

76. Kostic, A., Sap, J., & Sheetz, M. P. (2007). RPTP alpha is required for rigidity-dependent inhibition of extension and differentiation of hippocampal neurons. *J Cell Sci , 120*, 3895-3904.

77. Krylyshkina, O., Anderson, K. I., Kaverina, I., Upmann, I., Manstein, D. J., Small, J. V., et al. (2003). Nanometer targeting of microtubules to focal adhesions. *J Cell Biol. , 161*, 853-859.

78. Krylyshkina, O., Kaverina, I., Kranewitter, W., Steffen, W., Alonso, M. C., Cross, R. A., et al. (2002). Modulation of substrate adhesion dynamics via microtubule targeting requires kinesin-1. *J Cell Biol. , 156*, 349-359.

79. Lad, Y., Kiema, T., Jiang, P., Pentikainen, O. T., Coles, C. H., Campbell, I. D., et al. (2007). Structure of three tandem filamin domains reveals auto-inhibition of ligand binding. *EMBO J , 26* (17), 3993-4004.

80. Le Clainche, C., & Carlier, M.-F. (2008). Regulation of actin assembly associated with protrusion and adhesion in cell migration. *Physiol. Rev. , 88*, 489-513.

81. Lee, N. P., Mruk, D. D., Conway, A. M., & Cheng, C. Y. (2004). Zyxin, axin, and Wiskott-Aldrich syndrome protein are adaptors that link the cadherin/catenin protein complex to the cytoskeleton at adherens junctions in the seminiferous epithelium of the rat testis. *J. Androl. , 25*, 200-215.

82. Leiss, M., Beckmann, K., Giros, A., Costell, M., & Fassler, R. (2008). The role of integrin binding sites in fibronectin matrix assembly in vivo. *Curr Opin Cell Biol. , 20*, 502-507.

83. Locascio, A., & Nieto, M. (2001). Cell movements during vertebrate development: integrated tissue behaviour versus individual cell migration. *Curr Opin Genet Dev. , 11*, 464-469.

84. Loo, D. T., Kanner, S. B., & Aruffo, A. (1998). Filamin binds to the cytoplasmic domain of beta 1-integrin. Identification of amino acids responsible for this interaction. *J Biol Chem , 273*, 23304-23312.

85. Lynch, C. D., & Sheetz, M. P. (2011). Cellular mechanotransduction: filamin A strains to regulate motility. *Curr Biol , 21*, R916-918.

86. Lynch, C. D., Gauthier, N. C., Biais, N., Lazar, A. M., Roca-Cusachs, P., Yu, C.-H., et al. (2011). Filamin depletion blocks endoplasmic spreading and destabilizes force-bearing adhesions. *Mol Biol Cell , 22*, 1263-1273.

87. Margadant, F., Chew, L. L., Hu, X., Yu, H., Bate, N., Zhang, X., et al. (2011). Mechanotransduction in vivo by repeated talin stretch-relaxation events depends on vinculin. *PLoS Biol , 9*, e1001223.

88. Mathur, A., Moore, S. W., & Sheetz, M. P. (2012). Role of feature curvature in contact guidance. *Acta Biomater*.

89. Mendez, M. G., Kojima, S.-I., & Goldman, R. D. (2010). Vimentin induces changes in cell shape, motility, and adhesion during the epithelial to mesenchymal transition. *FASEB J , 24*, 1838-1851.

90. Minn, A. J., Gupta, G. P., Siegel, P. M., Bos, P. D., Shu, W., Giri, D. D., et al. (2005). Genes that mediate breast cancer metastasis to lung. *Nature , 436*, 518-524.

91. Minn, A. J., Kang, Y., Serganova, I., Gupta, G. P., Giri, D. D., Doubrovin, M., et al. (2005). Distinct organ-specific metastatic potential of individual breast cancer cells and primary tumors. *J Clin Invest , 115*, 44-55.

92. Miranti, C. K., & Brugge, J. S. (2002). Sensing the environment: a historical perspective on integrin signal transduction. *Nat Cell Biol. , 4*, E83-90.

93. Mitchison, T., & Kirschner, M. (1984). Dynamic instability of microtubule growth. *Nature , 312*, 237-242.

94. Moore, S. W., Roca-Cusachs, P., & Sheetz, M. P. (2010). Stretchy proteins on stretchy substrates: the important elements of integrin-mediated rigidity sensing. *Developmental Cell , 19*, 194-206.

95. Nakamura, F., Osborn, T. M., Hartemink, C. A., Hartwig, J. H., & Stossel, T. P. (2007). Structural basis of filamin A functions. *J Cell Biol , 179*, 1011-1025.

96. Nieminen, M., Henttinen, T., Merinen, M., Marttila-Ichihara, F., Eriksson, J. E., & Jalkanen, S. (2006). Vimentin function in lymphocyte adhesion and transcellular migration. *Nat Cell Biol , 8* (2), 156-162.

97. Nishida, T., Yasumoto, K., Otori, T., & Desaki, J. (1988). The network structure of corneal fibroblasts in the rat as revealed by scanning electron microscopy. *Invest Ophthalmol Vis Sci , 29*, 1887-1890.

98. Nishizaka, T., Shi, Q., & Sheetz, M. P. (2000). Position-dependent linkages of fibronectin-integrin-cytoskeleton. *PNAS , 97*, 692-697.

99. Nogales, E. (2000). Structural insights into microtubule function. *Annu. Rev. Biochem. , 69*, 277-302.

100. Oliver, T., Dembo, M., & Jacobson, K. (1995). Traction forces in locomoting cells. *Cell Motil Cytoskeleton , 31*, 225-240.

101. Pentikainen, U., & Ylanne, J. (2009). The regulation mechanism for the auto-inhibition of binding of human filamin A to integrin. *J Mol Biol , 393* (3), 644-657.

102. Pollard, T. D. (1986). Rate constants for the reactions of ATP- and ADP-actin with the ends of actin filaments. *J Cell Biol , 103*, 2747-2754.

103. Pollard, T. D., & Borisy, G. G. (2003). Cellular motility driven by assembly and disassembly of actin filaments. *Cell , 112* (4), 453-465.

104. Razinia, Z., Makela, T., Ylanne, J., & Calderwood, D. A. (2012). Filamins in mechanosensing and signaling. *Annu Rev Biophys* .

105. Riveline, D. E., Zamir, E., Balaban, N. Q., Schwarz, U. S., Ishizaki, T., Narumiya, S., et al. (2001). Focal contacts as mechanosensors: externally applied local mechanical force induces growth of focal contacts by an mDia1-dependent and ROCK-independent mechanism. *J Cell Biol. , 153*, 1175-1186.

106. Rossier, O. M., Gauthier, N., Biais, N., Vonnegut, W., Fardin, M.-A., Avigan, P., et al. (2010). Force generated by actomyosin contraction builds bridges between adhesive contacts. *EMBO J , 29*, 1055-1068.

107. Ryzhkov, P., Prass, M., Gummich, M., Kuhn, J.-S., Oettmeier, C., & Dobereiner, H.-G. (2010). Adhesion patterns in early cell spreading. *J Phys Condens Matter , 22*, 194106.

108. Sawada, Y., & Sheetz, M. P. (2002). Force transduction by Triton cytoskeletons. *J Cell Biol , 156*, 609-615.

109. Schiffers, P. M., Henrion, D., Boulanger, C. M., Colucci-Guyon, E., Langa-Vuves, F., van Essen, H., et al. (2000). Altered flow-induced arterial remodeling in vimentin-deficient mice. *Arterioscler Thromb Vasc Biol , 20* (3), 611-616.

110. Schiller, H. B., Friedel, C. C., Boulegue, C., & Fassler, R. (2011). Quantitative proteomics of the integrin adhesome show a myosin II-dependent recruitment of LIM domain proteins. *EMBO Rep. , 12*, 259-266.

111. Schmoller, K. M., Lieleg, O., & Bausch, A. R. (2009). Structural and viscoelastic properties of actin/filamin networks: cross-linked versus bundled networks. *Biophys J , 97*, 83-89.

112. Sharma, C. P., Ezzell, R. M., & Arnaout, M. A. (1995). Direct interaction of filamin (ABP-280) with the beta 2-integrin subunit CD18. *J Immunol , 154*, 3461-3470.

113. Shifrin, Y., Arora, P., Ohta, Y., Calderwood, D., & McCulloch, C. (2009). The role of FilGAP-filamin A interactions in mechanoprotection. *Mol Biol Cell* .

114. Sprague, B., Pego, R., & Stavreva, D. (2004). Analysis of binding reactions by fluorescence recovery after photobleaching. *Biophys J* .

115. Stossel, T. P., Condeelis, J., Cooley, L., Hartwig, J. H., Noegel, A., Schleicher, M., et al. (2001). Filamins as integrators of cell mechanics and signaling. *Nat Rev Mol Cell , 2*, 138-145.

116. Straight, A. F., Cheung, A., Limouze, J., Chen, I., Westwood, N. J., Sellers, J. R., et al. (2003). Dissecting temporal and spatial control of cytokinesis with a myosin II inhibitor. *Science , 299* (5613), 1743-1747.

117. Sweeney, H. L., & Houdusse, A. (2010). Structural and functional insights into the myosin motor mechanism. *Annu. Rev. Biophys. , 39* (1), 539-557.

118. Takafuta, T., Wu, G., Murphy, G. F., & Shapiro, S. S. (1998). Human beta-filamin is a new protein that interacts with the cytoplasmic tail of glycoprotein Ibalpha. *J Biol Chem. , 273*, 17531-17538.

119. Takala, H., Nurminen, E., Nurmi, S., Aatonen, M., Strandin, T., Takatalo, M., et al. (n.d.). Integrin beta 2 phosphorylation on Thr758 acts as a molecular switch to regulate 14-3-3 and filamin binding. *Blood* .

120. Tan, J. L., Tien, J., Pirone, D. M., Gray, D. S., Bhadriraju, K., & Chen, C. S. (2003). Cells lying on a bed of microneedles: an approach to isolate mechanical force. *PNAS , 100*, 1484-1489.

121. Tarin, D., & Croft, C. B. (1969). Ultrastructural feature of wound healing in mouse skin. *J. Anat. , 105*, 189-190.

122. Terasaki, M., & Reese, T. (1994). Interactions among endoplasmic reticulum, microtubules, and retrograde movements of the cell surface. *Cell Motil Cytoskeleton , 29*, 291-300.

123. Terzi, F., Henrion, D., Colucci-Guyon, E., Federici, P., Babinet, C., Levy, B. I., et al. (1997). Reduction of renal mass is lethal in mice lacking vimentin. Role of endothelin-nitric oxide imbalance. *J Clin Invest , 100*, 1520-1528.

124. Thaiparambil, J. T., Bender, L., Ganesh, T., Kline, E., Patel, P., Liu, Y., et al. (2011). Withaferin A inhibits breast cancer invasion and metastasis at sub-

cytotoxic doses by inducing vimentin disassembly and serine 56 phosphorylation. *Int J Cancer* .

125. Toyoda, H., Ina, K., Kitamura, H., Tsuda, T., & Shimada, T. (1997). Organization of the lamina propria mucosae of rat intestinal mucosa, with special reference to the subepithelial connective tissue. *Acta Anat , 158*, 172-184.

126. Tseng, Y., An, K., Esue, O., & Wirtz, D. (2004). The bimodal role of filamin in controlling the architecture and mechanics of F-actin networks. *Journal of Biological Chemistry* .

127. Tsuruta, D. (2003). The vimentin cytoskeleton regulates focal contact size and adhesion of endothelial cells subjected to shear stress. *J Cell Sci. , 116*, 4977-4984.

128. van der Flier, A., & Sonnenberg, A. (2001). Structural and functional aspects of filamins. *Biochim Biophys Acta. , 1538*, 99-117.

129. Vicente-Manzanares, M., Ma, X., Adelstein, R. S., & Horwitz, A. R. (2009). Non-muscle myosin II takes center stage in cell adhesion and migration. *Nat Rev Mol Cell Biol. , 10*, 778-790.

130. Wang, N., Tytell, J. D., & Ingber, D. E. (2009). Mechanotransduction at a distance: mechanically coupling the extracellular matrix with the nucleus. *Nat Rev Mol Cell Biol , 10*, 75-82.

131. Waterman-Storer, C. M., & Salmon, E. D. (1998). Endoplasmic reticulum membrane tubules are distributed by microtubules in living cells using three distinct mechanisms. *Curr Biol. , 8*, 798-806.

132. Weisenberg, R. C., Borisy, G. G., & Taylor, E. W. (1968). Colchicine-binding protein of mammalian brain and its relation to microtubules. *Biochemistry , 7* (12), 4466-4479.

133. Weisenberg, R. C., Deery, W. J., & Dickinson, P. J. (1976). Tubulin-nucleotide interactions during the polymerization and depolymerization of microtubules. *Biochemistry , 15* (19), 4248-4254.

134. Weiss, P. (1958). Cell contact. *International Review of Cytology , 7*, 391-423.

135. Xu, Y., Bismar, T. A., Su, J., Xu, B., Kristiansen, G., Varga, Z., et al. (2010). Filamin A regulates focal adhesion disassembly and suppresses breast cancer cell migration and invasion. *J Exp Med. , 207*, 2421-2437.

136. Yamazaki, M., Furuike, S., & Ito, T. (2002). Mechanical response of single filamin A (ABP-280) molecules and its role in the actin cytoskeleton. *J. Muscle Res. Cell. Motil. , 23*, 525-534.

137. Yang, J., & Weinberg, R. A. (2008). Epithelial-mesenchymal transition: at the crossroads of development and tumor metastasis. *Developmental Cell , 14*, 818-829.

138. Zaidel-Bar, R., Cohen, M., Addadi, L., & Geiger, B. (2004). Hierarchical assembly of cell-matrix adhesion complexes. *Biochem Soc Trans , 32*, 416-420.

139. Zaidel-Bar, R., Itzkovitz, S., Ma'ayan, A., Iyengar, R., & Geiger, B. (2007). Functional atlas of the integrin adhesome. *Nat Cell Biol. , 9*, 858-867.

140. Zhang, X., Jiang, G., Cai, Y., Monkley, S. J., Critchley, D. R., & Sheetz, M. P. (2008). Talin depletion reveals independence of initial cell spreading from integrin activation and traction. *Nat Cell Biol , 10*, 1062-1068.

141. Zhou, X., Tian, F., Sandzen, J., Cao, R., Flaberg, E., Szekely, L., et al. (2007). Filamin B deficiency in mice results in skeletal malformations and impaired microvascular development. *PNAS , 104*, 3919-3924.